UNIVERSITÀ POLITECNICA DELLE MARCHE
CORSO DI DOTTORATO DI RICERCA IN SCIENZE DELLA VITA E DELL'AMBIENTE
CURRICULUM IN PROTEZIONE CIVILE ED AMBIENTALE

Phase Change Materials (PCMs): an Opportunity for Energy Saving in the Cold Chain

Ph.D Dissertation of:
Benedetta Copertaro

Advisor:
Prof. Paolo Principi

XXIX Ciclo

Università Politecnica delle Marche
Dipartimento di Scienze della Vita e dell'Ambiente
Via Brecce Bianche — 60131 - Ancona, Italy

SUCCESS IS AN ICEBERG

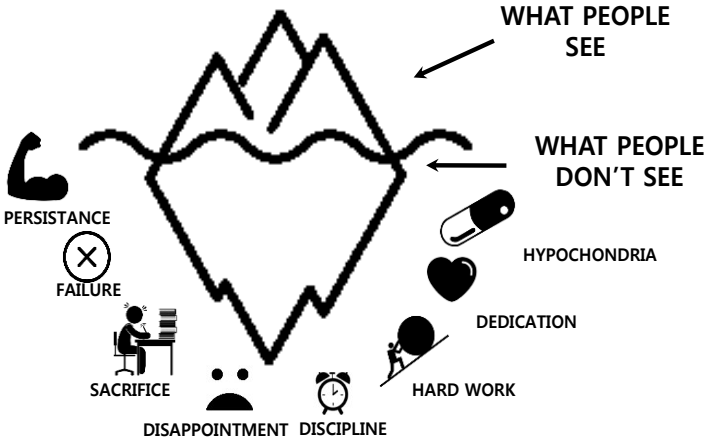

To my Family and my Love
which both sides they have experienced.

Publications

The presented thesis is based on five publications written during the doctoral research activity. Specifically, two of these have been published in scientific journals and the remaining three have been presented at international conferences. The list of publications is the following:

- **Journal papers**

Benedetta Copertaro, Paolo Principi and Roberto Fioretti. Thermal performance analysis of PCM in refrigerated container envelopes in the Italian context– Numerical modeling and validation. Applied Thermal Engineering: Volume 102, Pages 873-881. 5 June 2016.

Roberto Fioretti, Paolo Principi and Benedetta Copertaro. A refrigerated container envelope with a PCM (Phase Change Material) layer: Experimental and theoretical investigation in a representative town in Central Italy. Energy Conversion and Management: Volume 122, Pages 131-141. 15 August 2016.

- **Conference papers**

Benedetta Copertaro, Roberto Fioretti and Paolo Principi: Numerical and experimental analysis on thermal behavior of refrigerated chamber's envelope incorporated with Phase Change Materials (PCMs). International Conference in Energy Science and Technology, 20 – 22 May 2015 Karlsruhe, Germany.

Benedetta Copertaro, Roberto Fioretti and Paolo Principi. Numerical study on the thermal performance of a refrigerated container envelope provided by Phase Change Materials (PCMs). Environment and Electrical Engineering (EEEIC), 2015 IEEE 15th International Conference on Environment and Electrical Engineering. 10-13 June Rome. Pages 378-383.

Benedetta Copertaro, Roberto Fioretti and Paolo Principi. Experimental analysis on a novel air heat exchanger containing PCM (phase change material) in a cold room.11th IIR Conference on Phase Change Materials and Slurries for Refrigeration and Air Conditioning, Karlsruhe, 2016.

Benedetta Copertaro, Roberto Fioretti and Paolo Principi. Thermal analysis on a phase change material latent heat storage in a cold room in case of power outage. 16 IEEE International Conference on Environment and Electrical Engineering. 7-10 June Florence.

Sommario

Mantenere la qualità e la sicurezza degli alimenti lungo tutta la catena del freddo, rappresenta una delle principali sfide per il settore della refrigerazione. Allo stesso tempo, garantire una temperatura costante lungo la filiera del freddo determina un elevato consumo energetico, comportando elevate emissioni di CO_2 in atmosfera. A tale proposito l'attività di ricerca è stata finalizzata alla sperimentazione di diverse possibilità di utilizzo dei materiali in passaggio di fase (PCMs), per ottimizzare le prestazioni energetiche dei sistemi di trasporto e stoccaggio refrigerati. Inizialmente l'attività di ricerca si è focalizzata sull'applicazione del PCM nell'involucro di un container refrigerato, al fine di ridurre e sfasare temporalmente il carico di raffreddamento. Tale tecnologia è stata valutata mediante approccio numerico e sperimentale, consentendo pertanto di validare il modello numerico. In un secondo momento, sono stati valutati i benefici energetici legati ad uno scambiatore di calore contenete PCM posizionato in prossimità dell'evaporatore di una cella frigorifera. Gli obiettivi di tale attività sono stati quelli di ridurre il consumo di energia elettrica in condizioni di regime stazionario ed il tasso di incremento della temperatura all'interno del vano in caso di black-out. Inoltre, al fine di aiutare le compagnie di trasporto refrigerato ad implementare le giuste misure di efficienza per la produzione del freddo è stato prodotto un tool di calcolo. Infine, l'attività di ricerca è stata focalizzata sull'applicazione del PCM nelle pareti interne del vano refrigerato di una cella frigorifera, allo scopo di ridurre il picco di temperatura dell'aria ed il consumo di energia elettrica durante differenti aperture della porta. Complessivamente i risultati ottenuti hanno evidenziato come l'applicazione del PCM nelle diverse tecnologie refrigerate, determina una interessante riduzione dei consumi di energia elettrica e delle emissioni di CO_2 in atmosfera.

Parole chiave: *Refrigerazione, catena del freddo, materiali in passaggio di fase, efficienza energetica e riduzione gas effetto serra*

Abstract

Ensuring both food quality and safety to the global population through the cold chain is the major challenge for the refrigeration sector. At the same time guaranteeing, a constant temperature throughout the entire cold chain determines a high-energy consumption and related CO_2 emissions into the atmosphere. Therefore, in this dissertation, different approaches aimed at improving refrigerated storage and transport systems performance by Phase Change Materials (PCMs) application have been investigated. The first study have focused on the application of PCM layer to the external side of a refrigerated container envelope, in order to reduce and shift the cooling load in comparison with a conventional enclosure. To that end, the proposed technology was evaluated using a numerical and experimental study design. The calculation results were compared with the experimental values in order to validate the mathematical model. In the field of refrigerated storage, the application of a PCM air heat exchanger near the evaporator of a cold room was experimentally investigated. The study purposes were to reduce the cooling energy consumption during normal operating conditions and the rate of temperature increase throughout the course of a power failure event. Moreover, in order to help refrigerated transport companies to define and implement the right efficiency measures for cold production by using PCM, a calculation tool has been developed. The final study have focused on the application of PCM layer to the internal compartment walls of a storage cold room, in order to reduce the peak air temperature and energy consumption during different door openings. To that end, the proposed technology was evaluated using an experimental campaign. The overall dissertation results highlighted that the PCM addition in the proposed refrigerated technologies can lead to interesting reduction in both energy consumption and related CO_2 emissions into the atmosphere.

Keywords: *Refrigeration, cold chain, phase change materials (PCMs), energy efficiency and greenhouse gasses emission reduction*

Contents

List of Figures

List of Tables

Introduction

Climate change is a fact of life: mitigating greenhouse gas emissions

Climate Change in IPCC usage (Intergovernmental Panel on Climate Change) refers to the variation at global or regional level in the state of the climate (**IPCC, 2014**). Many things can cause climate to change all on its own: climate can be affected by changing in the Sun and volcanic eruptions but also by humans activities. Everything humans do such as driving cars, heating and cooling house, cooking foods, running factories and tropical deforestation and so on requires to burn coal, gas and oil releasing Green House Gasses (GHGs) into the atmosphere (**IPCC, 2014**). These gasses being opaque to the infrared radiation emitted by the Heart surface trap the heat into the atmosphere that was in its way out, causing global warming. Since 1950s many unequivocal changes have been observed. As an example the atmosphere and the ocean have warmed of 0.85°C (1880-2012) and 0.11°C (1971-2010) respectively (**IPCC, 2014**). Moreover concentrations of greenhouse gases have increased. It was found that in 2010 the concentration of GHG such as, carbon dioxide (CO_2), methane (CH_4), and nitrous oxide (N_2O) have exceeded the pre-industrial levels by about 40%, 150%, and 20%, respectively (**IPCC, 2014**). Therefore a further increase of GHGs concentration into the atmosphere will lead to a more warming and changes in all components of climate system, determining potentially irreversible damages to both natural and anthropic systems. For this purpose for evaluating potential responses of climate system to the increase of GHG concentration to the atmosphere, the IPCC since 90s produces several climate projections aimed at explore future climate (**Flato et al., 2013**). Substantially climate projections are based on a set of scenarios influenced by different human behavior and activities, economic growth and energy usage; practically on future global emissions of greenhouse gasses (**Flato et al., 2013**). The latest five assessment report of IPCC according to the new Representative Concentration Pathways RCP 4.5 and RCP 8.5 indicates an increase of global average temperature of about 1.4°C to 3.1°C and 2.6°C to 4.8°C respectively (**Flato et al., 2013**; **IPCC, 2013**).

In this context faced with the economic and population growth, which are considered the two main GHG driving force, a series of climate mitigation ad even adaptation actions should be planned (**IPCC, 2014**). By this way a reduction of climate change impact can be achieved. Although mitigation and adaptation are sharing the final purpose of reducing climate change impacts, the objective are considered differences. Climate Adaptation in **IPCC** (**2014**) usage refers to the "*human's capability of making changes in the way they live in order to become more resilient to changes in climate*". Adaptation occurs in two main ways. The first way consists on proactive practices such as seasonal climate forecasting, crop

and livelihood diversification, water storage and so on. The second way consists on reactive adaptations such as emergency response, disaster recovery and migration (**IPCC, 2007**). On the other hand, Climate Mitigation in **IPCC** (**2014**) usage refers to the "*human intervention aimed at reducing the sources or enhancing the sinks of GHGs*". Substantially there are two main ways to reduce or prevent emission of greenhouse gasses: reducing energy usage by the development of energy efficiency technologies and switching to energy sources that do not discharge greenhouse gases (**IPCC, 2014**). In accordance to **IPCC, 2014** "*the total anthropogenic GHG emissions risen rapidly from 2000 to 2010 reaching 49 (±4.5) gigatonnes CO2-equivalents per year (GtCO2eq/yr) in 2010*". In that way, five main sectors (energy supply, Agriculture, Forestry and Other Land Use AFOLU, industry, transport and buildings sectors) responsible for the improvement of GHG emission levels were identified by IPCC.

It is well known that the combustion of fossil fuel deriving from the energy supply sector is considered the largest contributor to global GHGs emission (**IPCC, 2014**). This sector which consists on the conversion of primary energy into electricity, heat, refined oil products, coke, enriched coal, and natural gas was estimated to be responsible of 35% of GHGs emission into the atmosphere in 2010 (**IPCC, 2014**). By this way a series of mitigation technology options, practices and behavioral aspects have been listed in the IPCC report. Summarizing, the report focused on the improvement of technologies energy efficiency, the reduction of the methane emission in the fuel supply chain and the development of carbon dioxide capture technologies (**IPCC, 2014**). Moreover the report focused on the reduction of the electrical losses in the transmission systems by the improvement of energy efficiency of cable and line electrical transmission (**Sims et al., 2007; Bruckner et al., 2014)**. Finally, regarding the GHGs mitigation options the attention was addressed to the Renewable Energy (RE) technologies and the nuclear energy usage. In the first case, RE technologies are considered one of the most effective way to supply electricity contributing to social and economic development, energy secure access, climate mitigation and reduction of environmental impacts (**IPCC, 2011**). As an example, was estimated (by using LCA, Life Cycle Assessment) that the GHG emissions for the electricity generation were lower from RE technologies than those associated with fossil fuel options. Moreover the use of biofuels could provide a higher GHG mitigation. In the second case, the nuclear power plant (**IPCC, 2014**) is considered a low carbon technology if compared to fossil power plants. Anyway a variety of barriers and risks have to be considered. New fuel cycles and reactor technologies are under progress and the development of advanced technologies for waste management and disposal are being studying. In accordance to **IPCC, 2014** the Agriculture, Forestry and Other Land Use sector "*is responsible for just under a quarter of anthropogenic GHG emissions mainly from deforestation and agricultural emissions from livestock, soil and nutrient*

management". Therefore, reducing deforestation and GHG emissions per unit of land/animal/product, changing food demand and reducing waste are considered the most effective mitigation options (**Smith et al. 2144**). The energy intensive industry sector was estimated to be responsible through direct and indirect emission of 30% of global GHG emissions in 2010 (**IPCC, 2014**). The processing of iron and steel, the petroleum refining and cement production are considered the most energy consumption sectors all over the world. Different factors such as insufficient operating and maintenance procedures, waste of materials and the not-recovery of heat, fuel and power from industrial process can cause an increase of the global GHG emissions (**Bernstein et al., 2007**). Therefore mitigation actions should be focused on the technological energy efficiency improvement, the design of energy efficient process aimed at increase the internal energy recovery and material recycling (**IPCC, 2014**).

In accordance to **IPCC, 2014** the transport sector "*produced 7.0 $GtCO_2eq$ of direct GHG emissions (including non-CO_2 gases) in 2010 and hence was responsible for approximately 23% of total energy-related CO_2 emissions*". Therefore by changing the behavior of travelers such as reducing the journey, choosing public transport and the substitution of oil-based products with natural gas, biofuel, electricity or hydrogen the direct GHG emissions can be reduced (**Kahn Ribeiro et al., 2007**). Finally the building sector was estimated to be responsible for 19% of global GHG emission in 2010 (**IPCC, 2014**). Overall there is a significant number of technologies aimed at reducing GHG emissions in the new and existing residential and commercial buildings. Summarizing, the IPCC report (**Levine et al., 2007**) focused on the reduction of heating ad solar heat loads by using high level of wall insulation material, the building envelope to accept or reject the solar radiation and by the improvement of building structure thermal inertia in order to shift the thermal loads. Moreover GHGs mitigation options for supermarkets and hypermarkets refrigeration system have been revised (**IPCC, 2014**). It is well known that by the leakage of refrigerant gasses and energy usage, the refrigeration sector is contributing to global warming significantly (**Garnett, 2007**). Therefore in the next section, a deepen discussion regarding the refrigeration sector development over the years, its importance in the modern society, the environmental impact and the technological advancement has been carried out.

Refrigeration: a necessity to mankind

A brief history of refrigeration

Refrigeration is a process which consists on cooling or maintaining a space, a substance and a product at temperature below the surrounding

environment. Since ancient time, people used different techniques in order to preserve perishable food. As an example the Pompeian were used to preserve food by using herbs and species. However, when people realized that foods is preserved better in the winter season than in summer, the attention was progressively addressed to ice using or to the evaporative cooling (**Krasner-Khait, 2016**). By this way the ice stared to be transported from cold regions, harvested in ice pills in order to be used in summer season and made during the night by cooling of water (**ASHRAE, 2004**).

Although there are not detailed informations about the beginning of artificial refrigeration technology development, it is generally agreed that the history of artificial refrigeration began in the year 1755 by William Cullen (**IIR, www.iifiir.org**). The professor discovered that by the evaporation of liquid in a vacuum was possible to produce a small quantity of ice. Subsequently an American inventor Oliver Evans in 1805 designed the first refrigerator which was able to produce ice by ether under vacuum (**www.madehow.com**). Finally in 1834, Jacob Perkins, an American working in Great Britain, built the first working vapor-compression refrigeration system in the world (**www.peakmechanical.com**). However 45 years passed before a commercial refrigerator was invented. In 1856 James Harrison developed the first practical vapor compressor refrigerator which was used in order to make ice for selling (**www.madehow.com**). Despite the quickly commercial refrigeration development numerous difficulties in translating this technologies in the domestic sector were found (**IIR, www.iifiir.org**). As an example, commercial refrigerators were far too heavy. In fact some of the commercial storage units being used in 1910 weighted until two hundred tons. Moreover commercial refrigerators were expensive and unsafe due to the leak of toxic gasses. For those reasons the only technology available for domestic use were the ice boxes (**IIR, www.iifiir.org**). Finally in 1911, the General Electric Company introduced the first domestic refrigerator leading to a wide diffusion of this technology all over the world during the Second World War and becoming available in developing countries also (**Garnett, 2007)**. In conclusion, the technological advancement of refrigeration allowed to break down barriers between food, season and climate offering the opportunity to preserve and cooling foods which are out of season and to meet the global food demand.

Refrigeration in the modern society

Nowadays refrigeration is everywhere and progressively changed the lifestyle of the society in different ways (**Çengel and Ghajar, 2010**). It is present in the health sector, where it is mainly used for preserving pharmaceutical products, vaccines and foods (**IIR, 2002**). As an example, the role of refrigeration was found crucial in the eradication of poliomyelitis worldwide and in the

transfusion blood but also organs preservation (**IIR, 2015**). Refrigeration can be also found in the building sector in order to provide cooling and dehumidification during summer season and in hot areas for personal comfort (**IIR, 2002**). Some studies highlighted that a high quality of indoor air has a significant influence on the productivity of both office workers and students in schools. Refrigeration is also used in the manufacturing industries such as petrochemical refining, refineries, chemical plants, nuclear fusion and so on (**IIR, 2015**).

Finally, refrigeration is particularly present in the food industry where almost 90% of the sector depends on refrigeration and more than a billion domestic refrigerators are used in the world. Specifically, refrigeration is a crucial task in food preservation due to the ability of inhibits bacteria and pathogens grow, preventing therefore the occurrence of foodborne diseases (**Garnett, 2007**). As an example the Food and Agriculture Organization (FAO) of the United Nations in conjunction with the World Health Organization (WHO) estimated that the consumption of food containing harmful pathogens, causes more than 200 diseases, ranging from diarrhea to cancer (**IIR, 2015**). Actually, there are many different foodstuffs such as fruits, vegetable, meet, fish and dairy products liable on temperature abuse. In this regard refrigeration have an essential role on reducing the post-harvest losses which account 30% of perishable food total production (**IIR, 2009**). Moreover the food system globalization led to an increase of volume and variety of refrigerated food traded globally. As an example, the trade in fruits and vegetable products is the most dynamic areas of international agricultural trade. **Legge et al.** (**2006**) estimated that annually over 73 million tons of fruits and vegetables are traded globally. As an example, according to an estimation made by **Wangler** (**2006**), the 40% of all fresh fruits and vegetables imported into the European Union derive from sub-Saharan Africa becoming a source of revenue for exporting countries. Finally, according to the Food and Agriculture Organization (FAO) of the United Nations there are 1 billion people who are chronically undernourished and that about a quarter of food is wasted in the developing world (**FAO, 2011**). In that way, refrigeration is actually considered a valid way for the reduction of hunger in the world (**IIR, 2009**). Therefore faced with the economic and population growth of the emerging countries, refrigeration is called to develop in a sustainable manner. It must face two main problems: ensuring high food quality to the whole world population and reducing the energy consumption and its impact on the environment.

Refrigeration and cold chain: global health and environmental issues

Ensuring both food quality and safety to the global population through the cold chain is the major challenge for the refrigeration sector (**IIR, 2009**). Providing

healthy and quality food products to the consumer means that a constant temperature throughout the entire cold chain (i.e. temperature controlled supply-chain) have to be maintained. In this context falling to keep product at the correct temperature can result in a reduced shelf-life or a deterioration of food quality (**IIR, 2015**). The latter may produce a large increase of food borne diseases becoming therefore a major public health issue in many countries. As an example FAO indicated that annually there are 1.5 billion cases of diarrhea in children under 5 years of age where the 70% of these cases are determined by insufficient food safety and hygiene (**IIR, 2002**). For those reasons the temperature control needs to be ensured at all stages of the cold chain avoiding therefore foodborne diseases even in developed countries. Currently the authorities are now requiring measures aimed at encouraging and assisting developed and developing countries in implementing efficient food control procedures. In fact, in accordance to **Coulomb** (**2008**) stringent regulations and standards are now being applied to food industry, storage operators and retailers. Only in this way will be possible to maintain the quality and safety of food throughout the cold chain system.

On the other hand refrigeration impact on the environment is huge. Around 20% of the global-warming impact of refrigeration systems are due to the leakage of fluorocarbons (direct emissions, **IIR 2002**), while the remaining 80% are due to energy consumption of refrigeration equipment (indirect emissions, **IIR 2000**). Therefore with the aim of contrasting global warming two main strategies such as, the reduction of both refrigerant emissions and energy consumption, should be adopted. Refrigerant gasses such as chlorofluorocarbons (CFCs) and the hydrochlorofluorocarbons (HCFCs) have been widely used as heat exchange gasses in different refrigeration equipment such as refrigerators, freezers and air conditioning systems. Although they have been considered highly efficient refrigerants, their leakage into the atmosphere (in which they are highly stable) damaged the ozone layer, contributing to global warming significantly **(James and James, 2010)**. As an example, according to **March Consulting Group (1998**) the 20% of refrigeration plant's global warming impact is due to the refrigerant leakage into the atmosphere **(James and James, 2010)**. Moreover the retail sector, which includes supermarkets, is considered one of the main fluorinated greenhouse gasses (F-gases) user. **James and James (2010)** reported that in the United Kingdom, the leakage of refrigerants from retail refrigeration system was responsible for about 1740.000 tons of CO_2 in the atmosphere in 2005. Moreover, **Gschrey et al. (2011)** estimated that fluorinated greenhouse gasses will contribute to increase until 7.9 %, the projected CO_2 global emissions in 2050. However, in order to reduce the refrigerants global warming impact, the Montreal Protocol is devoted to phase out all the refrigerant used in the refrigeration sector (**IPCC, TEAP**). Specifically CFCs have been banned in the developed countries and will need to be decommissioned by 2010 in developing countries. Although HCFCs

have a less impact on ozone depletion and global warming, the increasingly pressing regulations are requiring to ban those refrigerant gasses in 2030 (**Coulomb, 2008**). Moreover the Montreal Protocol pointed out the necessity of substituting those Ozone Depleting Substance (ODSs) with others characterized by a lower (hydrofluorocarbons, HFCs) or a negligible (natural refrigerants such as ammonia, CO_2, hydrocarbons, water, and air) global warming potential impact (**IIR, 2002**).

On the other hand according to **Mattarolo (1990)**, the 15% of the electricity consumed worldwide is used for refrigeration (**Coulomb, 2008**) and the cold-chain accounts for approximately 2.5 % of CO_2 emission in the world **(Evans et al., 2014; Guilpart, 2008)**. As an example in France, household refrigerators consumed about 26% of residential electricity and they are estimated to be responsible for 17% of greenhouse gases emission in the country **(Azzouz et al., 2009)**. **Tassou et al. (2011)** estimated that supermarkets are responsible for around 3% of the total electrical energy consumption and 1% of the total GHG emissions in the United Kingdom. Moreover transport of food, accounted for 10 million tons of carbon dioxide in the UK in 2002 (**James and James, 2010**). Finally, regarding the refrigerated transport in the United States, trucks consumed 65% of the total energy by freight transportation in 2005 **(Ahmed et al., 2010)**. Worldwide it is estimated that there are 18 000 hypermarkets, 322 000 supermarkets (that use more than 30 million display cabinets), 1 million temperature controlled transport vehicles and 1 billion household refrigerators **(Billiard, 2005)**. Therefore, considering the rate of global population and economic growth an increase in energy consumption and joined CO_2 emissions is also expected in the near future. In this context, energy efficiency is increasingly of concern to the food industry mainly due to substantially increased energy costs and pressure from the European Union to operate zero carbon system. As an example, the FRISBEE (Food Refrigeration Innovations for Safety, consumers' Benefit, Environmental impact and Energy optimization along the cold chain in Europe) European project aims to assess solutions for improving refrigeration technologies efficiency throughout the food cold chain **(www.frisbee-project.eu)**. Within the framework of the European Union FP7 project, software for optimizing quality of refrigerated food, energy use and the global warming impact of refrigeration technologies has been developed **(Gwanpua et al., 2015)**.

Refrigeration technical developments

Nowadays most of refrigeration technologies are based on standard vapor compression refrigeration system which consists in a circuit composed by a compressor, a condenser, an expansion valve and an evaporator. Although global warming is partially determined by refrigerant gasses leakage into the atmosphere,

the carbon dioxide produced as a result of energy consumption to run the refrigerator, represents the most affecting area (**IIR, 2003**). For this reason in past decades many researches focused on improving the energy efficiency of refrigerating system components **(Marques el al., 2014)**. Specifically most of technical developments lie in three main categories: 1) *The enhancement of heat transfer from heat exchangers, such as condenser and evaporator* (**IIR, 2003**). As an example it was found that the enlargement of the evaporator or condenser area by 50% can reduce the energy consumption by 10% and 6% respectively (**DKV, 1985**). 2) *Moreover, making modifications to the compressor is considered one of the most effective way to improve the performance of refrigeration unit.* By this way, electronically regulated variable-speed compressors are now being developed (**IIR, 2003**). The main advantages of this technology can be found in a continuous control, lower noise generator and a reduction of power consumption of about 30% (**Binneberg et al., 2002**). 3) *Finally, the improvement of thermal insulation of system walls* is considered a valid way to help the compartment to remain cold and to reduce the energy consumption of refrigerating unit as well (**Joybari et al. 2015**). Moreover, by using vacuum insulation panels (VIPs) the heat transfer resistant can reduced about 4 times more than a polyurethane board of equal thickness (**Joybari et al. 2015**). On the other hand Thermal Energy Storage (TES) and the use of Phase Change Materials (PCMs) may become a further approach aimed at achieving energy saving and CO_2 emission reduction in the refrigeration technology **(Orò et al., 2014; Orò et al., 2013)**.

Thermal Energy Storage

Thermal energy storage plays an important role in heat management and during last decade has received a great deal of attention, getting used in different applications. As an example, TES in buildings has the potential to decrease the energy demand or peak loads for both heating and cooling. Moreover, in the textile and clothing sector TES can provide an enhanced thermal comfort **(Sarier and Onder, 2007)**. In a recent study **Oró et al. (2014)** developed a model to assess the potential effect on the reduction in energy consumption and related CO_2 emissions by using thermal energy storage as a cold production system (Spanish and European Context). They estimated that in Europe the energy and environmental benefits due to a thermal energy storage system in the “cold road transport” sector could be between 3-40%. In this context TES can be considered the most effective way to reduce energy consumption and related CO_2 emissions becoming one of the most research topic. Overall, there are three main physical ways for thermal energy storage: Thermo-Chemical Reactions (TCR), Sensible Heat (SHS) and Latent Heat (LHS).

Chemical reactions

Thermo-chemical reactions can provide a high thermal energy storage capacity. The basic principle is the following (**Sharma et al., 2009**):

$$AB + \text{heat} \rightarrow A+B \qquad \text{endothermic reaction}$$
$$A+B \rightarrow AB + \text{heat} \qquad \text{exothermic reaction}$$

Firstly, during the endothermic reaction (charging period) the compound AB is broken into components A and B which can be stored separately. Secondly, bringing A and B together, AB is formed and heat is released (exothermic reaction). Thermo chemical Storage (TCS) based on chemical reactions has much higher thermal capacity than sensible heat being considered one of the main way to store thermal energy.

Sensible heat

Sensible heat storage (SHS) energy is based on the changes in temperature of a liquid or solid storage material during the process of charging and discharging. The amount of the stored energy depends on both the specific heat and amount of storage material. The sensible heat which can be stored in a material can be expressed as follow (**Sharma et al., 2009**):

$$Q = \int_{T1}^{T2} m \cdot Cp \cdot dT = m \cdot Cp \cdot (T2 - T1)$$

where Cp is the specific heat of the storage medium material and dT is the temperature change. Storage based on sensible heat is relatively inexpensive if compared to the chemical and latent storage system. Anyway it requires large amount of storage medium due to its low energy density.

Latent heat

Due to its high storage density and small temperature variation, the latent heat storage (LHS) is considered the most attractive way to store energy. In this context, heat storage materials are attractive compounds due to the ability of providing high energy storage density per unit mass and buffering effect against temperature changes. Phase Change Materials (PCMs) owing to their ability of absorbing and releasing large amount of energy during phase transition (solid to liquid or liquid to gas) are considered as subgroup of heat storage materials. The stored heat in a PCM medium can be calculated as follow (**Sharma et al., 2009**):

$$Q = \int_{T1}^{TPC} m \cdot Cp \cdot dT + m \cdot a_m \cdot \Delta h_m + \int_{TPC}^{T2} m \cdot Cp \cdot dT$$

where T_1 is the initial temperature, T_{PC} is the phase change temperature, T_2 is the final temperature, m (kg) is the mass of heat storage medium (kg), Cp (kJ/kg °C) is the specific heat (kJ/kg °C), a_m is the fraction melted and, Δh_m is the heat of fusion per unit mass (kJ/kg).

Phase Change Materials

PCMs are "latent" heat storage materials which use the chemical bonds to store and release a large amount of energy at an almost constant temperature. Multiple type of PCMs exist. The main classification (**Zhou et al., 2012**) consists on the differentiation between organic PCMs, inorganic PCMs and eutectic PCMs (Fig. 1).

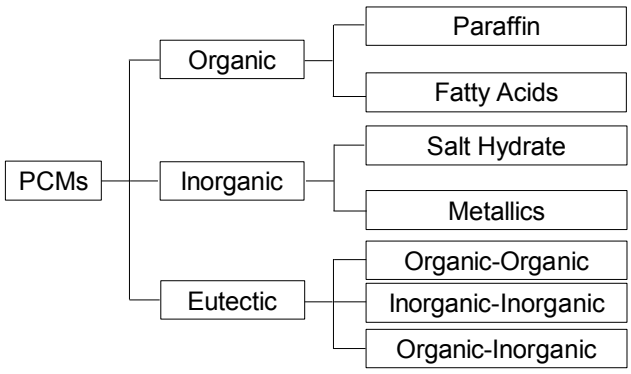

Figure 1: Phase Change Materials (PCMs) classification

Specifically, the organic PCMs include paraffin and fatty acids. Paraffin consists of an n-alkanes chain CH_3–(CH_2)–CH_3. The longer is the chain, the higher is the melting point and the latent heat value. Paraffin are chemically stable and inert below 500 °C. Moreover they are safe, less-expensive and non-corrosive. The fatty acids (CH_3 $(CH2)_{2n}$·COOH) have a latent heat of fusion which is similar to the paraffin. Moreover they are characterized by a capacity to complete melting and solidification cycles preserving capability of accumulating and releasing heat.

The inorganic PCMs are classified as salt hydrate and metallic. The general formula describing the salt hydrate is given by M nH2O, where M is an inorganic compound. It is well known that salt hydrate are characterized by a high latent heat of fusion and high density value. Moreover, their cost is lower than paraffin. The

metallic category includes the low melting metals and metal eutectic with a high thermal conductivity. Due to their weight, this type of PCMs are not being widely used. Finally the eutectic compound is a mixture of two or more components. Therefore it is possible to modify the material properties such as the melting temperature.

References

Ahmed, M., Meade, O., Medina, M.A., 2010. Reducing heat transfer across the insulated walls of refrigerated truck trailers by the application of phase change materials. Energ. Convers. Manage. 51(3), 383–392.

ASHRAE, 2004. A History of refrigeration. By George C and Briley, P.E. Fellow life member of ASHRAE.

Azzouz, K., Leducq, D., Gobin D., 2009. Enhancing the performance of household refrigerators with latent heat storage: An experimental investigation. Int. J. Refrig. 32(7), 1634 –1644.

Bernstein, L., Roy, J., Delhotal, K.C., Harnisch, J., Matsuhashi, R., Price, L., Tanaka, K., Worrell, E., Yamba, F., Fengqi, Z., 2007: Industry. In Climate Change 2007: Mitigation. Contribution of Working Group III to the Fourth Assessment Report of the Intergovernmental Panel on Climate Change [Metz, B., Davidson, O.R., Bosch, P.R., Dave, R., Meyer, L.A (eds)], Cambridge University Press, Cambridge, United Kingdom and New York, NY, USA.

Billiard, F., 2005. Refrigerating equipment, energy efficiency and refrigerants. Bulletin of the IIR.

Binneberg, P., Kraus, E., Quack, H., 2002. Reduction in power consumption of household refrigerators by using variable speed compressors. In: Int. Refrigeration and Air Conditioning Conference, Paper 615.

Bruckner, T., Bashmakov, I.A., Mulugetta, Y., Chum, H., de la Vega Navarro, A., Edmonds, J., Faaij, A., Fungtammasan, B., Garg, A., Hertwich, E., Honnery, D., Infield, D., Kainuma, M., Khennas, S., Kim, S., Nimir, H.B., Riahi, K., Strachan, N., Wiser, R., and X. Zhang, 2014: Energy Systems. In: Climate Change 2014: Mitigation of Climate Change. Contribution of Working Group III to the Fifth Assessment Report of the Intergovernmental Panel on Climate Change [Edenhofer, O., Pichs-Madruga, R., Sokona, Y., Farahani, E., Kadner, S., Seyboth, K., Adler, A., Baum, I., Brunner, S., Eickemeier, P., Kriemann, B., Savolainen, J., Schlömer, S., von Stechow, C., Zwickel, T., and Minx J.C. (eds.)]. Cambridge University Press, Cambridge, United Kingdom and New York, NY, USA.

Çengel, Y.A., Ghajar, A. 2010. Heat and mass transfer: Fondamental & Applications - McGraw-Hill Editor, 4 edition Chapter17 - Refrigeration and freezing of foods.

Change 2007: Mitigation. Contribution of Working Group III to the Fourth Assessment Report of the Intergovernmental Panel on Climate Change [Metz, B., Davidson, O.R., Bosch, P.R., Dave, R., Meyer L.A. (eds)], Cambridge University Press, Cambridge, United Kingdom and New York, NY, USA.

Coulomb, D., 2008. Refrigeration and cold chain serving the global food industry and creating a better future: two key IIR challenges for improved health and environment. Trends Food Sci Tech 19(8), 413–417.

DKV, 1985. M€oglichkeiten der Energieeinsparung bei Haushaltsku¨ hl- und Gefrierger€aten (Opportunities of Energy Savings for Household Refrigerators and Freezers).Statusbericht 1, second ed. Deutscher K€alte- und

Evans, J. A., Hammond, E.C., Gigiel, A.J., Fostera, A.M., Reinholdt, L., Fikiin, K., Zilio, C., 2014. Assessment of methods to reduce the energy consumption of food cold stores, Appl. Thermal Eng. 62, 697–705.

Flato, G., Marotzke, J., Abiodun, B., Braconnot, P., Chou, S.C., Collins, W., Cox, P., Driouech, F., Emori, S., Eyring, V., Forest, C., Gleckler, P., Guilyardi, E., Jakob, C., Kattsov, V., Reason, C., and M. Rummukainen, 2013: Evaluation of climate models. In Climate Change 2013: The Physical Science Basis. Contribution of Working Group I to the Fifth Assessment Report of the Intergovernmental Panel on Climate Change. T.F. Stocker, D. Qin, G.-K. Plattner, M. Tignor, S.K. Allen, J. Doschung, A. Nauels, Y. Xia, V. Bex, and P.M. Midgley, Eds. Cambridge University Press, 741-882.

FAO, 2011. Energy-Smart Food for people and climate, Issue Paper. Food and agriculture organization of the United Nations.

Garnett, T. Food Climate Research Network Centre for Environmental Strategy University of Surrey Food refrigeration: what is the contribution to greenhouse gas emissions and how might emissions be reduced? A working paper produced as part of the Food Climate Research Network April 2007.

Gschrey, B., Schwarz, W., Elsner, C., Engelhardt, R., 2011. High increase of global F-gas emissions until 2050. Greenh. GasMeas. Manag. 1, 85–92.

Guilpart, J., 2008. Froid et alimentation: Sécurité, sûreté ou procédé, Conférence Centenaire du froid, Paris.

Gwanpua, S.G., Verboven, P., Leducq, D., Brown, T., Verlinden, B.E., Bekele, E., Aregawi, W., Evans, J., Foster, A., Duret, S., Hoang, H.M., Van der Sluis, S., Wissink, E., Hendriksen, L.J.A.M., Taoukis, P., Gogou, E., Stahl, V., El Jabri, M., Le Page, J.F., Claussen, I., Indergård, E., Nicolai, B.M., Alvarez, G., Geeraerd, A.H., 2015. The FRISBEE tool, a software for optimising the trade-off between food quality, energy use, and global warming impact of cold chains.

IIR, 2000: Statement by the IIR. Sixth Session of the Conference of the Parties to the United Nations Framework Convention on Climate Change. The Hague. The Netherlands. November 20, 2000.

IIR, 2002: The Word Summit Sustainable Development Report on Refrigeration Sector Achievements and Challenges – IIR – September 2002.

IIR, 2003: 17th Informatory Note on Refrigerating Technologies How to improve energy efficiency in refrigerating equipment.

IIR, 2009: 5th Informatory Note on Refrigeration and Food. The Role of Refrigeration in Worldwide Nutrition.

IIR, 2015: 29th Informatory Note on Refrigeration Technologies. The Role of Refrigeration in the Global Economy.

International Institute of Refrigeration (IIR). A brief history of refrigeration (www.iifiir.org).

IPCC/TEAP Special Report: Safeguarding the Ozone Layer and the Global Climate System.

IPCC, 2007: Climate Change 2007: Impacts, Adaptation and Vulnerability. Contribution of Working Group II to the Fourth Assessment Report of the Intergovernmental Panel on Climate Change, M.L. Parry, O.F. Canziani, J.P. Palutikof, P.J. van der Linden and C.E. Hanson, Eds., Cambridge University Press, Cambridge, UK, 976pp.

IPCC, 2011: Summary for Policymakers. In: IPCC Special Report on Renewable Energy Sources and Climate Change Mitigation [O. Edenhofer, R. Pichs-Madruga, Y. Sokona, K. Seyboth, P. Matschoss, S. Kadner, T. Zwickel, P. Eickemeier, G. Hansen, S. Schlömer, C. von Stechow (eds)], Cambridge University Press, Cambridge, United Kingdom and New York, NY, USA.

IPCC, 2013: Summary for Policymakers. In: Climate Change 2013: The Physical Science Basis. Contribution ofWorking Group I to the Fifth Assessment Report of the Intergovernmental Panel on Climate Change [Stocker,T.F., D. Qin, G.-K. Plattner, M. Tignor, S.K. Allen, J. Boschung, A. Nauels, Y. Xia, V. Bex and P.M. Midgley (eds.)]. Cambridge University Press, Cambridge, United Kingdom and New York, NY, USA.

IPCC, 2014: Climate Change 2014: Mitigation of Climate Change. Contribution of Working Group III to the Fifth AssessmenT Report of the Intergovernmental Panel on Climate Change [Edenhofer, O., R. Pichs-Madruga, Y. Sokona, E. Farahani, S. Kadner, K.Seyboth, A. Adler, I. Baum, S. Brunner, P. Eickemeier, B. Kriemann, J. Savolainen, S. Schlömer, C. von Stechow, T. Zwickel and J.C. Minx (eds.)]. Cambridge University Press, Cambridge, United Kingdom and New York, NY, USA.

James, S.J., James, C., 2010. The food cold-chain and climate change. Food Res. Int. 43, 1944–1956.

Joybari, M.M., Haghighata, F., Moffat, J., Sra, P., 2015. Heat and cold storage using phase change materials in domestic refrigeration systems: The state-of-the-art review. Energy and Build.106, 111–124.

Kahn Ribeiro, S., S. Kobayashi, M. Beuthe, J. Gasca, D. Greene, D. S. Lee, Y. Muromachi, P. J. Newton, S. Plotkin, D. Sperling, R. Wit, P. J. Zhou, 2007: Transport and its infrastructure. In Climate Change 2007: Mitigation. Contribution of Working Group III to the Fourth Assessment Report of the Intergovernmental Panel on Climate Change [B. Metz, O.R. Davidson, P.R. Bosch, R. Dave, L.A. Meyer (eds)], Cambridge University Press, Cambridge, United Kingdom and New York, NY, USA.

Krasner-Khait, B. 2016. The impact of refrigeration. History Magazione.

Legge, A., Orchard, J., Graffham, A., Greenhalgh, P., Kleih, U., 2006. The production of fresh produce in Africa for export to the United Kingdom: mapping different value chains. Natural Resources Institute. Funded by the United Kingdom Department for International Development.

Levine, M., D. Ürge-Vorsatz, K. Blok, L. Geng, D. Harvey, S. Lang, G. Levermore, A. Mongameli Mehlwana, S. Mirasgedis, A. Novikova, J. Rilling, H. Yoshino, 2007: Residential and commercial buildings. In Climate Change 2007: Mitigation. Contribution of Working Group III to the Fourth Assessment Report of the Intergovernmental Panel on Climate Change [B. Metz, O.R. Davidson, P.R. Bosch, R. Dave, L.A. Meyer (eds)], Cambridge University Press, Cambridge, United Kingdom and New York, NY, USA.

Marques, A.C., Davies, G.F., Maidment, G.G., Evans, J.A., Wood, I.D., 2014. Novel design and performance enhancement of domestic refrigerators with thermal storage. App. Therm. Eng. 63 (2), 511–519. J. Food Eng.148, 2–12.

Mattarolo, L., 1990. Refrigeration and food processing to ensure the nutrition of the growing world population. Progress in the science and technology of refrigeration in

food engineering. Proceedings of meetings of commissions B2, C2, D1, D2-D3. Dresden, Germany. Paris, France: IIF (43–54).
Oro´, E., Miro´, L., Farid, M.M., Martin, V., Cabeza, L.F., 2014. Energy management and CO2 mitigation using phase change materials (PCM) for thermal energy storage (TES) in cold storage and transport. Int. J. Refrigeration 42, 26–
Oro´, E., Barreneche, C., Farid, M.M., Cabeza, L.F., 2013. Experimental study on the selection of phase change materials for low temperature applications. Renew. Energy 57, 130–136. 35.
Sarier, N., Onder, E., 2007. Thermal characteristics of polyurethane foams incorporated with phase change materials. Thermochim. Acta. 454, 90–98.
Sharma, A., Tyagi, V.V., Chen, C.R., Buddhi, D. 2009: Review on thermal energy storage with phase change materials and applications. Renew Sust Energ Rev 13 (2009) 318–345.
Sims, R.E.H., R.N. Schock, A. Adegbululgbe, J. Fenhann, I. Konstantinaviciute, W. Moomaw, H.B. Nimir, B. Schlamadinger, J. Torres-Martínez, C. Turner, Y. Uchiyama, S.J.V. Vuori, N. Wamukonya, X. Zhang, 2007: Energy supply. In Climate Change 2007: Mitigation. Contribution of Working Group III to the Fourth Assessment Report of the Intergovernmental Panel on Climate Change [B. Metz, O.R. Davidson, P.R. Bosch, R. Dave, L.A. Meyer (eds)], Cambridge University Press, Cambridge, United Kingdom and New York, NY, USA.
Smith P., M. Bustamante, H. Ahammad, H. Clark, H. Dong, E. A. Elsiddig, H. Haberl, R. Harper, J. House, M. Jafari, O. Masera, C. Mbow, N. H. Ravindranath, C. W. Rice, C. Robledo Abad, A. Romanovskaya, F. Sperling, and F. Tubiello, 2014: Agriculture, Forestry and Other Land Use (AFOLU). In: Climate Change 2014: Mitigation of Climate Change. Contribution of Working Group III to the Fifth Assessment Report of the Intergovernmental Panel on Climate Change [Edenhofer, O., R. Pichs-Madruga, Y. Sokona, E. Farahani, S. Kadner, K. Seyboth, A. Adler, I. Baum, S. Brunner, P. Eickemeier, B. Kriemann, J. Savolainen, S. Schlömer, C. von Stechow, T. Zwickel and J.C. Minx (eds.)]. Cambridge University Press, Cambridge, United Kingdom and New York, NY, USA.
Tassou, S.A., Ge, Y., Hadawey, A., Mariott, D., 2011. Energy consumption and conservation in food retailing. App. Therm. Eng. 31 (2-3), 147–156.
Wangler, Z. L., 2006. Sub-Saharan African horticultural exports to the UK and climate change: a literature review. Fresh Insights No.2, IIED. Funded by the UK Department for International Development.
www.peakmechanical.ca: history of refrigeration.
www.madehow.com: Refrigerator
Zhou, D., Zhao, C.Y., Tian, Y., 2012. Review on thermal energy storage with phase change materials (PCMs) in building applications. App. Energy 92, 593–605.

1. State of the art

1.1 PCMs application over refrigerated storage and transport systems

In the past decades PCMs have been widely used in the building sector. Specifically, a large number of studies have demonstrated that the addition of PCMs to the building envelope allows the thermal load to be reduced in warm climatic contexts especially during the summer season **(de Grassi et al., 2006; Carbonari et al., 2006; de Gracia et al., 2013; Evola et al., 2013)**. Moreover PCMs have been widely used in small containers **(Orò et al., 2013; Laguerre et al., 2008)** in order to stabilize the internal temperature during short journeys of perishable goods such as food, blood or medicines. In the last years, many researchers investigated PCM addition for different cold storage and transportation systems with the aim to increase their energy efficiency. Therefore, a number of case studies literature presented have been examined.

1.1.1 Refrigerated truck

Tassou et al. (2009) revised different technologies aimed at reducing the refrigerated food transport environmental impact. Specifically, hollow tubes, beams or plates can be filled with a eutectic solution (PCM) aimed at storing energy and producing the cooling effect necessary to maintain the refrigerated compartment at the desired thermal conditions. In the same study PCMs are charged during the night or before starting the journey, and discharged during transportation, thereby limiting the activation of the refrigeration system. In their study **Simard and Lacroix (2003)** validated a numerical model for simulating thermal behaviour of a parallel plates (filled with an aqueous-glycol mixture) operating in a typical refrigerated truck. The results highlighted that the latent cold storage unit helped to maintain the refrigerated compartment internal temperature below –8.15 °C for 8 hours. **Liu et al. (2012)** developed an advanced cooling system incorporating a PCM with the aim to keep refrigerated vans at the required thermal conditions during their journey. The special feature characterizing the proposed technology is that the van does not have the cooling system on- board. In fact the phase change thermal storage unit, charged by a refrigeration unit located off the vehicle, provides cooling when the truck is in service. In this way, a reduced energy consumption and lower greenhouse gas emission can be achieved. Following the promising thermal results obtained in lowering and shifting the peak heat load across building walls **(Medina et al., 2008; Zhang et al., 2005; Sun et al., 2014; Dubovsky et al., 2014; Thiele et al., 2015)** and roofs **(Li et al., 2015)** to off peak electricity demand, there has been a developing attention in the addition of PCMs in standard vehicle walls.

Ahmed et al. (2010) proposed a novel method for reducing heat transmission through the envelope of a refrigerated truck trailer by adding PCMs. This technology, based on the inclusion of copper pipes containing paraffin in standard vehicle walls, allowed an average daily heat flow reduction inside the refrigerated compartment equal to 16.3%. Moreover, for individual walls the peak heat transfer rate reduction was found to range between 11.3% - 43.8%. **Tinti et al. (2014)** analyzed the possibility to incorporate a microencapsulated phase change material (melting point 6 °C) into standard polyurethane foam designed for thermal insulation in refrigerated transport. This technology would be very useful in contrasting all events in which a temperature transient occurs, such as a temporary blackout of the refrigeration system, the frequent opening/closing of the compartment doors, the varying solar irradiation during the day and the vehicle journey. **Glouannec et al. (2014)** presented a numerical and experimental investigation of three different configuration walls of a refrigerated van. The reference wall thermal behavior was compared, in turn, with two different multilayer insulation walls containing: a first case with reflective multi-foil insulation and aero gel while a second case with the insertion of PCM (microencapsulated paraffin). Compared to the reference wall the authors found that for the RMS-aero gel wall, the heat flux density peak and the energy consumption were decreased by 27% and 36% respectively. Although during eight hours test a complete material melting and freezing was not reach, good results were obtained by increasing the wall thermal inertia using a PCM layer. Globally, during the daytime period, the energy consumption decreased by 25 % compared with the reference wall.

1.1.2 Household and freezer refrigerators

In a recent study, **Yuan and Cheng (2014)** proposed a novel multi-objective optimization method, with the aim to minimize the total cost and energy consumption of an ordinary household refrigerator. This novel method, which combines refrigerator dynamic model and Genetic algorithm NSGA-II, leads to an overall performance optimization of both novel and reference household refrigerators. However, by comparing the main optimization findings obtained for the ordinary and novel household refrigerators, the authors stated large energy and cost saving in the PCM added system. **Azzouz et al. (2005, 2008, and 2009)** studied the inclusion of a thick PCM slab on the back of a household refrigerator evaporator both numerically and experimentally with the aim to improve its energy efficiency and to keep the refrigeration system at constant temperature during power failure. Encouraging results were obtained by the authors. In fact, the PCM integration allows 5–9 h of continuous operation without the electrical supply and a 10–30% increase in the coefficient of performance.

Yusufoglu et al. (2015), presented a new household refrigerator incorporating phase change materials on the evaporator tubes in order to improve energy saving. In this study, four different PCMs have been tested in two different refrigerator prototypes. In addition, a new PCM packaging system has been developed in order to have a good thermal contact with the evaporator tubes. As a results the compressors on/off cycle times were optimized and reduced energy consumption achieved. Considering the first refrigerator prototype (1.8 kg of distilled water placed in slab-like container) the achieved energy saving was equal to 8.8%. On the other hand, a higher energy saving (9.4%) was reached in the second refrigerator prototype by using only 0.950 kg of PCM (melting temperature of -5.6 °C) placed in very thin metallic film packages. **Cheng et al. (2011)** adopted a shape-stabilized phase change materials to construct a heat storage condenser in order to improve the overall heat-transfer performances of household refrigerator's condenser. Specifically 0.5 kg of PCM consisting of paraffin, high-density polyethylene, and expanded graphite was mounted around the condenser tubes. A phase temperature range between 25 °C – 60 °C characterized this type of PCM, matching therefore the condenser temperature. Experimental results showed lower energy consumption for the PCM added system (about 12% energy saving). In addition, thanks to PCM application, a higher evaporator temperature (3 °C) and a higher COP were obtained. Further on, the system was modeled in order to analyze the work characteristics of the novel refrigerator and the effect of some parameters like ambient temperature, freezer set point and phase change temperature on the energy saving (**Cheng and Yuan, 2013**). It was found that increase of the ambient temperature and the decrease of the freezer temperature promotes the energy saving effect (between 20% and 26%). Moreover the amount of energy consumption showed a minimum value at 49 °C, matching the phase change temperature of the SSPCM. These results highlighted the importance of choosing a proper PCM melting point temperature. **Gin et al. (2010)** demonstrated that through the application of PCM panels against the internal walls of a domestic freezer, a reduction in temperature variations in case of heat loads (such as opening of door, defrosting and loss of electrical power) can be achieved. The energy consumption tests showed that the addition of PCM can reduce energy consumption during the defrost cycle and door opening by 8% and 7% respectively.

1.1.3 Commercial freezers and open multi-deck display cabinets

A study of the use of PCM to a commercial freezer was developed by **Orò et al. (2012).** The aim of the study was to improve the thermal conditions inside the refrigerated compartment during door opening and electrical power failure events. To that end a PCM, with a phase change temperature of -18 °C, was encapsulated

inside a 10mm thick of stainless steel and positioned inside the freezer. The experimental tests were conducted considering different time of both door openings and electrical power failure. The results demonstrated that after 3 hour of no electrical power, the PCM can maintain the freezer temperature 4-6 °C lower and allowed the M-pack temperature to stay about 2 °C. In a further study **Orò et al. (2012)** considered the previously described application in order to study the PCM response during a refrigeration system failure. By this way two different PCMs, Climsel C-18 from CLIMATOR and E-21 from CRISTOPIA, were used during the experiments. Due to a melting temperature near to the storage conditions of commercial freezer, the PCM E-21 performed better than the PCM C-18. **Lu et al. (2010)** proposed a novel design of display cabinet's shelf aimed at improving the heat transfer and lowering the food temperature. To that end the cabinet's shelf were implemented with heat pipes and PCM (a mixture of 98% deionized water and 2% borax). The results showed that the heat pipes application resulted in a reduced product temperature variations by between 3 °C and 5 °C. Furthermore by combining the heat pipes with PCM, a reduction in food temperature during the defrost period can be obtained.

Lu and Tassou (2013) realized a deep study devoted to increase the thermal capacity of a food refrigerated cabinet by using different PCMs with a melting temperature range between 0 °C and 5 °C. The authors found that water based PCM with nucleate agents, which can reduce significantly super cooling effect, are suitable for such application. **Alzuwaid et al. (2015)** experimentally investigated the performance of a refrigerated open-type multi-deck display cabinet with integrated phase change material (PCM). A PCM composed by deionised water, 1.2% silver iodide, 0.9% guar and 0.15% sodium tetra borate with a freezing temperature of -2.0 °C was used in this work. Specifically, it was charged in two single panel radiators installed after the cabinet evaporator in order to enhance the system performance and reducing the energy consumption. Moreover the PCM radiator can operate as a cooling coil during the defrost period (when the compressor is switched off) maintaining the cabinet temperature within an acceptable range. Tests were carried out for this cabinet without PCM integration first, then with two single plate radiators containing water gel PCM. The test results showed that by installing PCM radiator the energy saving of the cabinet significantly improved to around 5%. Moreover PCM radiator increased the defrost time, which was 5 min longer than the basic cabinet. The overall effect consisted on a significant reduction of air and products temperature. On the condenser side of the refrigerator system, PCM can extend condenser's heat rejection process to compressor OFF time leading to a lower condensation temperature.

1.1.4 Beverage and food containers

Orò et al. (2013) experimentally and numerically analyzed a chilly bean, incorporating phase change materials, used to store hot and cold beverage and food respectively. Firstly, during the experimentation a PCM, with a phase change temperature of 2-5 °C was used. Secondly, during the numerical modeling PCMs characterized by a phase change temperature of -15 °C and 63 °C were applied to the bin. This choice was made, in order to simulate the storage and transportation of ice cream and coffee respectively. The authors found that by using PCM an increase of transportation time (by 400% and 320%) of ice cream and hot water can be achieved. **Orò et al. (2013)** realized an active phase change material package for the thermal protection of ice cream containers. The used PCM was a E-21 (from CRISTOPIA) with a phase change temperature of -21.3 °C and a latent heat of fusion of 233 (kJ/kg). Moreover, in order to prevent the PCM leaking a thickening agent was added. Regarding the test procedure the ice cream was stored at -28 °C in a freezer and then exposed, for almost three hours, at an external temperature of 25 °C. The results demonstrated the effectiveness of using PCM in the container in terms of ice cream temperature decrease.

Leducq et al. (2015) analyzed the possibility of improving the ice cream long term storage and transportation conditions by using a phase change material packaging system. The impact of temperature fluctuations and ice crystal size distribution on the PCM added system were then compared with the polystyrene packaging configuration. Specifically, the selected PCM was a eutectic solution of water and sodium chloride with a melting temperature of 21 °C. Firstly, the packaging systems containing the ice cream were kept at a constant temperature of -22 °C (140 days) in a horizontal freezer. Secondly, the ice cream boxes were kept at a constant temperature of -23 °C for three days and then exposed to a temperature abuse (20 °C ambient temperature) during 40 minutes. The long term storage results allow to evaluate significant differences, on both ice crystal size distribution and temperature variations, between the two insulated packaging types and the carton board box. The small thickness necessary to have the same buffering effect of the insulated materials, represented the main advantages of using PCM. Finally, regarding the temperature abuse test results the use of both PCM and polystyrene, had a significant impact on reducing the rate of temperature increase of the ice cream. In this case the PCM thermal protection provided the best results, enabling temperature to remain below zero. Finally in a recent study, **Hoang et al. (2015)** developed a numerical model in order to study the heat transfer of a plate, made with encapsulated PCM, for food packaging applications. The selected PCM was the Rubitherm RT5, characterized by a phase change temperature suitable for chilled food. The electro-hydrodynamic process was used for encapsulating the PCM. Specifically, two plates of different PCM mass fraction ((30% for the plate 1

and 38% for the plate 2) were experimentally tested during a cooling and heating process. The obtained results were then used to validate the numerical method. The results demonstrated a better thermal buffering capacity, on product shelf-life, of the encapsulated PCM material compared to a standard one (carton board).

1.2 Research work objective

The aim of this PhD thesis is to assess the effectiveness of PCMs application through different refrigerated storage and transportation systems in terms of CO_2 emission reduction derived by the energy saving amount. It is well known that the refrigerated compartments have to be maintained below the ambient air temperature that represents a driving force for heat flow towards the refrigerated compartment from the external environment. In this regard the total heat gain, which generally affect the refrigerated systems, is determined by the surrounding environment (heat conducted through the insulated envelope), door openings (infiltration load), power failure events and products loading (heat that have to be removed by stored products). These letters in conjunctions with a low efficiency-refrigerating unit, determine the increase of energy consumption. By this way, the PhD thesis purpose is the implementation of thermal energy storage systems by using PCM in a cold room in order to reduce the total heat gain and to improve the energy efficiency of the refrigeration unit. This can be translated into both a lower energy consumption and a reduction in combined greenhouse gas (CO_2) emissions into the atmosphere.

In this regard, during the first PhD research year a technology to improve the thermal performance of reefer container envelopes by using PCM was investigated. In fact, due to external climatic conditions, radiation and warm temperature, refrigerated containers are subjected to high thermal stresses during storage in yards, warehouses, ships or during transport by rail or road. Moreover the consequent high thermal load has a great influence on both the electric and fuel energy consumption and on combined greenhouse gas emissions into the atmosphere. Therefore, the research activity focused on evaluate the thermal effectiveness of a Phase Change Material (PCM) layer application to the external side of a refrigerated container envelope. By this way, numerical and experimental analysis were carried out. The aims of the theoretical analysis are the preliminary investigation of the benefits deriving from this technology under several climatic conditions and the selection of the most suitable PCM, while a methodology to predict the PCM thermal behavior is also suggested. On the other hand, the aims of the experimental analysis were to study the thermal behaviour of a prototype panel inside a climatic test room and to evaluate the behaviour of this technology under defined environmental conditions. For the outdoor experimental campaign, the PCM is added to the all-external surfaces of a real refrigerated cold room and its

thermal behaviour compared with the reference envelope. Furthermore, the outdoor experimental results were compared with numerical modelling results in order to test the accuracy of the numerical model and to validate it. Regarding the refrigerated storage sector, during the second PhD research year a technology to improve the energy efficiency of a cold room, by using a PCM air heat exchanger, was investigated. The growing attention to the global environmental issue and the rising in energy costs are increasingly promoting the necessity of developing sustainable and energy efficient cooling technologies among the refrigerated equipment manufactures. By this way, making changes in refrigeration system and its components such as evaporator, condenser and compressor can increase the efficiency of the refrigeration unit. Therefore, the research activity focused on evaluate the performance of a cold room with an air heat exchanger containing PCM positioned in a channel near the evaporator. By this way an experimental analysis was carried out. The aims of the experimental activities were to reduce cooling energy consumption and temperature variations on steady state operating conditions. Moreover, the PCM air heat exchanger capability of providing several hours of refrigeration without power supply has been analyzed. Lastly, in order to help companies to define and implement the right energy efficiency measures for cold production during transport, a calculation tool has been developed. It is also intended that this methodology determines which parameters such as door opening, external temperature, products respiration rate and duration of journey have a greater influence in energy consumptions. The operator will be able to select the most suitable PCMs in order to obtain a possible energy saving and a higher quality and safety of stored products.

Finally during the third PhD research year, a technology to reduce energy consumption and compartment temperature variations during door openings and power failure by using PCM was investigated. It is well known that the maintenance of suitable conditions during refrigerated cargoes storage, represents a compelling food industry concern mainly due to the relevant economic value behind the entire agricultural and food chain. In fact during transportation or storing, fresh products may undergo temperature fluctuation especially during door openings and electric power blackout. If compared with frozen food, chilled products, which include fruits and vegetables, result to be more liable to temperature abuse. Therefore maintaining the optimum carriage temperature can prevent the problem of the cargo being deemed unfit for consumption. Moreover the heat loads deriving from door openings can be translated in an energy consumption increase. This is due to the necessity by the refrigeration unit, of providing and additional cooling capacity to contrast these types of extra heat loads. Therefore, the research activity focused on evaluate the energy and thermal effectiveness of PCM layer application inside a refrigerated compartment. To that end PCM polyethylene panels were placed against the internal walls of a

refrigerated cold room. By this way, an experimental analysis was carried out. The aims of the experimental investigation were to decrease the peak air temperature and energy consumption during different door openings. Moreover the PCM panels capability of reducing the rate of compartment temperature increase during an electrical power blackout was investigated.

Acknowledgments

The present work was partially developed in collaboration with ENEA (Italian National Agency for New Technologies, Energy and Sustainable Economic Development) during the program agreement with the Economic Development Ministry regarding the Electrical System Research (www.enea.it). The author want to thanks ENEA for the technical and financial support.

References

Ahmed, M., Meade, O., Medina, M.A., 2010. Reducing heat transfer across the insulated walls of refrigerated truck trailers by the application of phase change materials. Energ. Convers. Manage. 51(3), 383–392.

Alzuwaid, F., Ge, Y.T., Tassou, S.A., Raeisi, A., Gowreesunker, L., 2015. The novel use of phase change materials in a refrigerated display cabinet: An experimental investigation. App. Therm. Eng. 75, 770–778.

Azzouz, K., Leducq, D., Guilpart, J., Gobin, D. improving the energy efficiency of a vapor compression system using a phase change material. In: Proceedings 2nd Conference on Phase Change Material & Slurry, Yverdon les Bains, 15 – 17 June 2005 Switzerland.

Azzouz, K., Leducq, D., Gobin, D., 2008. Performance enhancement of a household refrigerator by addition of latent heat storage. Int. J. Refrig. 31, 892–901.

Azzouz, K., Leducq, D., Gobin D., 2009. Enhancing the performance of household refrigerators with latent heat storage: An experimental investigation. Int. J. Refrig. 32(7), 1634 –1644.

Carbonari, A., De Grassi, M., Di Perna, C., Principi, P., 2006. Numerical and experimental analyses of PCM containing sandwich panels for prefabricated walls. Energ Buildings. 38, 472–483.

Cheng, W. L., Mei, B.J., Liu, Y.N., Huang, Y.H., Yuan, X.D., 2011. A novel household refrigerator with shape-stabilized PCM (Phase Change Material) heat storage condensers: An experimental investigation. Energy 36 (10), 5797–5804.

Cheng, W. L., Yuan, X.D., 2013. Numerical analysis of a novel household refrigerator with shape stabilized PCM (phase change material) heat storage condenser. Energy 59, 265–276.

de Gracia, A., Navarro, L., Castell, A., Cabeza, L.F., 2013. Numerical study on the thermal performance of a ventilated facade with PCM. Appl. Thermal Eng. 61, 372–380.

de Grassi, M., Carbonari, A., Palomba, G., 2006. A statistical approach for the evaluation of the thermal behavior of dry assembled PCM containing walls, Build. Environ. 41, 448–485.

Dubovsky, V., Ziskind, G., Letan, R., 2014. Effect of windows on temperature moderation by a phase-change material (PCM) in a structure in winter. Energ. Convers. Manage. 87, 1324-1331.

Evola, G., Marletta, L., Sicurella, F., 2013. A methodology for investigating the effectiveness of PCM wallboards for summer thermal comfort in buildings. Build Environ. 59, 517–527.

Gin, B., Farid, M.M., Bansal, P.K. 2010. Effect of door opening and defrost cycle on a freezer with phase change panels. Energ. Convers. Manage. 51:2698–2706.

Glouannec, P., Michel, B., Delamarre, G., Grohens, Y., 2014. Experimental and numerical study of heat transfer across insulation -+wall of a refrigerated integral panel van. Appl. Therm. Eng. 73, 196–204.

Hoang, H.M., Leducq, D., Perez-Masia, R., Lagaron, J.M., Gogou, E., Taoukis, P., Alvarez G., 2015. Heat transfer study of submicro-encapsulated PCM plate for food packaging application. Int. J. Refrig. 52, 151–1 60.

Laguerre, O., Ben Aissa, M.F., Flick, D., 2008. Methodology of temperature prediction in an insulated container equipped with PCM, Int. J of Refrigeration. 31, 1063–1072.
Leducq, D., NDoye, F.T., Alvarez, G., 2015. Phase change material for the thermal protection of ice cream during storage and transportation. Int. J. Refrig. 52,133–139.
Li D, Zheng Y, Liu C, Wu G., 2015. Numerical analysis on thermal performance of roof contained PCM of a single residential building. Energ. Convers. Manage. 100, 147-156.
Liu, M., Saman, W., Bruno, F., 2012. Development of a novel refrigeration system for refrigerated trucks incorporating phase change material. Appl. Energy. 92, 336-342.
Lu, W., Tassou S.A., 2013. Characterization and experimental investigation of phase change materials for chilled food refrigerated cabinet applications. Appl. Energy 112, 1376–1382.
Lu, Y.L., Zhang, W.H., Yuan, P., Xue, M.D., Qu, Z.G., Tao, W.Q., 2010. Experimental study of heat transfer intensification by using a novel combined shelf in food refrigerated display cabinets (Experimental study of a novel cabinets). Appl. Therm. Eng. 30, 85–91.
March Consulting Group, 1998. Opportunities to minimize emissions of hydrofluorocarbons (HFCs) in the European Union. March Consulting Group.
Medina, M.A., King, J.B., Zhang, M., 2008. On the heat transfer rate reduction of structural insulated panels (SIPs) outfitted with phase change materials (PCMs). Energy. 33, 667–678.
Oro´, E., Miro´, L., Farid, M.M., Cabeza, L.F., 2012. Improving thermal performance of freezers using phase change materials. Int. J. Refrig. 35, 984–991.
Oro´, E., Miro´, L., Farid, M.M., Cabeza, L.F., 2012. Thermal analysis of a low temperature storage unit using phase change materials without refrigeration system. Int. J. Refrig. 35, 1709–1714.
Oró, E., Cabeza, L.F., Farid, M.M., 2013. Experimental and numerical analysis of a chilly bin incorporating phase change material. Appl. Therm. Eng 58, 61–67.
Oro´, E., de Gracia, A., Cabeza, L.F., 2013. Active phase change material package for thermal protection of ice cream containers. . Int. J. Refrig. 36, 102–109.
Oro´, E., Barreneche, C., Farid, M.M., Cabeza, L.F., 2013. Experimental study on the selection of phase change materials for low temperature applications. Renew. Energy 57, 130–136.
Simard, A.P., Lacroix, M., 2003. Study of the thermal behavior of a latent heat cold storage unit operating under frosting conditions. Energ. Convers. Manage. 44, 1605-1624.
Sun, X., Zhang, Q., Medina, M.A., Lee, K.O., 2014. Energy and economic analysis of a building enclosure outfitted with a phase change material board (PCMB) Energ. Convers. Manage. 83, 73-78.
Tassou, S.A., De-Lille, G., Ge, Y.T., 2009. Food transport refrigeration – Approaches to reduce energy consumption and environmental impacts of road transport. Appl. Therm. Eng., 29 1467-1477.
Thiele, A.M., Jamet, A., Sant, G., Pilon, L., 2015. Annual energy analysis of concrete containing phase change materials for building envelopes. Energ. Convers. Manage. 103, 374-386.

Tinti, A., Tarzia, A., Passaro, A., Angiuli, R., 2014. Thermographic analysis of polyurethane foams integrated with phase change materials designed for dynamic thermal insulation in refrigerated transport. Appl.Therm. Eng. 70, 201–210.

Yuan, X.D., Cheng, W.L., 2014. Multi-objective optimization of household refrigerator with novel heat-storage condensers by Genetic algorithm. Energ. Convers. Manage. 84, 550-561.

Yusufoglu, Y., Apaydin, T., Yilmaz, S., Paksoy, H.O., 2015. Improving performance of household refrigerators by incorporating phase change materials. Int. J. Refrigeration 57, 173–18.

Zhang, M., Medina, M.A., King, J.B., 2005. Development of a thermally enhanced frame wall with phase-change materials for on-peak air conditioning demand reduction and energy savings in residential buildings. Int J Energy Res. 29, 795–809.

2. A refrigerated container envelope with a PCM layer: theoretical and experimental investigation

---

This chapter has previously been published in Applied Thermal Engineering (Copertaro et al. 2016), Energy Conversion and Management (Fioretti et al. 2016), IEEE EEEIC Rome 2015 Conference Proceedings (Copertaro et al. 2015). The work was also orally presented at Energy Science and Technology International Conference, Karlsruhe, Germany 2015 (Copertaro et al. 2015). Some paragraphs have been added for the purpose of this dissertation.

2.1 Introduction

The first study concerning the implementation of thermal heat storage on refrigerated transport systems, focalized on the reduction of cooling energy required to break down the heat load deriving from the external environment.

Nowadays, there is a growing consumer demand for chilled or frozen products and refrigerated containers carry many of these products over long distances. In fact, due to the considerable latitudinal extension and complex morphology characterising the Italian peninsula, containers often have to travel for more than 1100 km to reach their destination. Therefore, the total heat load during transport by rail, road and ship using containers is subject to high oscillation due to the changing external climatic conditions. Moreover, especially throughout loading and unloading phases containers undergo different duration power failure. Therefore, depending on the external climatic conditions, the quality of the refrigerated cargo could be affected by the internal operative temperature oscillations caused by the lightweight envelopes. For those reasons, the purpose of this study is to investigate the effect of the addition of a PCM layer to a reefer enclosure, ideally stacked in the container terminal, in order to reduce and shift the cooling load in comparison with a conventional enclosure. The proposed technology was evaluated using a numerical and experimental design study. The calculation results were compared with the experimental values in order to validate the mathematical model, achieving a high reliability.

2.2 Theoretical analysis

2.2.1 Physical model and dynamic thermal simulations

The numerical analysis was carried out using the COMSOL Multiphysics **(www.comsol.it)** software finite element method. To verify the thermal improvement deriving from PCM application to the external envelope, unidirectional and time-dependent simulations were performed (Fig. 2).

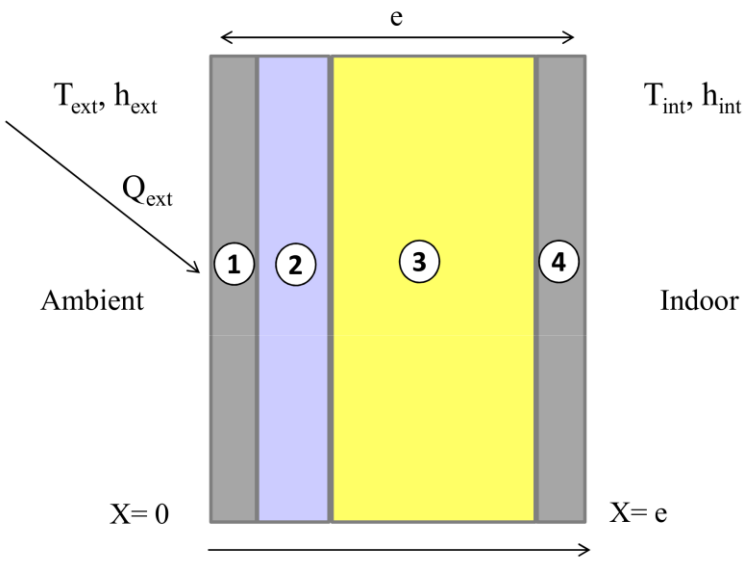

Figure 2: Cross-section of the new composite envelope: (1) steel (0.001 m); (2) PCM (0.03 m); (3) expanded polyurethane (0.10 m); (4) steel (0.001 m)

A 20' ISO **(EN ISO 6346:1995)** refrigerated container with dimensions 6.058m x 2.438m x 2.591m was considered during the numerical analysis. The considered global heat load inside the container takes into account the contribution of the incoming heat flux through the four lateral walls and the ceiling applied, in turn, with nine different phase change materials. In particular, eight kinds of paraffin and one kind of salt hydrate, with a melting temperature ranging between 27.5 °C and 46.5 °C, were used. Moreover, in order to select the most suitable PCM layer thickness, the same numerical study had previously been carried out prior to application and, on the basis of the results obtained, a three-centimetre thick PCM layer was chosen. It is well known **(Joybari et al., 2015)** that a lower PCM thickness and a subsequent lower latent heat of fusion cannot counter the heat

gain through the envelope during critical summer conditions. On the other hand, any increase in the PCM thickness means that not all the thickness can be involved in the phase change process. Therefore, the selected PCM layer thickness was the minimum amount of PCM that was able to absorb the energy passing through the compartment walls under critical summer conditions as latent heat of fusion. During this study, simulations were also performed for different exposures: north (2.428m x 2.591m), south (2.428m x 2.591m), west (6.058m x 2.591m), east (6.058m x 2.591m) and horizontal (6.058m x 2.438m) facing. Moreover, the chosen external conditions (Fig. 3) were related to the extreme weather conditions on a summer day in three different towns, specifically Milan, Ancona and Palermo, located in the North, Center and South of Italy respectively **(UNI 10349).** In total, 150 different combinations were simulated. The program accuracy was tested by calculating reference cases in accordance with **EN ISO 10211-1**, Annex A**.** In addition, the present numerical procedure was previously validated for a different PCM application obtaining a highest error equal to 3.13% **(Principi and Fioretti, 2012).** Therefore, in order to estimate the effective heat capacity of PCM (ceff), due to sensible and latent heat, an equation that calculates the heat capacity as a function of the temperature was developed and implemented in the calculation software **(Darkwa and Callaghan, 2006; Zukowski, 2007; Farid, 1989).** The equation is reported below:

$$c_{eff} = c_s + c_L \cdot e^{-0.5 \cdot \left(\frac{T - T_m}{b}\right)^2}$$

where c_L is the total amount of latent heat and b is a dimensionless parameter which produces the amplitude of the Gaussian curve and hence the width of the phase change zone. The governing equation for the heat transfer process within the panel is the energy equation for conduction, expressed as:

$$\rho \cdot c_{eff} \cdot \left(\frac{\partial T}{\partial t}\right) = \nabla \cdot (\lambda \cdot \nabla T)$$

The energy balance at the external and internal surfaces takes into account the solar energy absorbed, and the energy exchanged with the air and surrounding environment by convective and irradiative heat transfer:

$$-(-\nabla T) = \alpha \cdot I + h \cdot (T_{amb} - T)$$

The boundary conditions used during the numerical analysis are reported in Table 1.

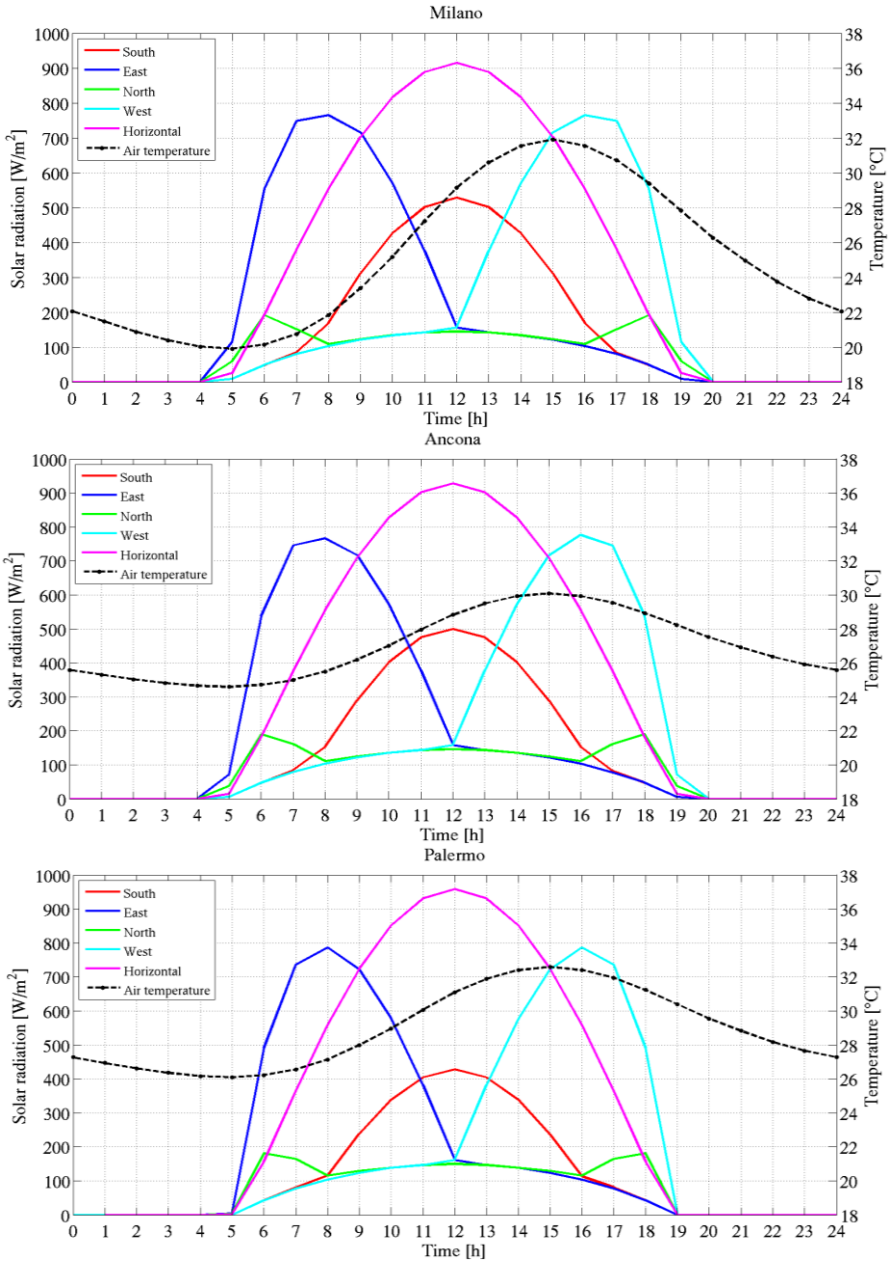

Figure 3: Daily heat load during a typical summer day in Milano, Ancona and Palermo

Table 1: Boundary conditions used for the simulation

	Air Temperature [°C]	Superficial Thermal Resistance (EN ISO 6946) (Çengel and Ghajar, 2010)	Other thermal sources
Internal refrigerated environment	0	0.13 ($m^2 \cdot K$)/W horizontal flow 0.10 ($m^2 \cdot K$)/W climbing flow	–
External environment	External climatic conditions in accordance with **UNI 10349**	0.04 ($m^2 \cdot K$)/W	Solar radiation – External climatic conditions in accordance with **UNI 10349**

The model built in the software is a mesh that consists of 19998 elements and the number of degrees of freedom is 40355. Moreover, in order to rule out any influence of the number or size of the grids on the computational results, a mesh-independent study was performed. Specifically four mesh densities characterized by tetrahedral elements were tested. The mesh-independent study details are listed in Table 2.

Table 2: Mesh-independent study details

Number of elements	Number of degrees of freedom	Average heat flux [W/m^2]	Maximum displacement [%]
1173	2516	9.46930	0.03%
2066	4329	9.46898	0.02%
6084	12423	9.46685	0%
19998	**40355**	**9.46685**	**0%**
84892	170499	9.46685	-

The main assumptions considered for the simulation process are:

- all the thermo physical properties (except the heat capacity of the PCM) were kept constant.
- isotropic conductivity;
- thermal resistance of the voids calculated according to B.3 of EN ISO 6946:1996;
- no mass transfer;
- no convective heat transfer in the liquid PCM phase.
- surface heat resistance is constant, in accordance with EN ISO 6946: 1996, Annex A.

Table 3 shows the thermophysical parameters related to the materials making up the simulated envelope structure. For standard materials, like aluminum, steel and polyurethane foam, standardized parameters **(UNI 10351:1994; UNI 12524:2001)** were used. For PCMs, the thermo physical parameters such as sensible heat (C_s), latent heat of fusion (C_l), width of phase change zone (b) and melting temperature (T_m) were obtained from values measured (through the 3-layer-calorimeter) and declared by the PCM manufacturers **(www.climator.com; www.rubitherm.de)**.

Table 3: Thermophysical properties of materials

Material	Thickness [m]	Melting temperature [°C]	Heat conductibility [W/(m·K)]	Sensible heat [J/(kg·K)]	Latent heat of fusion [J/kg]	Density [kg/m^3]	Width of phase change zone
Steel	0.001	-	50	475	-	7800	-
Expanded polyurethane	0.1	-	0.032	1400	-	40	-
PCM – paraffin RT27	0.03	27.5	0.2	2000	55000	880	0.12
PCM – paraffin RT28HC	0.03	28	0.2	2000	140000	880	0.32
PCM – paraffin RT31	0.03	30.5	0.2	2000	24350	880	0.02
PCM – paraffin RT35	0.03	32.5	0.2	2000	26000	880	0.025
PCM – paraffin RT35HC	0.03	35	0.2	3000	105000	770	0.2
PCM – paraffin RT42	0.03	41	0.2	2000	30000	880	0.037
PCM – paraffin RT44HC	0.03	43	0.2	2000	94500	780	0.135
PCM – paraffin RT47	0.03	45	0.2	2000	20000	880	0.0169
PCM – C48	0.03	46.5	0.6	3600	110000	1360	0.6

2.2.2 Results

In order to assess the increase in envelope thermal inertia obtained with the addition of a PCM layer, two case studies were analyzed. The first investigates the envelope system without PCM, considering the layer of polyurethane foam sandwiched between the two layers of metal sheet (reference case). The second considers the integration, in turn, of different PCMs into the traditional insulated envelope. Fig. 4 reports the daily heat load on the inside of the refrigerated container compared with the composite envelope using different phase change materials during a typical summer day in Milan. The graphs show a reduction and a phase displacement in peak heat load as well as a reduction in overall heat load inside the refrigerated container fitted with different PCMs (area under each curve). Data analysis shows that the heat load of the reference container varies between 282.12 W and 669.37 W with an amplitude, defined by the difference between the maximum and the minimum thermal load value during the day, equal to 387.15 W. In this specific case the peak heat load is reached at 4 PM, one of the most critical times in the day (in terms of high ambient temperature and global solar radiation). On the other hand, for RT27 and RT28HC a shift in peak heat load, of approximately three hours, is also noticeable.

In fact the heat loads peaked at times closer to 8 PM with a reduction, as a result of using PCM, of 17.56%, and 20.93% respectively. As regards RT31, RT35 and RT35HC, a greater reduction in peak heat load is evident (24.56%, 23.57% and 25.01% respectively) as well as a more constant heat load trend during the day if compared with RT27 and RT28HC. In fact, for RT31 the heat load is between 375.88 W and 504.96 W, with an amplitude of 129.08 W. For RT35 and RT35HC the amplitude is estimated to be equal to 159.88 W and 150.53 W respectively. Furthermore it is also worth noting that during the night RT35 and RT35HC release the stored energy, thereby becoming completely solidified three hours earlier (at 8 AM) than RT27, RT28HC and RT31. A different situation can be observed considering RT42, RT44HC, RT47 and C48. The graph shows that the reduction in peak heat load decreases with the increase in the PCM melting temperature. Furthermore a greater heat load amplitude can be observed. In fact, the latter PCMs activate the thermal energy storage later (approximately at 12 PM) than the other phase change materials characterized by lower melting temperature. Specifically, for RT42, RT44HC, RT47 and C48 the peak heat load reduction with respect to the reference, as a result of using PCM, is equal to 18.24%, 18.85%, 16.64% and 13.42% respectively.

Fig. 5, which compares the daily heat load of the reference container with the composite envelope during a typical summer day in Ancona, also shows a significant reduction in both peak heat load and overall heat load inside the refrigerated container fitted with different PCMs. Data analysis shows that the heat

load of the reference container varies between 345.75 W and 646.56 W with an amplitude of 300.81 W. Also in this case the main peak heat load is reached during the most critical part of the day. On the other hand for RT27 and RT28HC the heat loads peaked at around 6 PM with a reduction, with respect to the reference value, of 10.56% and 11.55 % respectively. RT31, RT35 and RT35HC also show a higher reduction in peak heat load (17.94%, 19.44% and 20.01% respectively) as well as a more constant heat load trend during the day if compared with RT27 and RT28HC. Furthermore it is also worth noting that during the night RT35HC, releases the latent heat, becoming completely solidified two hours earlier than the PCMs characterized by lower melting temperatures. As far as RT42, RT44HC, RT47 and C48 are concerned, a different situation can be observed. In fact the graph shows that the reduction and the phase displacement in peak heat load decrease with the increase in PCM melting temperature. For RT42, the heat load ranges from a minimum value of 339.38 W to a maximum of 550.70 W with an amplitude of 211.32 W. In this case the peak heat load reduction, with respect to the reference container, is approximately 14.82%. Considering RT44HC, the peak heat load is 556.00 W and occurs at 4PM, 2 hours earlier than PCMs characterized by a lower melting temperature (ranging between 27.5 °C and 41 °C). A similar thermal behavior, due to the comparable melting temperature, can be identified for RT47. As regards the salt hydrate C48, the heat load ranges between a minimum value of 351.50 W and a maximum of 573.14 W. In this case the heat load peaked closer to 6 PM with a reduction of 11.35% with respect to the reference container.

Fig. 6 illustrates the comparison of the daily heat load for the reference container with the composite envelope during a typical summer day in Palermo. Data analysis shows that the heat load of the reference container varies between 367.27 W and 681.54 W with an amplitude of 314.27 W. On the other hand, for RT27 and RT28HC the peak heat load reduction, with respect to the reference, is equal to 7.54% and 8.86% respectively. RT31 and RT35 also show a higher reduction in peak heat load (14.48 % and 18.01% respectively) as well as a more constant heat load trend during the day if compared with RT27 and RT28HC. A better thermal behavior can be identified considering RT35HC. In fact the heat load peaked at around 6 PM, with a reduction, as a result of using PCM, of 20.87%. It is also worth noting that during the night RT35HC releases the latent heat and therefore starts to store energy three hours earlier than RT31 and RT35.Also in this case a worsening of thermal behavior can be noticed considering RT42, RT44HC, RT47 and C48. For RT42 the heat load is between 362.24 W and 574.39 W, with a peak heat load reduction of 15.72% with respect to the reference value. As regards RT44HC, the heat load peaked at about 6. PM, with a 16.44% reduction compared with the reference container. A similar thermal behavior can be identified for RT47 and C48, with a peak heat load reduction of 16.44% and 13.32% respectively.

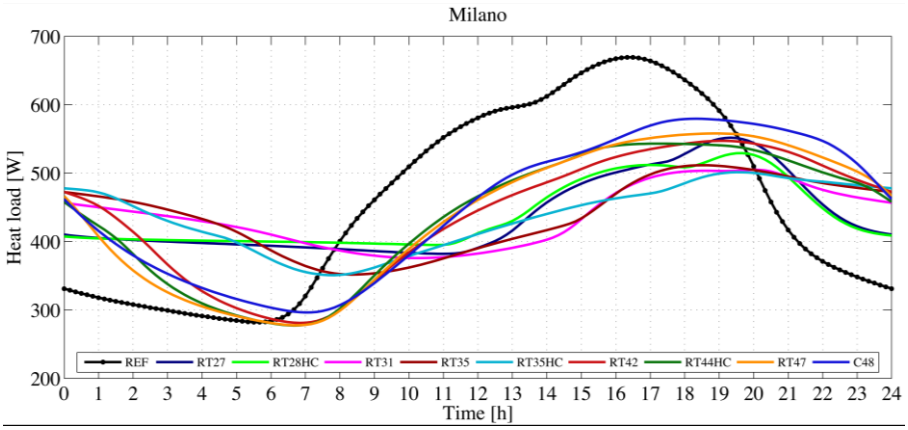

Figure 4: Daily heat load during a typical summer day in Milano

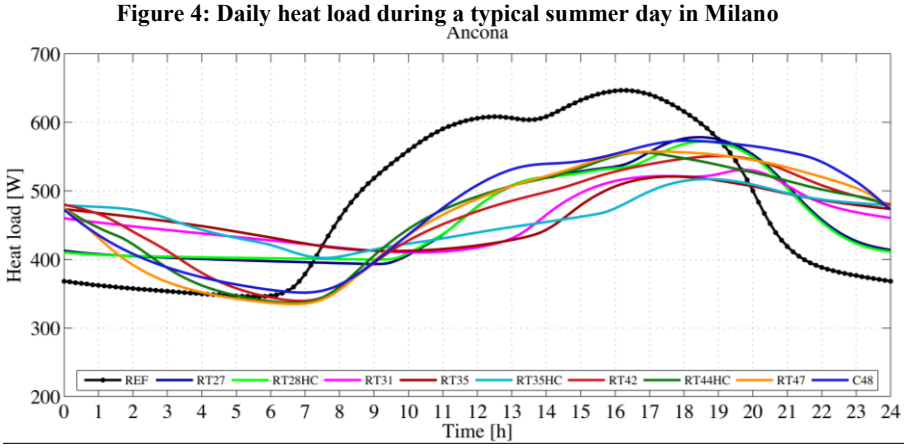

Figure 5: Daily heat load during a typical summer day in Ancona

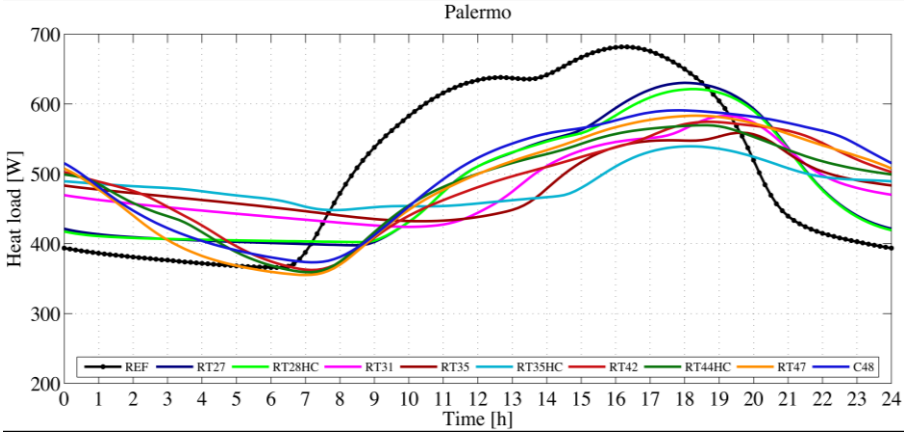

Figure 6: Daily heat load during a typical summer day in Palermo

Table 4 summarizes the average daily energy rate data and the corresponding percentage reduction of the reference container compared with the envelope fitted with different PCMs.

Table 4: Average daily energy data and corresponding percentage reductions

PCM	MILAN		ANCONA		PALERMO	
	Total energy [kWh]	Percentage Reduction [%]	Total energy [kWh]	Percentage Reduction [%]	Total energy [kWh]	Percentage Reduction [%]
REFERENCE	11.056	0	11.665	0	12.27	0
RT27	10.570	4.39	11.138	4.52	11.699	4.65
RT28HC	10.612	4.01	11.127	4.61	11.659	4.97
RT31	10.559	4.49	11.131	4.57	11.682	4.79
RT35	10.561	4.47	11.136	4.53	11.687	4.75
RT35HC	10.552	4.55	11.123	4.65	11.688	4.74
RT42	10.558	4.50	11.137	4.53	11.689	4.73
RT44HC	10.519	4.85	11.154	4.38	11.680	4.81
RT47	10.561	4.48	11.138	4.52	11.691	4.71
C48	10.866	1.72	11.462	1.74	12.027	1.98

2.2.3 Discussion

It is well known **(Baentes et al., 2010)** that the performance of a PCM enhanced container envelope depends on several factors such as the melting temperature of the PCM, the latent heat capacity, the external climatic conditions and solar heat gains. In fact, an overall view of the previously described results shows that a phase change temperature outside the practical operational temperature range makes the PCM enhanced container envelope useless as the temperature never reached the melting point. Specifically PCMs like RT42, RT44HC, RT47 and C48 did not work properly due to the high melting and solidification temperatures. In fact, the external temperature and solar radiation characterizing each Italian climatic context, only partially allowed the PCM melting point temperature to be reached, thereby producing an unfinished melting process. Therefore the PCM latent heat capacity was not completely used and resulted in a slight reduction and phase displacement of the incoming peak heat load with respect to a traditional container envelope. Conversely, it was found that PCMs characterized by low phase change temperature were not able to meet the required energy demand throughout the entire critical summer day for each climatic zone. In fact, PCMs like RT27, RT28HC and RT31 were completely

melted in the early hours of the day, thereby excluding the possibility to store energy during the critical times characterized by high temperature and solar radiation. Moreover, due to a nighttime external temperature that did not drop below the PCM melting point these materials were not able to completely discharge the stored heat and were therefore unable to accumulate latent heat the following day. However, thanks to the proper phase change temperature, RT35 and RT35HC were perfectly suited to the present PCM application. In fact, once the temperature surrounding the PCM rose to the melting point, the PCM started to change its state from solid to liquid with the consequent absorption of latent heat. Therefore, most of the energy was stored in the PCM until the local temperature dropped below the melting point, when the PCM started to discharge heat and become fully solidified. This storage-release cycle normally produces a double effect: a reduction and a phase displacement of incoming heat load with respect to a traditional envelope. In the first case, the peak heat load reduction can be translated into a reduced cooling capacity of the refrigerating unit. In this way, a reduction in refrigeration equipment size and a decrease in pollution from electrical and diesel driven refrigeration units can be achieved **(Ahmed et al., 2010)**. In the second case, the overlapping of the heat load peaks due to air exchanges from infiltrations and transmission through the walls can be avoided. This means that the transmitted heat load stored during the day reaches the internal refrigerated environment during the night, which is characterized by high refrigeration system performance (due to lower environmental temperature) and reduced energy costs.

Considering all the PCMs analyzed, the results show that the best thermal behavior during a typical summer day in Milano, Ancona and Palermo is obtained by applying paraffin wax RT35HC. In fact, thanks to its high heat storage capacity and a melting temperature similar to the external environmental conditions, this material changes its state completely, absorbing and phase displacing the overall heat flow through the refrigerated container envelope. In addition, a reduction in the total energy rate in a range between 4.55% and 4.74% was observed. Nevertheless, due to the limited daily energy input reduction (also considering correct all the hypotheses and model assumptions) a good management of the peak heat load inside the container is of fundamental importance. This means that the shift in time of the air exchanges and the transmitted peak heat loads through the walls lead to a high refrigeration system performance (due to a lower external environmental temperature) and a shift in electricity consumption from peak demand periods to off-peak periods, hence also leading to economic savings.

2.2.4 Conclusion

This chapter presents the first numerical investigation of the energy behavior (in the Italian climatic context) of a refrigerated container envelope fitted with PCMs. Due to the light weight of the envelope, refrigerated containers are subject to overheating problems when they are irradiated, especially during the summer. A low thermal inertia envelope, even if characterized by high thermal resistance, leads to overheating when irradiated by the sun with a consequent high energy consumption. In this context, the PCM application can confer high thermal inertia to the envelope, leading to a reduction and a phase displacement in the peak heat load through the envelope. In addition a reduction in the daily total energy rate can be observed. These results are due to the absorption of the heat load during the PCM melting phase. Considering all the PCMs analyzed, RT35HC was found to perform best on a typical summer day in Milan, Ancona and Palermo (heat load peak reduction – between 20.01% – 20.87%; delay in peak – between 2-3 h; daily energy rate reduction 4.55-4.74%). In fact the analysis of the numerical data provides encouraging results for lowering the energy rate and the peak heat load through the refrigerated container envelope. This can potentially be translated into both a lower energy consumption and a reduction in combined greenhouse gas (CO_2) emissions into the atmosphere. To that end RT35HC was employed for the experimental campaign in order to validate the numerical method.

2.3 Experimental analysis

2.3.1 Multilayer insulation envelope development

The insertion of a PCM in a reefer container envelope is aimed at reducing and displacing the phase of cooling load in comparison with a conventional panel (generally with low thermal inertia) made simply with insulating materials. Thanks to the high thermal storage capacity of PCM, it is able to reduce the heat transfer rate coming from the outside environment. When the outdoor temperature is higher than the melting temperature, a PCM starts to modify its state (from solid to liquid) with the resulting absorption of latent heat and the stabilisation of its temperature. The most notable effect is the reduction in the incoming heat flux peak due to a temperature difference between the external and the internal side of the envelope. Moreover, PCM absorbs heat when the external envelope surface is affected by the maximum incoming heat flux occurring during the hours of highest solar irradiation. The latent heat stored by PCM is subsequently released when the temperature decreases to below the melting point. This storage-release cycle generally causes a phase displacement of heat flux in comparison with a conventional enclosure, and a reduced cooling peak load between the daytime and the night time can be achieved.

In accordance with the obtained theoretical analysis results, Rubitherm RT35HC **(www.rubitherm.de)** paraffin wax was selected. It has an average density of 770 kg/m^3, a latent heat of fusion equal to 220000 J/kg, a fusion temperature of 35°C and a volume expansion equal to 12%. Due to the nature of PCM (solid-liquid transition), it can only be used in containers or if encapsulated. Therefore the solution developed for this study requires the material to be inserted in polyethylene panels (with dimensions of 0.6 x 0.6 x 0.03 m) each of which is internally divided into 81 small square tanks (Fig. 7a). The resistance and elastic characteristics of these panels allow the PCM to be contained without any notable shape loss despite the volume expansion that occurs during the phase change. The polyethylene panels were manually filled with the previously oven-melted (50 °C) paraffin wax (Fig. 7b). Finally the packaging system was hermetically closed (three bars of pressure, 170°C) using a thin multilayer film (Fig. 7c).

For the indoor campaign the previously described PCM layer was assembled in a prototype panel (0.6 m x 0.6 m) (Fig. 8b) made with a perimeter wood frame (2), internal and external plastified metal sheet (1-6) surfaces and finally filled with polyurethane foaming (5). A reference panel (Fig. 8a) was also assembled. The latter is made up of a sheet metal interior layer (1), a perimeter wood frame (3) an insulating layer made up of polyurethane (5) and an external sheet metal finishing layer (6). The PCM-added panel is the same as the reference one but with a layer of RT35HC between the external metal sheet and the

polyurethane foam. The thickness of the panels was 0.10 m and 0.13 m, respectively, for the reference and the PCM-added prototypes. For the outdoor campaign, the PCM layers were implemented on all the external surfaces of a cold room (Fig. 9a) using a wood frame (Fig. 9b) and then closed with a thin plastified metal sheet layer (Fig. 9c).

Figure 7: Phase Change Material layer development: (a) Polyethylene panel (b) RT35HC encapsulation (c) Polyvinyl chloride closing layer

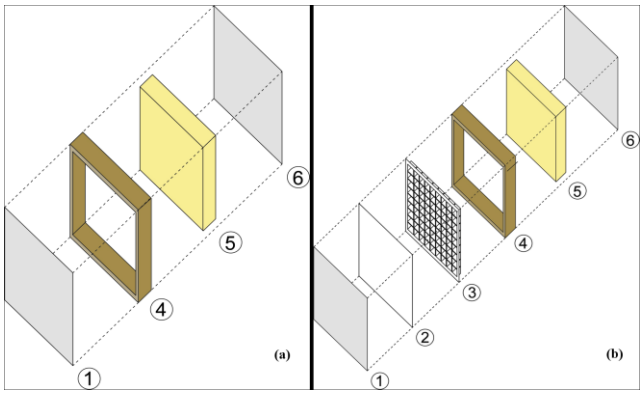

Figure 8: Surveyed prototypes: (a) Reference panel (b) PCM-added panel

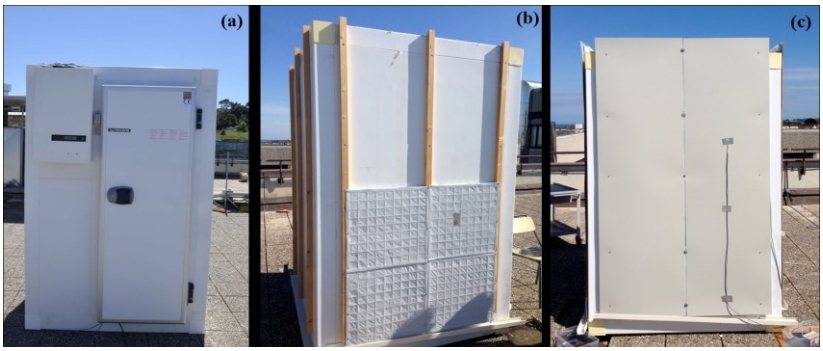

Figure 9: Steps in fitting the cold room with PCM: (a) Cold room (b) RT35HC layer implementation (c) Addition of a plastified metal sheet closing layer

2.3.2 Experimental indoor analysis set-up

The goal of the indoor analysis was to develop a PCM-added prototype panel and to compare its thermal behaviour with the reference panel under defined environmental conditions. Specifically, the indoor tests were held inside a climatic test room where it is possible to reproduce the most realistic environmental conditions. The test room (Fig. 10) has the same characteristics of the one used and described by **Carbonari et al. (2006)**.

Figure 10: Climatic test room

For the present research purposes, a refrigerated test box was placed inside the climatic test room (Fig. 11). The prototype panels (with and without PCM) were tested in sequence, assembled on the external side of the refrigerated test box. In order to reproduce solar irradiation flux, a solar simulator was used **(Carbonari et al., 2006)**.

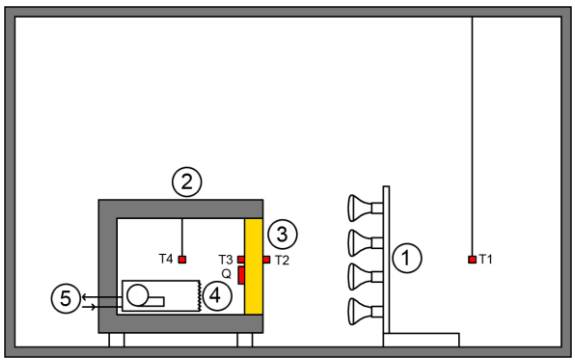

Figure 11: Climatic test room with the refrigerated test box inside (2): Solar simulator (1), Prototype panel (3), Cooling unit (4), Thermostatic bath (5) Developed monitoring system (T_1) Air temperature inside the cold room, (T2) Prototype panel external surface temperature, (T3) Prototype panel internal surface temperature, (T4) Refrigerated test box internal temperature and (Q) Heat flux)

The data were acquired with a data recorder Datataker DT500, set to one reading every 5 min. In order to measure the internal and external surface of prototype panels Resistance Thermal Detectors (RTDs, "Pt 100") characterized by ± 0.1 °C sensitivity, were employed. Air temperature was measured using T-type thermocouples, placed inside the climatic chamber and refrigerated test box. A flux meter (Hukseflux HP01) was used to measure the flux passing through the panels.

2.3.3 Outdoor experimental campaign set-up

The outdoor experimental campaign was conducted in order to test the related energy benefits due to PCM addition in a refrigerated cold room envelope. Specifically the outdoor experimental tests were carried out during a typical Italian summer, in order to verify the behaviour during extreme weather conditions when the PCM should act as a peak reducing cooling technology. In fact, during the summer days the effect of the higher external temperature generates high thermal load thereby reducing the cooling capacity of the refrigeration unit. Therefore, the thermal inertia of the PCM layer can contribute to maintaining the internal thermal conditions needed despite the loss of electricity. The outdoor experimental set-up consisted of two identical cold rooms one of them fitted with a PCM external layer.

The cold rooms (MISA MINI COLD ROOM mod. KLM 20) are parallelepipeds in shape, with an external size of 2.20 m x 1.4 m x 1.4 m (height x width x length) and a capacity of 2.88 m^3. The door dimensions are 1.90 m x 0.68 m x 0.11 m (height x width x length). The envelope of the cold rooms was made up of internal and external 0.001 m thick metal sheet that sandwiched a 0.10 m thick insulation layer made of expanded polyurethane, whose density was equal to 38-40 kg/m^3. The sandwich panels are lined internally and externally with a white plastic membrane. Each cold room is equipped with a direct expansion vapour-compression refrigeration unit with a cooling capacity of 1120 W. The evaporator is in direct contact with the internal air. A fan (120 W) provides air circulation inside the cold room and it stops working when the compressor of the cooling system is switched to the "OFF" position.

Both the novel and the reference cold rooms were fully instrumented (Fig. 12) to measure the temperatures of the internal/external surfaces, the PCM surface layer and the internal cold room compartment. To that end, Pt 100" resistance thermal detectors (RTDs) with a four-wire connection, having a 0.1 °C sensitivity, were used. Moreover, the heat flux passing through the south-oriented wall of the cold room with or without PCM was detected (flux meter Hukseflux HFP01). The sensor names and positions are reported in Table 5. All the experimental data were acquired with a data acquisition system (Datataker DT500) sets to one reading every 5 min. Moreover, in order to measure the external climatic conditions a meteorological station has been employed.

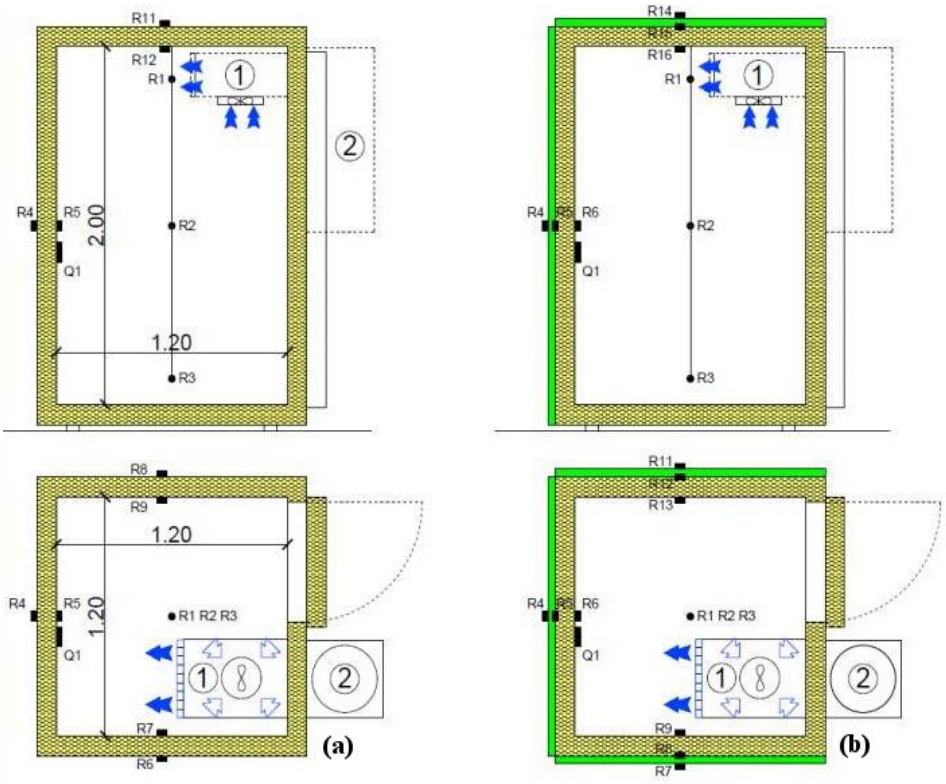

Figure 12: Monitoring system developed (a) Reference cold room (b) Cold room with PCM-added layer (in green) Refrigeration unit evaporator (1) and condenser (2)

Table 5: Sensor name and locations

Sensor name	Sensor location reference cold room	Sensor location PCM cold room
R1	Compartment air temperature at 1.8 meters	Compartment air temperature at 1.8 meters
R2	Compartment air temperature at 1.5 meters	Compartment air temperature at 1.5 meters
R3	Compartment air temperature at 1 meter	Compartment air temperature at 1 meter
R4	South external surface temperature	South external surface temperature
R5	South internal surface temperature	South surface temperature between PCM layer and polyurethane foam
R6	East external surface temperature	South internal surface temperature
R7	East internal surface temperature	East external surface temperature
R8	West external surface temperature	East surface temperature between PCM layer and polyurethane foam
R9	West internal surface temperature	East internal surface temperature
R11	Horizontal external surface temperature	West external surface temperature
R12	Horizontal internal surface temperature	West surface temperature between PCM layer and polyurethane foam
R13	–	West internal surface temperature
R14	–	Horizontal external surface temperature
R15	–	Horizontal surface temperature between PCM layer and polyurethane foam
R16	–	Horizontal internal surface temperature
Q1	Heat flux of south-oriented wall	Heat flux of south-oriented wall

2.3.4 Indoor experimental results

During the indoor experimental analysis, the thermal behaviour of the prototype panels (with and without PCM) was analysed under defined boundary conditions. The indoor experimental analysis procedure followed the here mentioned phases: 1) the prototype panel was implemented on the external side of the refrigerated box and its surface irradiated by a radiant flow (1000 W/m^2) with the electromagnetic spectrum similar to the highest solar irradiation. 2) a temperature gradient of 19 °C between the internal and external environment was reproduced; 3) the indoor experimental test ended after 3.5 hours when the incoming heat flux reached a constant value. This could be inferred by the steady-state heat flux reached at 03:15 as shown in Fig. 13.

The test results of the indoor experimental analysis include the internal and external surface temperatures and the heat flux passing through the panel. The data lines in Fig. 13 compare the heat transfer rate per unit area across the reference

panel with that of the PCM-added panel. In the considered time range, the chart evidently shows a decrease in peak heat transfer rate per unit area as well as a reduction in the total energy for the prototype panel with PCM (equal to 59.31%). Fig. 14 shows that, during its melting phase, the PCM layer absorbs the heat flux coming from the outside environment, remaining at a nearly constant temperature of 63 °C for almost two hours. The use of halogens lamps determines higher values of external surface temperature with respect to the realistic operational conditions. It is therefore evident that the RT35HC is decisive in countering solar irradiation and reduces the internal surface temperature trend. In fact, the use of PCM maintained the internal surface temperature constant and lower (1-2 °C) during the 3.5 hours of the experimental test (Fig. 15).

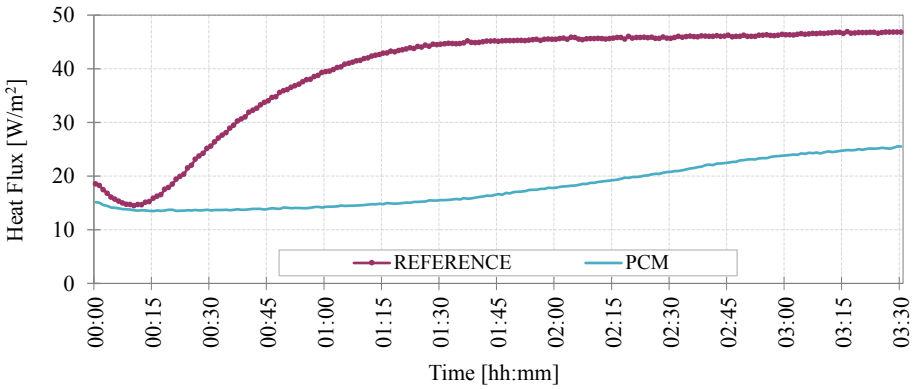

Figure 13: Heat flux through the prototype panel with and without PCM

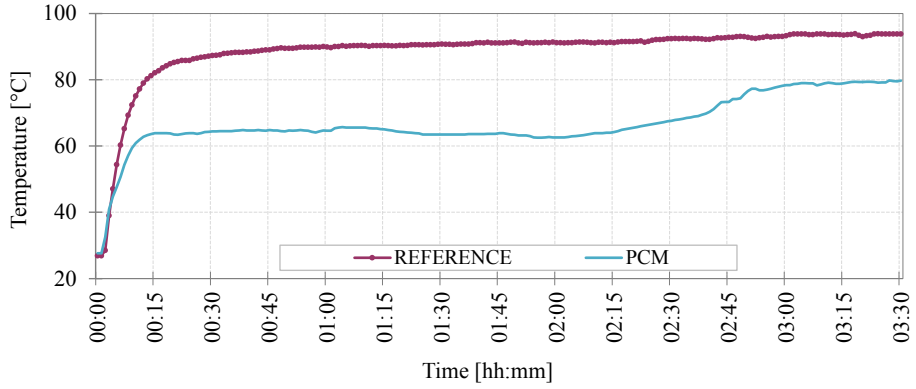

Figure 14: External surface temperature of the prototype panel with and without PCM

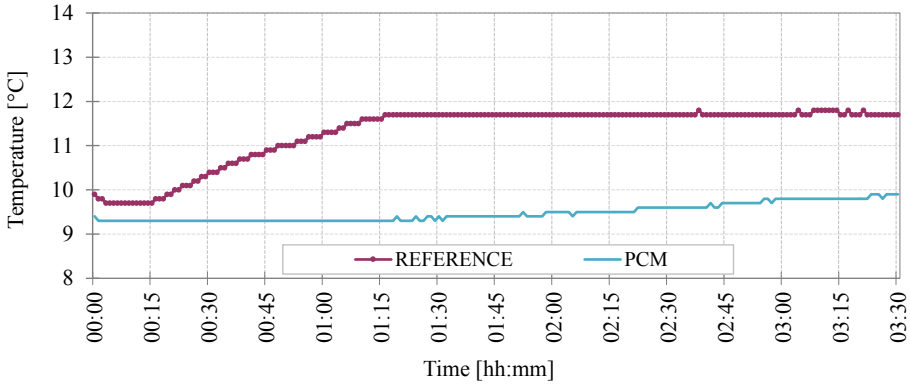

Figure 15: Internal surface temperature of the prototype panel with and without PCM

2.3.5 Numerical model validation

A comparison of the experimentally measured and numerically calculated heat flux distribution through the prototype panel provided by PCM is shown in Fig. 16. Specifically, the incoming heat flux measured by flux meter during the indoor experimental campaign was compared with the numerical one. The agreement between the numerical solution and the measurement is rather good. In fact, the cross-correlation statistical analysis, which estimates the degree to which the numerical and experimental time series are correlated, provided a correlation coefficient (r) of 0.97.

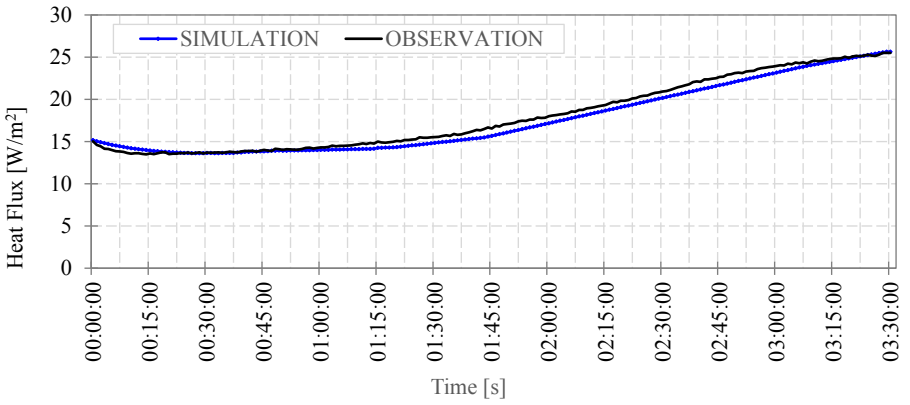

Figure 16: Comparison of the experimentally measured and numerically calculated heat flux distribution through the PCM prototype panel

2.3.6 Outdoor experimental results

The reference and the novel cold room thermal behaviour were monitored for most of the summer in 2014. To make the results clear and readable, two test days (30/08/2014 and 09/09/2014) are reported and discussed here. In Ancona both high solar gains and outdoor temperature characterised this period. In fact, as can be observed in Fig. 17a and Fig. 18a, the maximum solar irradiation value was equal to 830 (W/m^2) and 770 (W/m^2) respectively and the air temperature ranged between 13 °C and 28 °C. Fig. 17a and Fig. 18a also show the comparison in measured temperatures at each interface of the south-oriented wall of the PCM-added cold room compared with the reference one. On the first day considered (Fig. 17a), comparing the external surface temperature of the PCM-added wall (R4-PCM) with the measured temperature value between the PCM layer and polyurethane foam (R5-PCM), it is possible to note a decrease (by 12 °C) and a peak shift (almost 5 h) of the two temperature trends. In fact, due to the PCM changing phase (that starts at 30 °C) the wall can store the heat load coming from the external environment, reducing and delaying the incoming thermal flux. It is also important to observe the comparison between the measured temperature value between the PCM layer and the polyurethane foam (R5-PCM) and the reference external surface temperature (R4-REF). In this case, the maximum temperature value is 7 °C lower than the maximum temperature value of the reference external surface temperature. This is mainly due to the storage of the solar gains as latent heat in the PCM layer, therefore leading to a reduction in temperature. Due to the on-off cycles of the refrigerating unit, no relevant differences between the reference and PCM internal temperature compartment have been observed. Heat flux data for the south-oriented wall were also collected during the experimental campaign. Fig. 17b shows the heat transfer rate per unit area across the reference wall for the room fitted with a PCM layer. As can be observed in Table 6, the heat transfer rate of the reference cold room peaked at 4:30 PM while the heat flux in the novel cold room peaked at 9:00 PM. In this case, the thermal heat flux peak reduction is equal to 5.55 %. A similar thermal behaviour was observed on the second day reported in this paper (Fig. 18). The data lines in Fig. 18a illustrate the comparison in measured temperature on each interface of the south-oriented wall of the PCM-added cold room and the reference. Once again, by comparing the reference external surface temperature (R4-REF) with the measured temperature between the PCM layer and the polyurethane foam (R5-PCM) it is possible to observe different behaviour. In fact, the storage of the incoming thermal flux as latent heat led to a reduction in temperature (by 8 °C) compared with the maximum value of the reference external surface temperature. Furthermore, comparing the external surface temperature (R4-PCM) of the PCM-added wall with the interface temperature between the PCM layer and the polyurethane foam (R5-PCM) it is

possible to observe a reduction (by 14 °C) and a phase displacement (almost 4 h) of the two temperature trends. Fig. 18b depicts the comparison in heat transfer rate per unit area across the reference south wall compared with the wall fitted with a PCM layer. Specifically, the thermal heat flux peak reduction and phase displacement were found to be equal to 8.57 % and 3.5 h respectively (Table 6). These results show that the PCM layer can be considered a way to absorb a large quantity of heat when there is both intensive solar irradiation and a high external environmental temperature. However, it is also worth noting that along with the heat flux peak reduction, a consistent reduction of the total amount of heat per unit area was not obtained. In fact, during the night time and the early hours of the morning, the incoming heat flux of the PCM cold room became higher than that for the reference case (Fig. 17b and Fig. 18b). This drawback, in the case of high night time temperature, is due to the PCM energy-releasing process that increases the incoming heat flux.

Table 6: Comparison between heat flux peak phase displacement and reduction for the reference and novel cold rooms

	Reference		**PCM**			
Day	**thermal flux peak [W/m²]**	**time [hh:mm]**	**thermal flux peak [W/m²]**	**time [hh:mm]**	**peak reduction [%]**	**delaying [hh:mm]**
2014-08-30	10.99	16:30	10.38	21:00	**5.55**	**4:30**
2014-09-09	11.55	17:30	10.56	21:00	**8.57**	**3:30**

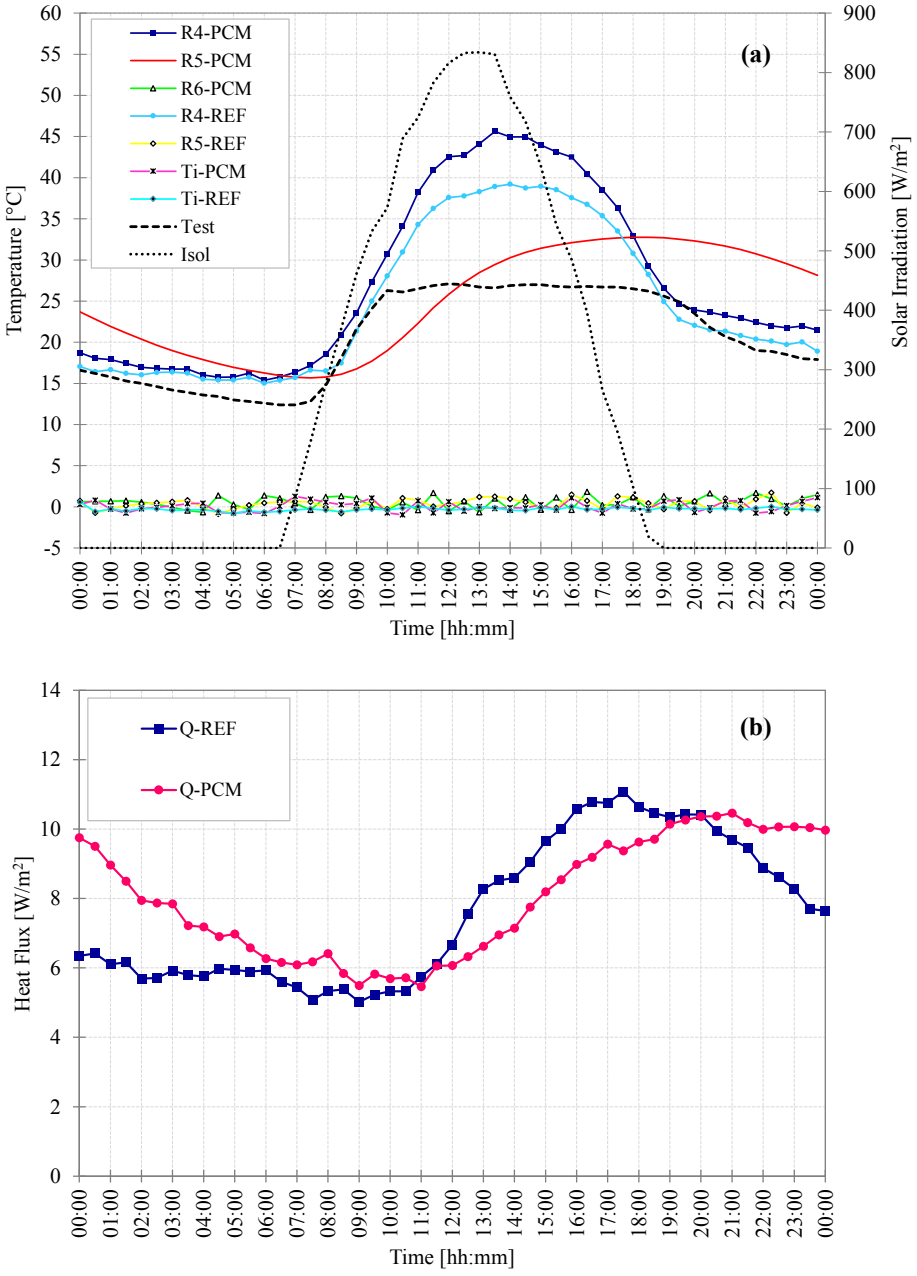

Figure 17: 2014-08-30 (a) internal compartment, surface temperatures and climatic data. (b) thermal flux through the south-oriented wall

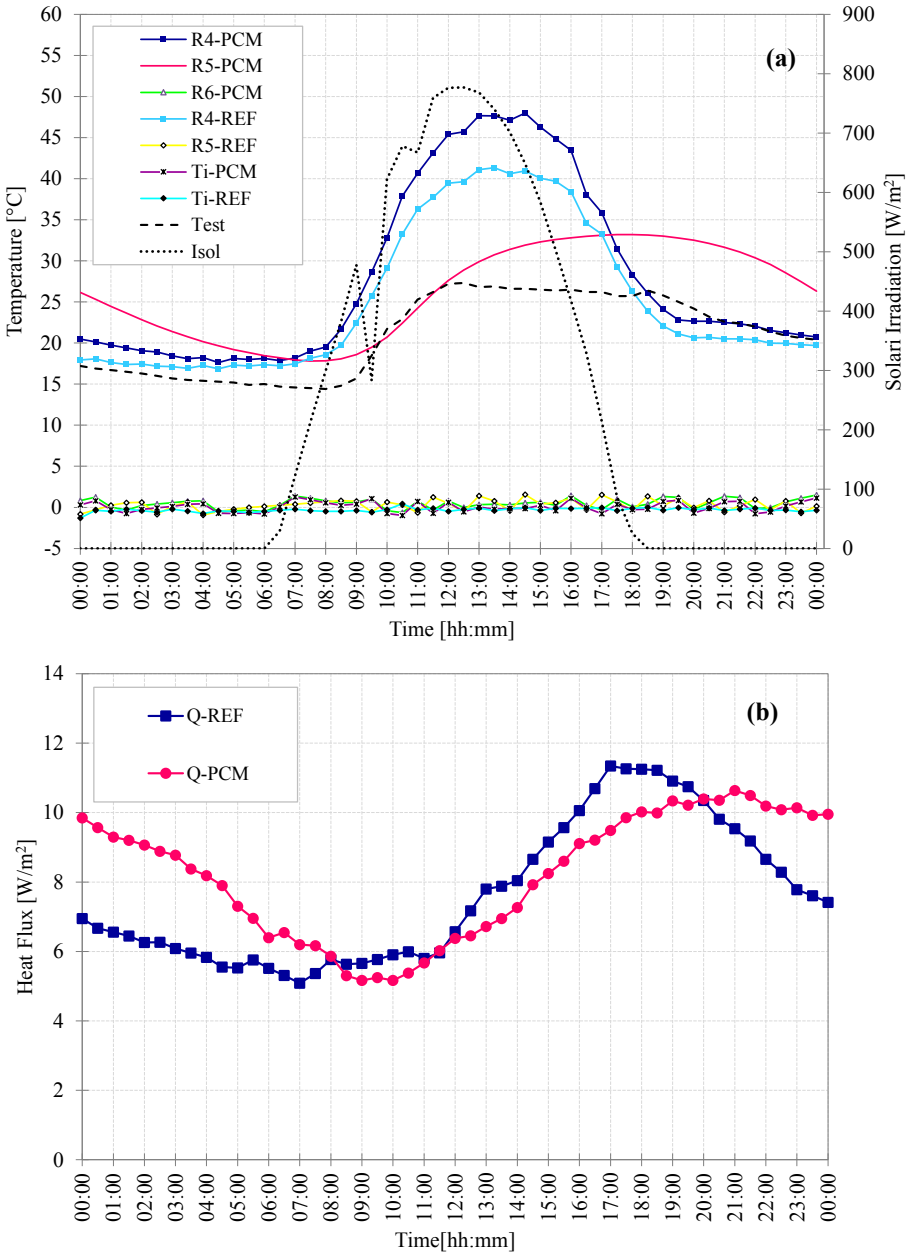

Figure 18: 2014-09-09 (a) internal compartment, surface temperatures and climatic data. (b) thermal flux through the south-oriented wall

2.3.7 Numerical model validation

In this paragraph, the outdoor experimental data (2014-08-30) are compared with the numerical results obtained from numerical modelling. For simplicity sake, the results concerning the heat flux data across the refrigerated cold room wall are reported. In this way, during the numerical modeling validation process the acquired external climatic conditions were used and applied as boundary conditions. As can be observed in Fig. 19, the theoretical and the experimental curve demonstrated a rather close agreement for all the transient periods, including the PCM melting phase. In fact, the cross-correlation statistical analysis, which estimates the degree to which the numerical and experimental time series are correlated, provided a correlation coefficient (r) of 0.95.

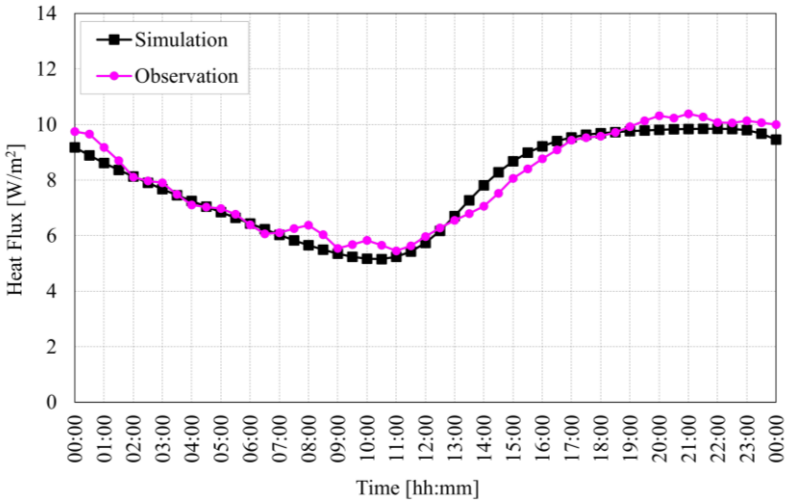

Figure 19: Comparison of the experimental and predicted heat flux data

Fig. 20 shows the Probability Density Function (PDF) of the observed and simulated heat flux data. The distribution amplitude is generally well represented even if a moderate underestimation of the observed values can be noted. In particular, a noticeable misrepresentation of values at left and right distribution tails is resulted. This is most likely due to the model inability to represent the start-and-stop phases of the refrigeration unit that are evident in the experimental heat flux curve upper described (Fig. 19). The obtained results are in accordance with the probability plot distribution (Quantile - Quantile plot) reported in Fig. 21a, where larger discrepancies have been found in lower and higher heat load and external surface temperature values Fig. 21b.

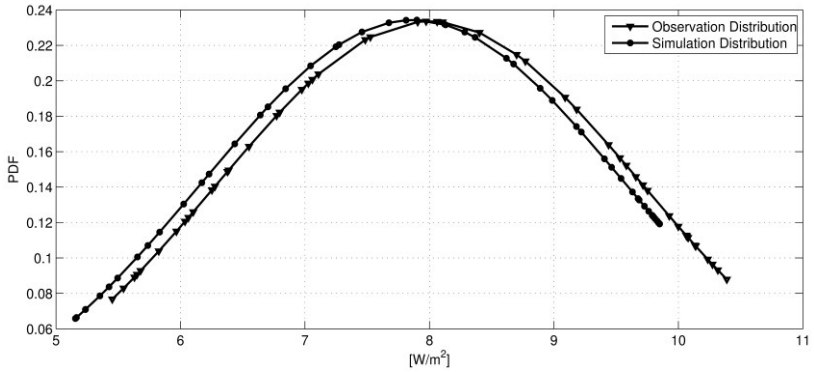

Figure 20: Heat fluxes observed and simulated PDF comparison

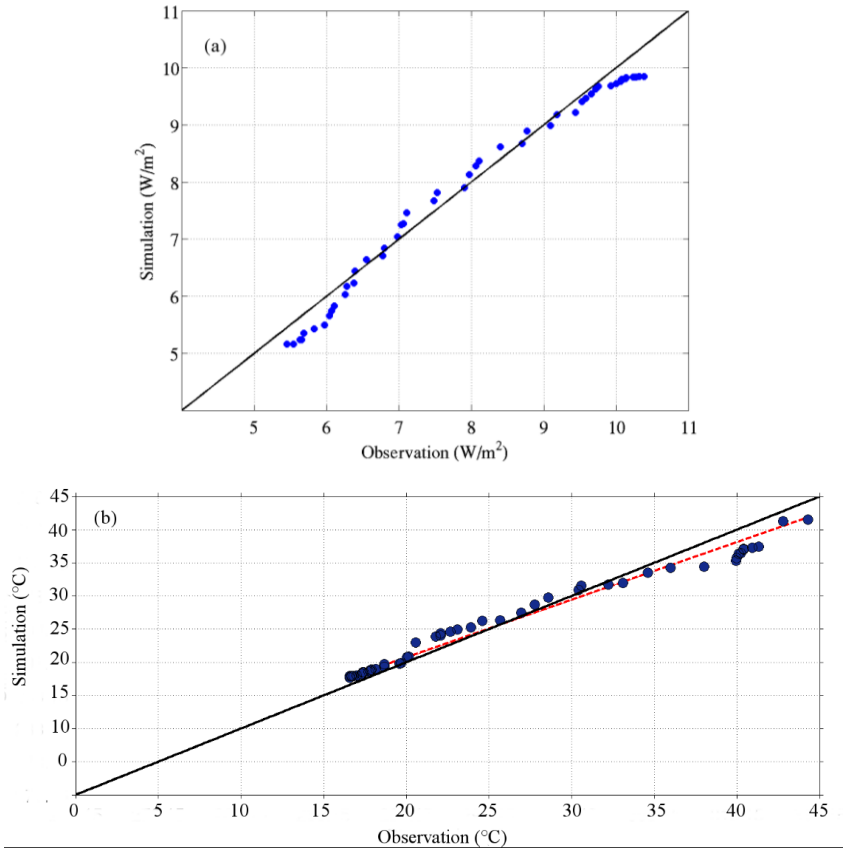

Figure 21: Observed-Simulated heat flux (a) and external temperature (b) Quantile-Quantile plot

2.3.8 Discussion

This study focuses on improving the thermal performance of a reefer container enclosure by using PCM. A low thermal inertia envelope, even if characterised by high thermal resistance, leads to overheating when irradiated by the sun, with a consequent increase in the internal refrigerated temperature, energy consumption and the possibility of food quality loss. Specifically the addition of PCM can provide the envelope with high thermal inertia (due to the heat load absorbed during the melting phase) determining a lower thermal load and its shift in time. It is also worth noting that a PCM application to the envelope of refrigerated containers allows the recommended storage temperature to be maintained during transportation or while they are stacked in container terminals. PCM addition helps to protect food from temperature abuse in cold chain transport by reducing heat transfer from the outside environment. In particular, when the PCM reaches its melting temperature, large amounts of heat are absorbed at a constant temperature, thereby enabling the internal surface and compartment temperature buffering function. In this way, temperature variations and fluctuations during the transportation of refrigerated cargo can be avoided. In this regard, future research studies could focus on evaluating the specific effect of PCM installation on the product temperature inside the refrigerated container. Moreover, PCM can also provide temperature control and consequently prevent both wear and extensive use of the compressor-driven cooling system. In fact, the shift in time of the air exchanges and the transmitted peak heat loads through the walls do not allow the refrigeration unit to remove the two thermal loads simultaneously.

To the best of the authors' knowledge promising results have been obtained by integrating PCM in insulation walls of refrigerated transport systems. As an example, **Ahmed et al. (2010)** proposed a novel insulation technology based on the inclusion of copper pipes containing paraffin in standard truck trailer walls. For individual walls, the peak heat transfer rate was reduced in the range of 11.3–43.8%. Overall, average daily heat flow reductions of 16.3% were observed in the refrigerated compartment. In comparison with the results obtained in the present work, the experimental data observed by **Ahmed et al. (2010)** are more encouraging. Although the experimental analyses are similar, the results obtained are not comparable due to different boundary conditions and different characteristics of the refrigerated trailer envelope and the PCM packaging system. **Glouannec et al. (2014)** modified a standard insulation wall of a refrigerated panel van by the addition of thin layers of new materials with the aim to increase both the insulation performance and thermal inertia. Specifically, the addition of a reflective multi-foil insulation (RMS) and aerogel layers gave good results in reduced peak heat transfer and energy consumption. Encouraging results were also obtained by adding a PCM layer. However, due to the indoor experimental test conditions the

PCM layer did not work perfectly. In fact a partial melt and freeze was observed. This underlines the importance of optimising the size, the position and the choice of PCM. Finally, **Tinti et al. (2014)** analysed the possibility of incorporating a microencapsulated phase change material (melting point 6 °C) into standard polyurethane foam designed for the thermal insulation of refrigerated transport systems. The developed technology would be very useful in contrasting all events in which a temperature transient occurs. In fact the thermo graphic analysis revealed the possibility of developing a hybrid insulation panel that, thanks to its low thermal conductivity and latent heat storage capacity, is able to reduce temperature abuse during the vehicle journey.

In this study, a novel packaging system to apply to new container envelopes was developed and thermally analysed. It is advisable to insert the PCM layer during the polyurethane foaming in order to have both better thermal contact and mechanical stress resistance. The promising results obtained during the indoor experimental analysis perfectly described the PCM thermal behaviour under defined environmental conditions. The results have shown an effective reduction in the thermal flow entering through the PCM-added panel compared with the reference one. It is evident that the PCM-added layer can absorb the heat load while the PCM remains at a constant temperature during the melting phase. Therefore, the PCM layer addition proves to be decisive in reducing solar irradiation and the surface temperature trend. These aspects were confirmed by the outdoor experimental campaign during which the PCM layer was added to all the external surfaces of a cold room and its thermal behaviour was studied under real summer environmental conditions. In general, the PCM-added layer reduced and shifted the peak of the thermal load during periods of sunlight. These results can be attributed to the high thermal inertia of the envelope. This means that the heat load stored during the day reaches the internal refrigerated environment during the night, which is characterised by high refrigeration system performance (due to a lower environmental temperature) and reduced energy costs. It is also important to underline that the present technology is aimed at reducing the thermal peak heat load and its shift in time especially during hot summer weather conditions. Consequently, a reduction in energy or fuel consumption by the refrigeration unit, especially during the daytime, which is characterised by high external temperatures, can be achieved. However, the external environmental conditions, such as temperature and solar irradiation, are not controllable during the container journey **(Laguerre et al., 2008)**. The ambient temperature can be less than 0 °C in winter or higher than 30 °C in summer while the solar irradiation may vary from 600 W/m^2 to 1000 W/m^2. Therefore, the selected PCM operating temperature (35°C) may not be applicable for the wintertime, hence representing one disadvantage of the presented technology. Despite this, it is worth noting that during the winter season the peak heat load does not vary significantly throughout

the day therefore, especially in refrigeration systems, a high thermal inertia envelope is not so relevant. Moreover, the refrigeration unit operates with high efficiency due to a reduced temperature gradient between the external and the internal environment and therefore requires low energy or fuel demand.

2.3.9 Concluding remarks

In this study, a technology aimed at improving the energy performance of a reefer container enclosure using PCM was numerically and experimentally investigated. The mathematical model was used to simulate the refrigerated container envelope during a typical summer day in the Italian climatic context. The model predicted that the paraffin wax RT35HC performed best on a typical summer day in Milan, Ancona and Palermo (heat load peak reduction – between 20.01% – 20.87%; delay in peak – between 2-3 h; daily energy rate reduction 4.55-4.74%). Specifically, during the experimental campaign, indoor and outdoor analyses were carried out. The analysis of the thermal performance during the indoor test has shown that a PCM-added layer helps to store the incoming heat load at a constant temperature during the phase change material melting phase. In this way, a 1-2 °C reduced internal surface temperature was observed compared with the reference container. The energy evaluation of the PCM-added envelope under real summer environmental conditions was carried out during the outdoor experimental campaign. The two experimental days (30/08/2014 and 09/09/2014) showed a reduction in peak heat transfer rate, compared with the reference, of 5.55% and 8.57% respectively. Moreover, a peak delay of 4.30 h and 3.30 h was obtained. In fact, PCM acting as an energy storage medium can absorb and displace the incoming heat flux during its melting phase. Despite this, during the outdoor experimental analysis, a consistent reduction of the total amount of incoming heat through the envelope was not observed. In fact the higher night-time outdoor temperature does not allowed the PCM to fully discharge the daily energy, determining an increase of the incoming heat flux. Regarding the numerical model validation, the cross-correlation coefficient value highlights the reliability of the numerical model, and hence it can be deduced that the model describes the latent absorption phenomenon correctly.

Acknowledgments

The author wants to thank the manufactory SA.M.E. Sargentini Materiali Edili (http://www.same-foil.com/) for the development of the phase change materials packaging system.

References

Ahmed, M., Meade, O., Medina, M.A., 2010. Reducing heat transfer across the insulated walls of refrigerated truck trailers by the application of phase change materials, Energ. Convers. And Manage. 51, 383-392.

Aung, M.M., Chang, Y.S., 2014. Temperature management for the quality assurance of a perishable food supply chain. Food Control 2014; 40:198–207.

Baentes, R., Jelle, B.P., Gustavsen, A., 2010. "Phase change materials for building applications: A state-of-the-art review, Energ. Buildings. 42, 1361–1368.

Carbonari, A., De Grassi, M., Di Perna, C., Principi, P., 2006. Numerical and experimental analyses of PCM containing sandwich panels for prefabricated walls. Energ. Buildings. 38: 472-483.

Çengel, Y.A., Ghajar, A. 2010. Heat and mass transfer: Fondamental & Applications - McGraw-Hill Editor, 4 edition Chapter17 - Refrigeration and freezing of foods.

Climator website. Available from: http://www.climator.com/en/climsel/ (Access on: 8 September 2015).

Comsol website. Available from: https://www.comsol.it/ (Access on: 8 September 2015).

Darkwa, K., O'Callaghan, P.W., 2006. Simulation of phase change drywalls in a passive solar building, Appl. Thermal Eng. 26, 853–858.

EN ISO 6346:1995 Freight container – coding, identification and marking.

EN ISO 10211-1, Thermal bridges in building construction, Heat flows and surface temperatures, Part1: general calculation methods, European Committee for Standardization, 1995.

EN ISO 6946:1996, Building components and building elements, Thermal resistance and thermal transmittance, calculation method, European Committee for Standardization.

Farid, M.M. A new approach in the calculation of heat transfer with pahse change, 9th International Congress on Energy and Environment, 1–19, Miami,1989.

Glouannec, P., Michel, B., Delamarre, G., Grohens, Y., 2014. Experimental and numerical study of heat transfer across insulation wall of a refrigerated integral panel van. Appl. Therm. Eng. 73:196–204.

Joybari, M.M., Haghighata, F., Moffat, J., Sra, P., 2015. Heat and cold storage using phase change materials in domestic refrigeration systems: The state-of-the-art review, Energy and Build. 106: 111–124.

Laguerre, O., Ben Aissa, M.F., Flick, D., 2008. Methodology of temperature prediction in an insulated container equipped with PCM. Int. J. Refrig. 31: 1063-1072.

Mosaffa, A.H., Infante Ferreira, C.A., Talati, F., Rosen, M.A., 2013. Thermal performance of a multiple PCM thermal storage unit for free cooling. Energ. Convers. Manage. 67: 1-7.

Principi, P., Fioretti, R., 2012. Thermal analysis of the application of pcm and low emissivity coating in hollow bricks, Energ. Buildings. 51, 131-142.

Rubitherm GmBH website. http://www.rubitherm.de/english/ (Access on: 8 September 2015).

Sari, A., 2016. Thermal energy storage characteristics of bentonite-based composite PCMs with enhanced thermal conductivity as novel thermal storage building materials. Energ. Convers. Manage. 117: 132-141.

Tinti, A., Tarzia, A., Passaro, A., Angiuli, R., 2014. Thermographic analysis of polyurethane foams integrated with phase change materials designed for dynamic thermal insulation in refrigerated transport. Appl. Therm. Eng. 70: 201–210.
UNI 10349, Heating and cooling of buildings, Climatic data, Italian Standard, 1994.
UNI 10351:1994, Building materials. Thermal conductivities and vapour permeabilities.
UNI 12524:2001, Building materials and products — Hygrothermal properties — Tabulated design values
Zukowski, M., 2007. Experimental study of short term thermal energy storage unit based on enclosed phase change material in polyethylene film bag, Energ. Convers. Manage. 48, 166–173.

3. Experimental investigation on a novel air heat exchanger containing PCM in a cold room

---

This chapter has previously been published in
11th IIR Conference Proceedings on Phase-Change Materials and Slurries for Refrigeration and Air Conditioning. (Copertaro et al. 2016) and IEEE EEEIC 2016 Conference Proceedings (Copertaro et al. 2016). Some paragraphs have been added for the purpose of this dissertation.

3.1 Introduction

After investigating the application of PCM to the external side of a refrigerated container envelope, the attention was paid to the reduction of cooling energy required to run a low efficiency refrigerating unit and to contrast the incoming heat load which occurs during a power outage event.

The growing attention to the global environmental issue and the rising in energy costs are increasingly promoting the necessity of developing sustainable and energy efficient cooling technologies among the refrigerated equipment manufactures. Making changes in refrigeration system and its components such as evaporator, condenser and compressor can increase the efficiency of the refrigeration unit. In this context, the application of PCM within the equipment is considered the most common techniques to reduce energy consumption of cooling system (**Marques el al., 2014**) and the rate of temperature increase during power loss (**Orò et al., 2012**). In fact, by accumulating the excess of cold energy produced by the evaporator, an extension of on and off cycle's periods can be obtained. By the way, a minimized number of cycles per unit time and a consequent reduced energy consumption are desirable **(Marques el al., 2014)**. Moreover, PCMs owing to their high heat storage capacity are able to accumulate and release large amounts of energy during the phase change process (**Leducq et al., 2011**). Therefore, the use of PCM in the refrigerated compartment has the potential to keep the internal temperature at desired level for longer period of time when a power failure occurs. For those reasons, the application of a PCM air heat exchanger near the evaporator of a cold storage room was investigated.

3.2 Air heat exchanger operating principle

In this study, PCM was placed in air heat exchanger near the evaporator with the purpose of reducing energy consumption, increase and stabilize the evaporator outgoing air temperature. Specifically, the PCM heat absorption and releasing process take place when the evaporator outgoing air temperature is above or below the temperature set point. The PCM works as "thermal flywheel": when the evaporator outgoing air temperature drops below the cold room temperature set point, heat is released by PCM; conversely, when the evaporator outgoing air temperature is higher than cold room temperature set point heat is absorbed by PCM. Therefore, there are two possible situations:

1) The evaporator outgoing air temperature is lower than cold room temperature set point and PCM (Fig. 22): air leaving the evaporator absorbs heat from the PCM, which changes its state (solidifies). Consequently, the air temperature increase, resulting close to the cold room temperature set point.

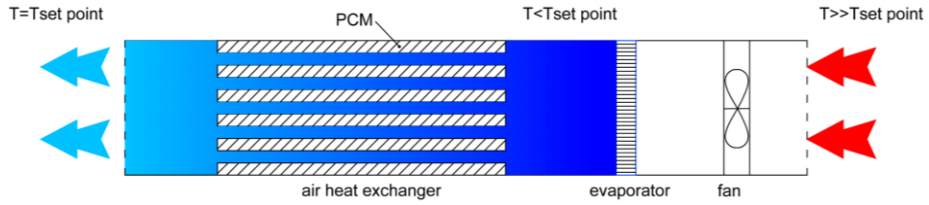

Figure 22: Air heat exchanger operating principle: first case

2) The evaporator outgoing air temperature is higher than cold room temperature set point and PCM (Fig. 23): air leaving the evaporator releases heat to the PCM, which changes its state (melts). Consequently, the air temperature decrease, resulting close to the cold room temperature set point.

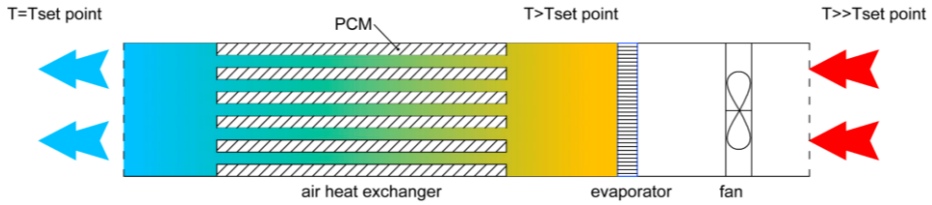

Figure 23: Air heat exchange operating principle: second case

3.3 PCM and air heat exchanger

The experimental campaign consists of cold room (KLM 20 MISA MINI COLD ROOM) which was previously described in Chapter 2, subparagraph 2.3.3. A paraffin wax with a phase change temperature of 5 °C was used since this temperature is near to the cold room set point temperature (5°C). The used paraffin wax (Rubitherm RT 5 HC) is characterized by an average density of 760 (kg/l), heat storage capacity of 240 (kJ/kg) and a heat conductivity of 0.2 [W/ (m·K)]. During the experimental activities, the selected PCM was stored in six air heat exchangers in pairs assembled. Each air heat exchanger consists of anodized aluminum and finned surface with internal dimensions of 1.00 m x 0.03 m x 0.14 m (length x height x width), equal to a $4.2 \cdot 10^{-3}$ m^3 in volume (Fig. 24). The exchange surface area is equal to 1.44 m^2 per meter of length. In order to obtain a better heat exchange between the evaporator outgoing air and the PCM air heat exchanger a polystyrene channel was constructed around the heat exchanger (Fig. 25) and a fan system (electric power of 20 W) was added on the outlet section of the channel (Fig. 26).

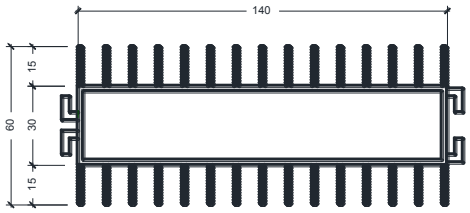

Figure 24: Section of the air heat exchanger

Figure 25: Positioning of the air heat exchanger in the cold room

Figure 26: Heat exchanger with polystyrene channel and fan system

3.4 Improving energy efficiency of a cold room by using PCM

3.4.1 Measurement and test conditions

The cold room was instrumented to measure temperatures of the evaporator during ON and OFF cycles, PCM air heat exchanger surface and internal cold room compartment. Fig. 27 shows the monitoring system developed.

Figure 27: Monitoring system

Specifically temperatures were measured using thermal resistance detectors (RTDs) “PT100” with a four-wire connection. All thermal resistance detectors were calibrated in an oil Micro-Bath (FLUKE CALIBRATION 7102) by using a reference sensor “PT25” characterized by a well-known high level of accuracy (0.002 °C). Therefore taking into account the temperature stability during calibration process and the residual error of the interpolating curve, the accuracy for each RTDs resulted equal to 0.05 °C. The heat flux passing through the cold room envelope was measured using a fluxmeter Hukseflux HFP01. The cold room compressor and additional fan system electricity consumption was measured with a digital wattmeter Christ Elektronik CAC 140. The experimental set-up was equipped with a data logger system (Datataker DT500) linked to a computer for monitoring experimental data. The sensor names and locations are given in Table 7.

Table 7: Sensor names and locations

Sensor name	Location
$T_{a\ 1m}$	Compartment air temperature at 1 meter high
$T_{a\ 1.5m}$	Compartment air temperature at 1.5 meter high
$T_{a\ 1.8m}$	Compartment air temperature at 1.8 meter high
$T_{a\ ext}$	External air temperature
T_{in}	Evaporator inlet air temperature
$T_{EVAPout}$	Evaporator outlet air temperature
T_{s6}	Cold room internal surface temperature
T_{s7}	Cold room external surface temperature
T_{S8}	Cold room external surface temperature
T_{R3}	PCM surface temperature
T_{R4}	PCM surface temperature
T_{R5}	PCM surface temperature
T_{R6}	PCM surface temperature
T_{R7}	PCM surface temperature
T_{R8}	PCM surface temperature
T_{PCMout}	Heat exchanger outgoing air temperature
Flux	Heat Flux

A series of preliminary tests were carried out in order to find out the optimum operating settings. Consequently, the cold room temperature set point chosen was equal to 5 °C, with a differential temperature of 2 °C. The energy performance test of the cold room was carried out in the "Renewable Energies Laboratory" of Università Politecnica delle Marche. The energy and thermal behavior of the cold room (with/without PCM air heat exchanger) was studied in steady state operating conditions during a typical Italian summer conditions (July 2015). The laboratory room was kept at a constant temperature of 32±1 °C.

3.4.2 Results and discussion

The test results of the reference and the novel cold room under steady state conditions includes the evaporator outgoing air temperature, internal compartment temperature and power consumption. All these parameters were measured during a 24h-test. To make it clear and readable 2h test results are here reported and discussed.

In Fig. 28, the comparison between the evaporator outgoing air temperature in the reference and in the novel cold room is shown. In addition, both PCM surface temperature and the heat exchanger outgoing air temperatures (hereafter "T_{pcmout}") are reported. For the reference cold room, evaporator outgoing air temperature ranged between –1.2 °C and 4.9 °C and the average value was 1.9 °C over a whole cycle. For the novel cold room, evaporator outgoing air temperature ranged between –1.4 °C and 5.18 °C and the average value was 2.3 °C. As shown in Fig. 28 the novel cold room, evaporator outgoing air temperature was cooled down at a faster rate during the "ON" period, whereas during the "OFF" period, a slower warming was observed. This effect can be observed in the data line describing the phase change material thermal behavior (T_{PCM}). The freezing phase is short and the melting is slightly wider. It is also worth noting that the PCM air heat exchanger allowed the increase and stabilization of the air temperature leaving the evaporator. In fact, the evaporator outgoing air passing through the PCM air heat exchanger, absorbs heat from the PCM which changes its state (solidifies). Consequently, the air temperature leaving the heat exchanger (T_{pcmout}) increased. It indicates that the lowest temperature value reached was equal to 1.63 °C (instead of -1.2°C, for the reference evaporator outgoing air temperature) and the average temperature was 4.29 °C (instead of 1.9°C, for the reference evaporator outgoing air temperature) over a whole cycle. In addition, the heat exchanger outgoing air temperature varied through smaller range (5.2 °C) if compared to the reference evaporator outgoing air temperature (6.4°C).

These results suggested that the PCM air heat exchanger helps keeping compartment temperature near to selected set point, providing also benefits to the

stored refrigerated products. In fact, the lowest value of the T_{pcmout} was 2.9 °C higher than the lowest value of the reference evaporator outgoing air temperature. By this way, the freezing of the refrigerated goods in contact with the evaporator temperatures could be avoided. It is well known that the exposure at warm or too cold temperature can significantly deteriorate fresh product. Under warm temperature, fruits and vegetables could improperly ripen. On the other hand, the exposure to close or below 0 °C temperature can cause a partial freeze, cracks formation and products drying.

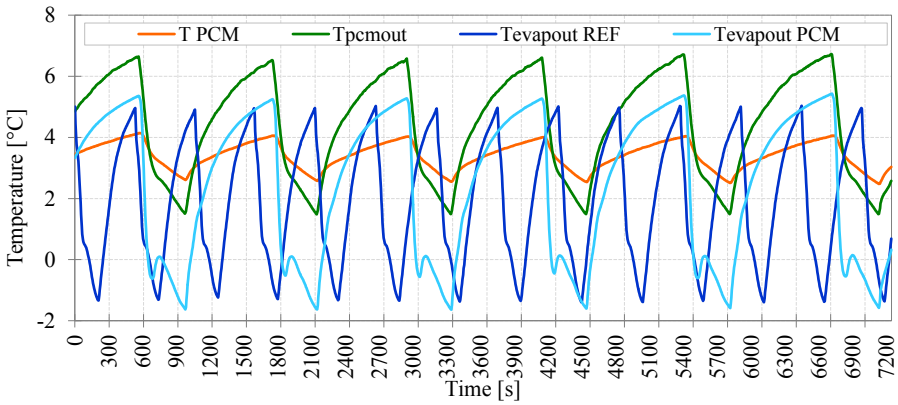

Figure 28: Evaporator outlet air temperature with/without PCM, temperature of PCM and air leaving the air heat exchanger

As shown in Fig. 29 for the reference cold room, the compartment air temperature ranged between 2.6 °C and 4.6 °C and the average temperature was 3.68 °C over a whole cycle. For the novel cold room, the compartment air temperature oscillates between 4 °C and 6 °C and the average temperature was 5 °C. Also in this case it is evident that the PCM air heat exchanger is useful in maintaining the desired thermal conditions into the refrigerated compartment.

Even though the compartment air temperature was in an acceptable range for both with and without PCM, the number of fluctuations over the time was significantly reduced in the PCM added system. In case of without PCM during the "off" period, the compartment air temperature has increased quickly (due to the high heat gain through the wall) and reached sooner the set point temperature. As a result, the compressor started to run quickly. On the other hand, when the PCM air heat exchanger is used the heat gain is absorbed by PCM (due to its latent heat) avoiding a rapid rise in air temperature compartment. The compressor was not triggered quickly. Therefore, the longer "off" time period can be useful in preventing the destructive effect on food quality due to frequent compressor start/stop **(Joybari et al., 2015**).

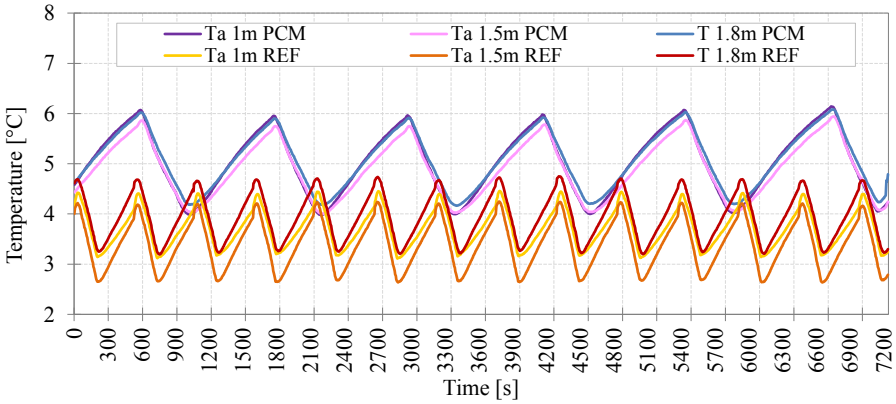

Figure 29: Compartment air temperature with/without PCM

The comparison of the power of compressor between the reference and the novel cold room is shown in Fig. 30. Under two hours of stable operating conditions, the number of the ON/OFF compressor cycles was equal to thirteen in the reference cold room; in the novel cold room was six. The total cycle time was 8.83 min and the ratio ON and OFF time to the total cycle time of the reference cold room was 38% and 62% respectively. Regarding the novel cold room the total cycle time was 19.75 min and the ratio ON and OFF time to the total cycle time were 33% and 67% respectively. Therefore, despite longer compressor ON time in each cycle to charge PCM, the global ON-time percentage ratio decreased from 38% to 33% due to longer compressor OFF time. This phenomenon can be explained as follows:

- During the "ON" period the evaporator outlet air passing through the PCM air heat exchanger absorbs heat from the PCM, which changes its state (solidifies). Therefore, due to the PCM freezing process the ON cycle time increased from 3.33 min to 6.5 min.

- During the "OFF" period the internal temperature compartment increases due to the heat gain form the external environment. Therefore the warmed air passing through the heat exchanger releases heat at PCM, which changes its state (melts). By this way, due to the PCM melting process, the OFF cycle time increased from 5.5 min to 13.25 min.

Thanks to the PCM air heat exchanger, the refrigerating unit energy efficiency was increased and the electric power consumption reduced as well. It is

well known that immediately after the start of the compressor, the electric power is used to get on steady conditions the refrigeration cycle and the cooling capacity is lower. In this lapse time, the refrigerating unit energy efficiency is reduced (**Marques et al., 2014**).

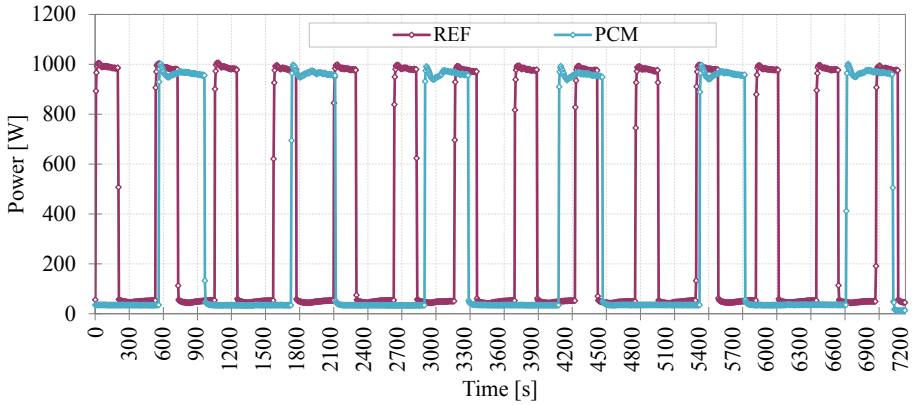

Figure 30: Electrical power consumption with/without PCM

Therefore reducing the number of compressor ON/OFF cycles over time and increasing their length, the period in which the energy efficiency of the refrigerating unit is lower can be reduced. Under two hours of stable operating conditions, the total electric power consumptions of the reference and the novel cold room were 2957.22 (kJ) and 2477.93 (kJ) respectively, which implied that the novel cold room could save energy by about 16% (Fig. 31).

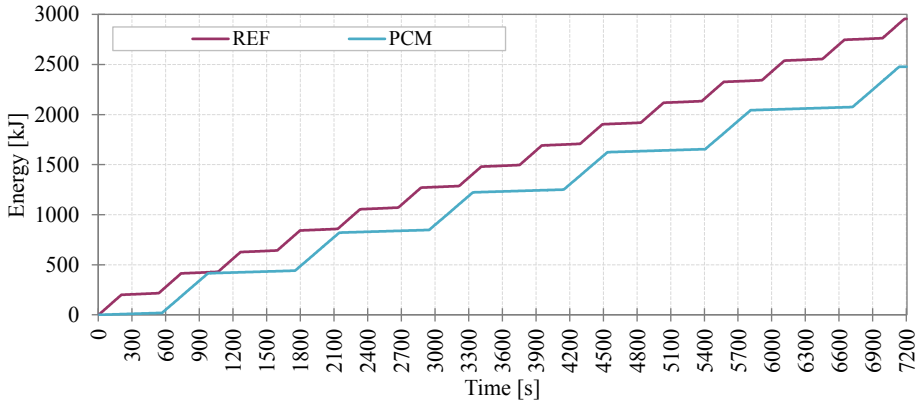

Figure 31: Energy consumption

For discerning individual contribution of the temperature gradient and ON/OFF cycle's reduction on the total electric consumption, further analysis was performed. First consideration is related to the temperature gradient, equal to 27.30 °C and to 29.14 °C for the novel and reference cold room respectively. Secondly, deriving the total electric consumption as a linear function of the temperature gradient we obtained an electrical consumption of 2644.95 kJ, considering the novel cold room operating at the reference ΔT (29.14 °C). This means that the net saving due to the reduction of ON-OFF cycles resulted equal to 10.55%. Finally, by difference, the residual ~ 5.44% reduction derived by the slight decrease of ΔT operating conditions.

3.5 Thermal analysis of a latent heat cold storage in a cold room in case of power outage

3.5.1 Measurement and test conditions

The experimental device consists of a cold room (KLM 20 MISA MINI COLD ROOM) which was previously described in Chapter 2, subparagraph 2.3.3. In order to better understand the PCM beneficial effect on reducing the rate of foodstuff temperature increase, a huge quantity of product has been stored inside the compartment. Specifically, the product used during the experimental test was 160 kg of polyethylene terephthalate (PET) plastic water bottles in order to have a defined quantity of material with known thermal characteristics. This choice was made taking into consideration the water content of fruits and vegetables, where the water makes up about 80% of the body's weight **(ASHRAE, 2006)**. The air temperature inside the cold room, the PCM air heat exchanger temperature and the product temperature (water bottles) were measured and monitored. For this purpose, seventeen between surface and air temperature sensors were located inside the cold room (Fig. 32). The sensor name and location are given in Table 8. Specifically, surface and air temperatures were measured using thermal resistance detectors "PT100" with four-wire connections (0.10 °C accuracy). Product temperature was measured using temperature sensor inserted into the middle of 2-liter bottle and the sensor was the same used for surface and air temperature. Due to the air stratification inside the cold room, an average air temperature (between Ta1m, Ta1.5m and Ta1.8m) was calculated. The heat flux passing through the cold room envelope was measured using a fluxmeter Hukseflux HFP01.

The experimental set-up was equipped with a data logger system (Datataker DT500) linked to a computer for monitoring experimental data. The behaviour of the cold room with and without PCM air heat exchanger was measured and analysed during a typical Italian summer condition (July 2015). Once the compartment temperature was stabilised at an average temperature of 5 °C, a power outage for almost twelve hours, was simulated. The laboratory room of DIISM (Department of Industrial Engineering and Mathematical Science at Università Politecnica delle Marche) was kept at a constant temperature of 32±1 °C. Under this condition, the average cold room compartment's heat loss due to heat transmission resulted approximately equal to 60 W.

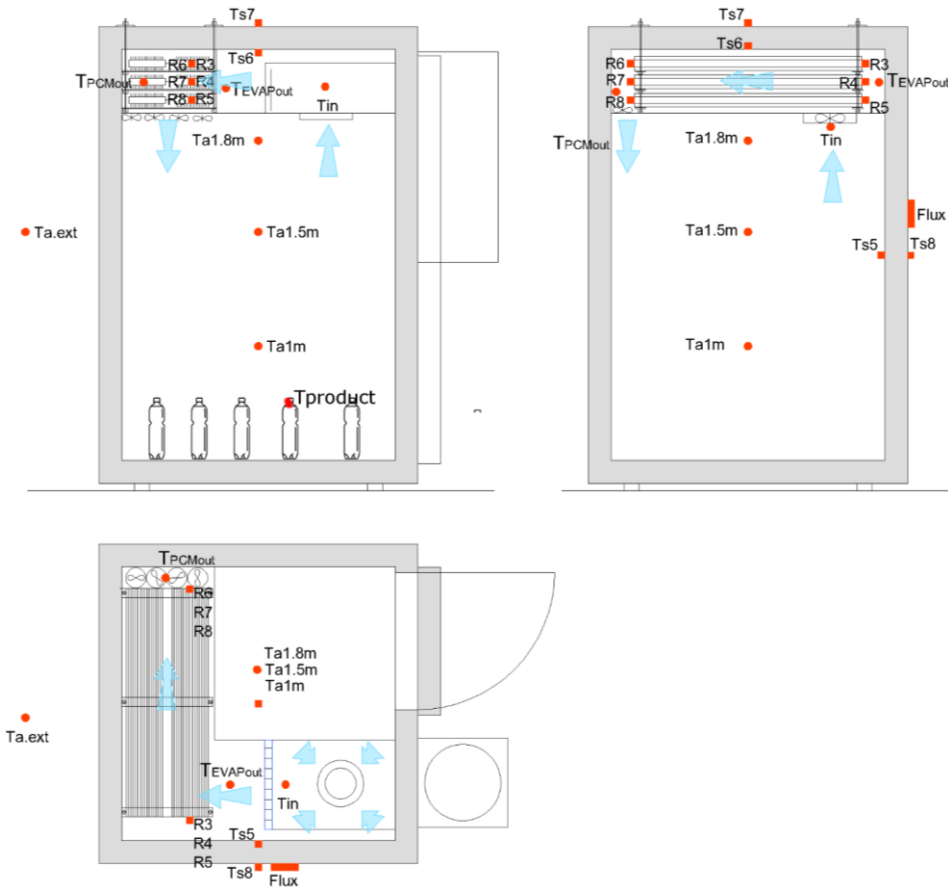

Figure 32: Monitoring system

Table 8: Sensor name and locations

Sensor name	Location
$T_{a\ 1m}$	Compartment air temperature at 1 meter high
$T_{a\ 1.5m}$	Compartment air temperature at 1.5 meter high
$T_{a\ 1.8m}$	Compartment air temperature at 1.8 meter high
$T_{a\ ext}$	External air temperature
T_{in}	Evaporator inlet air temperature
$T_{EVAPout}$	Evaporator outlet air temperature
T_{s6}	Cold room internal surface temperature
T_{s7}	Cold room external surface temperature
T_{S8}	Cold room external surface temperature
T_{R3}	PCM surface temperature
T_{R4}	PCM surface temperature
T_{R5}	PCM surface temperature
T_{R6}	PCM surface temperature
T_{R7}	PCM surface temperature
T_{R8}	PCM surface temperature
T_{PCMout}	Heat exchanger outgoing air temperature
$T_{product}$	PET temperature
Flux	Heat Flux

3.5.2 Results and discussion

Test results of the reference and the novel cold room include the temperatures of cold room compartment air, refrigerated product (160 kg of PET water bottle) and PCM air heat exchanger surface. All these parameters were measured during of 12h-power outage test. Fig. 33 shows the average air temperature inside the cold room with and without PCM during 12 hours of no refrigeration system. The graph shows that the times of the cold room compartment to reach 8 °C were 0.54 h when no PCM was used, instead of 2.08 h when PCM was used. Moreover, with PCM, the cold room took 6.79 h for average air temperature to reach 10 °C as compared to without PCM that took only 1.33 h. It is also worth noting that after 12 hours of power outage the internal compartment temperature of the reference cold room reached the maximum value of 16.89 °C. On the other hand, in the novel cold room the same temperature value resulted equal to 13.83 °C. The inflection point shown at 9.5h is an indication of the complete melting of phase change material. This effect can be better observed in the data line (Fig. 34) describing the phase change material thermal behaviour

(T_{PCM}). It is worth noting that the melting process takes place for almost 9.5 h, during which time the PCM acts as cooling unit.

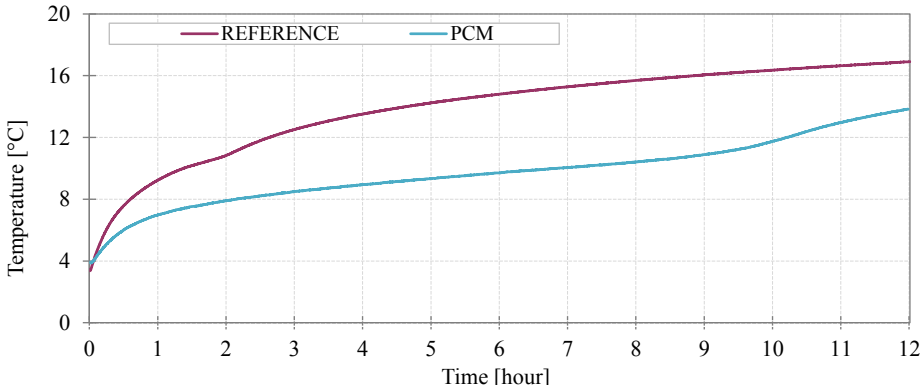

Figure 33: Average air temperature inside the cold room with and without PCM

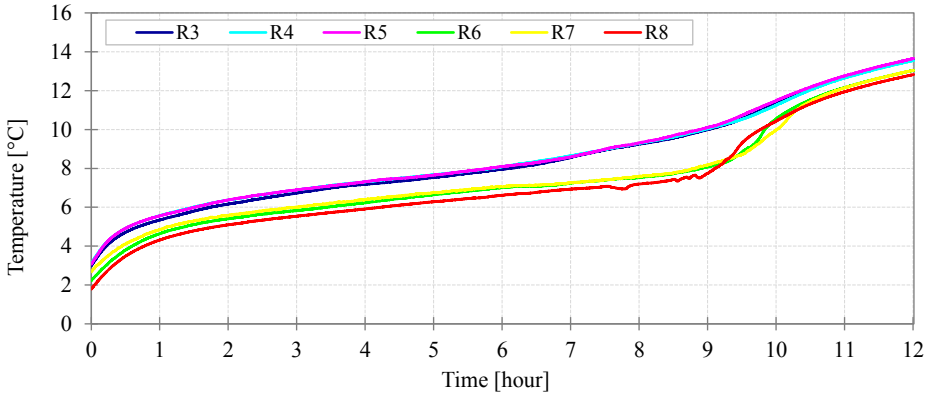

Figure 34: PCM air heat exchanger surface temperature

The PCM benefit in reducing the rate of temperature increase when no refrigeration system is used can be more evident considering the data lines in Fig. 35. The graph shows the rate of compartment temperature increase with and without PCM during the first seven hours of power loss. The graph shows the rate of compartment temperature increase with and without PCM during the first seven hours of power loss. After 0.5 h, the rate of change of temperature in the compartment is resulted equal to 1.67 °C/h for the novel cold room instead of 2.89 °C/h for the reference cold room.

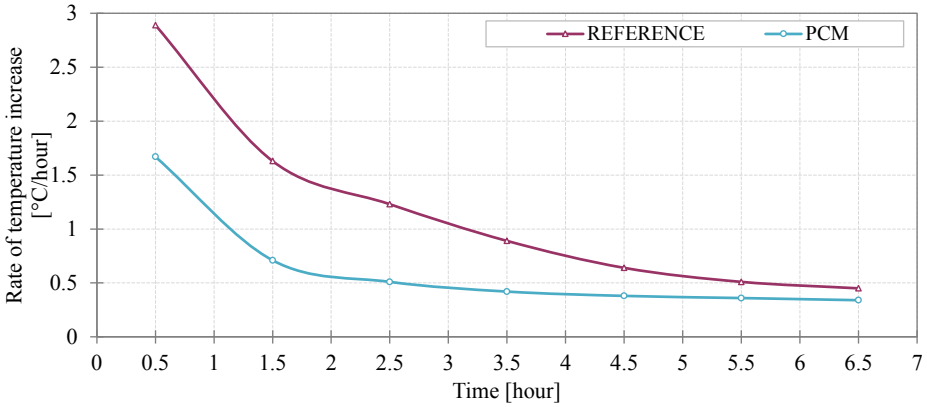

Figure 35: Rate of compartment temperature increase with and without PCM

These results showed that the PCM melting process slowed down the heating rate of the compartment air helping to reduce temperature abuse of refrigerated products as well. It is well known that the preservation of food quality and safety can be achieved when the perishable product is maintained at a storage temperature where metabolic and microbial deterioration are minimised (**Aung and Chang, 2015**). Therefore, maintaining the storage temperature near to the desired holding temperature and reducing the rate of temperature increase represent the most effective ways to protect the perishable foods. The PCM beneficial effect can be observed in Fig. 36 where the detected product temperature in the novel and reference cold room is compared.

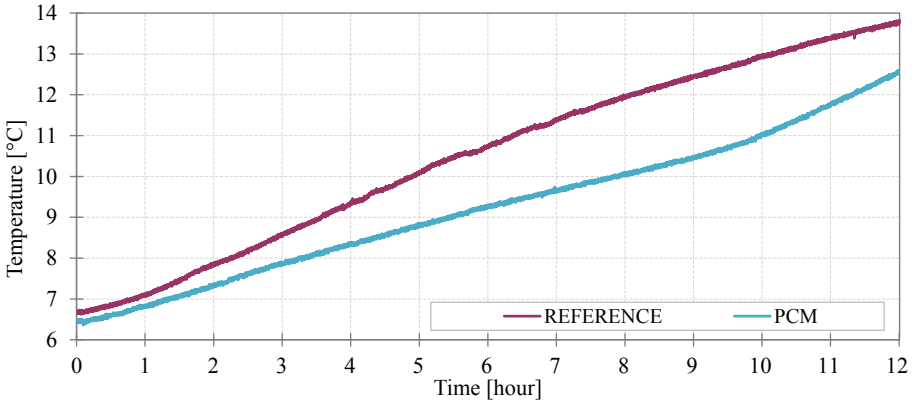

Figure 36: Product temperature with and without PCM

The measurement of the temperature was carried out with a RTD sensor positioned in the middle of the bottle. The graph shows that to reach 7 °C the cold room compartment took 0.97 h when no PCM was used against 2.02 h when PCM was used. Moreover, the rate of product temperature increase resulted faster without phase change material (Fig. 37). After 0.5 h, the rate of change of product temperature resulted equal to 0.35 °C/h for the novel cold room instead of 0.55 °C/h for the reference cold room. The rate continues to rise reaching the value of 0.47 °C/h after 3.5 h, whereas without PCM a value of 0.75 °C/h was reached. Therefore, these results confirm that the purpose of the PCM air heat exchanger is to act as cooling unit reducing and damping out temperature abuse of the stored products.

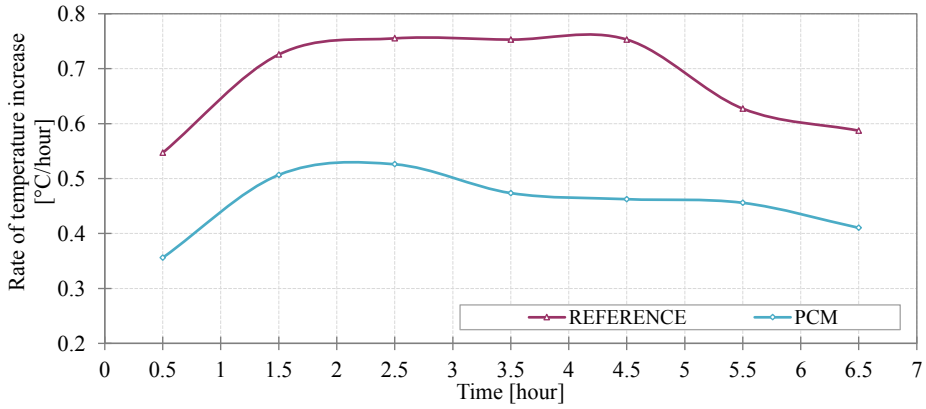

Figure 37: Rate of product temperature increase with and without PCM

3.6 Conclusion

In this experimental study, the performance of a cold room with a novel air heat exchanger containing PCM was investigated. Firstly, experimental activity was devoted to investigate the effect of PCM air heat exchanger on the temperature of the evaporator, cold room compartment and finally on electricity consumption. Results indicate that the PCM freezing/melting process allowed the reduction of compartment temperature fluctuations over time, avoiding the destructive effect of frequent compressor starts and stops on food quality. Moreover, the results clearly show an overlay of two effects that led to a reduction of the overall energy consumption in the novel cold room: the reduction of the compressor ON/OFF cycles (10.55%) and a slight decrease of ΔT operating conditions (5.44%). For further improvement of energy efficiency, the amount and the melting temperature of PCM should be optimized in accordance with heat gain of the cold room at environment temperature. In the later study, the thermal behaviour of a cold room

with and without a PCM latent heat storage system during 12 h of power outage was investigated. Experimental activity was devoted to investigate thermally the effect of PCM air heat exchanger on the temperature of cold room compartment and stored product. Results indicated that the PCM melting process allowed to minimize temperature rise of the air and stored product in the cold room compartment. After 12 h of power outage the maximum compartment temperature value of the novel cold room was 3.06 °C lower than maximum compartment temperature value of the reference cold room. Moreover, a slower rate of both cold room compartment and product temperature increase was observed. In accordance with the results of this work, the presented technology can be considered a valid method for delaying the deterioration of stored products during power outage. In fact, the PCM air heat exchanger acts as cooling unit reducing and damping out the rate of temperature increase inside the cold room compartment. Finally, it is important to underline that the present technology can be easily applicable to other compartments involved in refrigerated goods storage and transport. Obviously future researches should be focused on a deeper analysis aimed to evaluate the effective advantages related to the use PCMs for food conservation. Only in this way will be possible to understand the time requirement to preserve the food quality in a real application.

References

ASHRAE Handbook—Refrigeration (SI) THERMAL PROPERTIES OF FOOD, 2006. Thermal properties of food. Section 9.

Aung, M.M. and Chang, Y.S. 2015. “Temperature management for the quality assurance of a perishable food supply chain.” Food Control. 40,198–207.

Gin, B. and Farid, M.M. 2010. “The use of PCM panels to improve storage condition of frozen food.” J. Food Eng.100, 372–376.

Joybari, M.M., Haghighata, F., Moffat, J., Sra, P., 2015. Heat and cold storage using phase change materials in domestic refrigeration systems: The state-of-the-art review. Energy and Build.106, 111–124.

Leducq, D., Schalbart, P., Trinquet, F., Alvarez, G., Verlinden, B. et al. Thermal energy storage: a key technology for the food cold chain. 23rd IIR International Congress of Refrigeration, Aug 2011, Prague, Czech Republic. 3 p. <hal-00765882>I.S.

Marques, A.C., Davies, G.F., Maidment, G.G., Evans, J.A., Wood, I.D., 2014. Novel design and performance enhancement of domestic refrigerators with thermal storage. App. Therm. Eng. 63, 511–519.

Orò, E., Mirò, L., Farid, M.M., Cabeza, L.F. 2012. “Thermal analysis of a low temperature storage unit using phase change materials without refrigeration system.” Int. J. Refrig. vol. 35, 1709–1714.

4. Effect of door opening on a cold room provided by PCM

4.1 Introduction

After exploited the PCM beneficial effect on reducing the cooling energy required to break down the heat gain determined by surrounding environment, power failure event and to run low efficiency refrigerating unit, the attention was paid to the reduction of infiltration load (door opening). The application of PCM on the internal compartment walls of a cold room, would be an ultimate step in achieving significant energy saving on refrigeration technologies.

Thermal energy storage by using phase change materials is considered the most effective way to reduce energy consumption of refrigeration systems. Specifically the door openings, the defrost cycle and the potential electrical power failure can cause the increase of both compartment air temperature and energy consumption. In fact when a door is opened, due to the temperature differences between the external warm air and the cold compartment air, a heat load is suddenly introduced. In the same way, when a loss of electrical power occurs the heat load coming through the walls determines an increase of the refrigerated compartment temperature. Therefore the refrigeration unit needs to improve the cooling capacity in order to remove this excessive heat loads. In this context the improvement of compartment thermal inertia by using PCM can be considered the most effective way to reduce such thermal load and the electrical energy usage. Therefore the objective of this work is to demonstrate the PCM beneficial effect in terms of both air temperature and energy consumption reduction during such events by experimental approach.

4.2 Experimental set-up

4.2.1 PCM and packaging system

The experimental campaign consists of the same cold room (KLM 20 MISA MINI COLD ROOM) used in Chapter 2, subparagraph 2.3.3. In this study, a paraffin wax with a phase change temperature of 5 °C was used since this temperature is near to the cold room set point temperature (4°C). The used paraffin wax (Rubitherm RT 5 HC) is characterized by a density liquid at 20 °C of 760 (kg/l), heat storage capacity of 240 (kJ/kg) and a heat conductivity of 0.2 [W/(m·K)]. During the experimental activities, the selected PCM was stored in twenty six low density polyethylene containers (21 cm length x 38 cm high x 2 cm depth equal to a 1.6 liter in volume), particularly suited for holding the material during its phase transition. (Fig. 38).

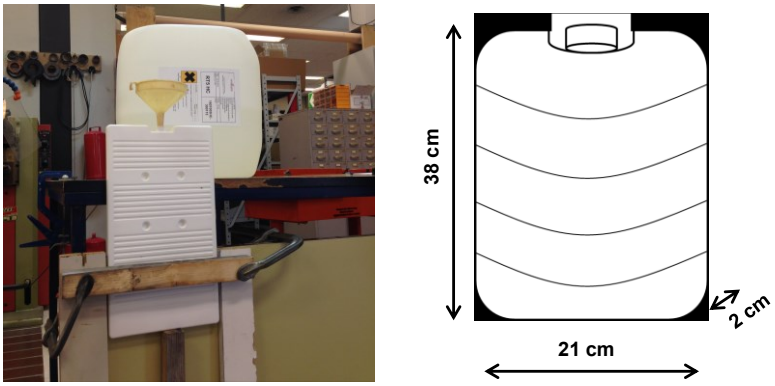

Figure 38: Low density polyethylene panels

Moreover in order to improve heat exchange between the cold outgoing evaporator air and the warm external air that enters during door opening, the PCM panels were placed on the upper compartment walls (Fig. 39).

Figure 39: Low density polyethylene panels positioning

Specifically, ten panels were placed on the central and right compartment walls respectively. Due to the lack of space, only six panels were placed on the left compartment wall.

4.2.2 Temperature measurements

The cold room was instrumented to measure temperature the PCM panels surface and internal cold room compartment. Specifically temperatures were measured using thermal resistance detectors (RTDs) "PT100" with a four-wire connection. The heat flux passing through the cold room envelope was measured using a fluxmeter Hukseflux HFP01. The cold room compressor and additional fan system electricity consumption was measured with a digital wattmeter Christ Elektronik CAC 140. The experimental set-up was equipped with a data logger system (Datataker DT500) linked to a computer for monitoring experimental data. Fig. 40 shows the monitoring system developed. The sensor names and locations are given in Table 9.

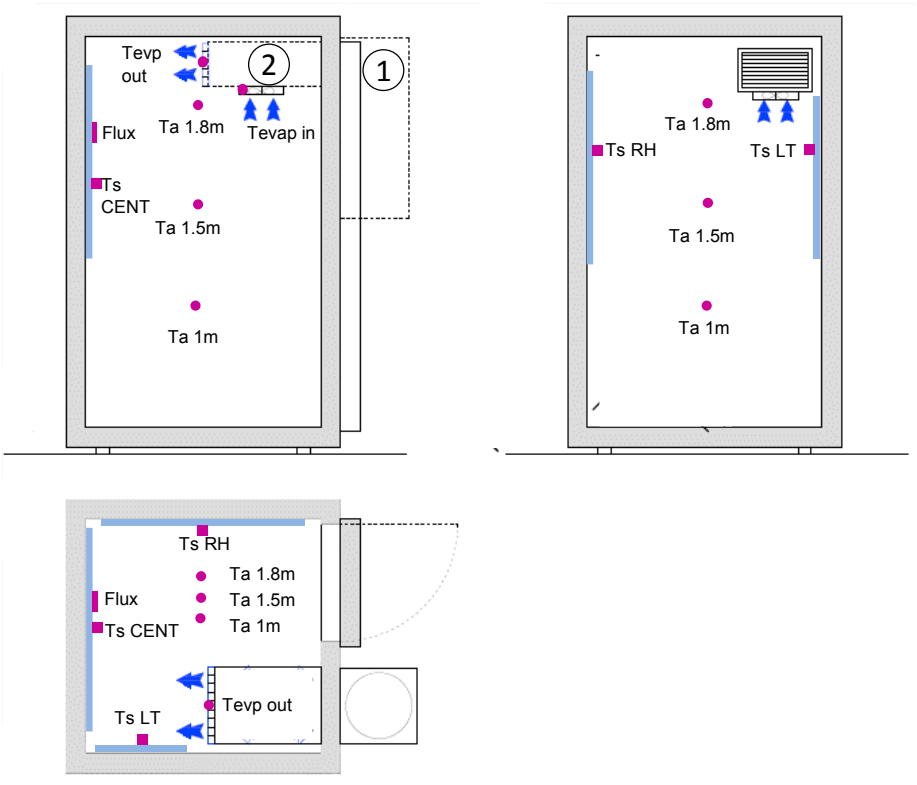

Figure 40: Monitoring system

Table 9: Sensor name and locations

Sensor name	Location
$T_{a\ 1m}$	Compartment air temperature at 1 meter high
$T_{a\ 1.5m}$	Compartment air temperature at 1.5 meter high
$T_{a\ 1.8m}$	Compartment air temperature at 1.8 meter high
$T_{a\ ext}$	External air temperature
$T_{evap\ in}$	Evaporator inlet air temperature
$T_{evap\ out}$	Evaporator outlet air temperature
$T_{s\ CENT}$	PCM panel central surface temperature
$T_{s\ RH}$	PCM panel right surface temperature
$T_{s\ LT}$	PCM panel left surface temperature
Flux	Heat Flux

4.2.3 Test procedure

A series of preliminary tests were carried out in order to find out the optimum operating settings. Consequently, the cold room temperature set point chosen was equal to 4 °C, with a differential temperature of 2 °C. The energy performance test of the cold room was carried out in the "Renewable Energies Laboratory" of Università Politecnica delle Marche. The laboratory room was kept at a constant temperature of 25 ± 1 °C. In order to better understand the PCM beneficial effect on reducing both air temperature and energy consumption, an empty cold room (with and without PCM) was used during the experimentations.

Specifically, testing consisted of three main part. During Part A the cold room was operated with and without PCM at steady state operating conditions in order to understand the effect of PCM addition over the energy consumption. Part B involved door openings with different duration. In this test, door openings were spaced out throughout eight hours period to represent on average how an operator of refrigerated transport, food industry and restaurant may open the cold room during activities such as loading and unloading of large quantities of food stuffs. Specifically, the door was opened three times for a total of five, three and two minutes. Between the three openings the authors waited to restore the steady state operating conditions in order to calculate the effective energy consumption determined by each door opening. Finally Part C was devoted to investigate temperature response to heat loads due to power loss situation. For this study the compressor was switched ''OFF" until the average air temperature reached the maximum extreme value of 10 °C, and then the compressor was restarted. Table 10 outlines the details of the three different parts as mentioned earlier.

Table 10: Experimental procedure

	Without PCM	With PCM
Steady operation Part A	**X**	**X**
Door openings Part B		
5 Minutes	**X**	**X**
3 Minutes	**X**	**X**
2 Minutes	**X**	**X**
Power failure Part C		
1.5 Hour	**X**	**X**

4.3 Results and discussion

4.3.1 Effect of heat load

It is expected that the door openings can cause and increase of energy consumption. In fact when the door is opened, due to the temperature differences between the external warm air and the cold compartment air, a heat load is suddenly introduced. Therefore the refrigeration unit needs to improve the cooling capacity in order to remove this excessive heat load. Fig. 41 shows that the compressor is ‘‘ON” for longer continuous period during the door openings, thus resulting in the higher energy consumptions compared to steady state operating conditions. Looking at Table 11 it is possible to appreciate that without PCM, the energy consumption (in eight hours period) is higher than the steady state conditions by 27.4 %, and with PCM, higher by 25 %. **Liu et al. (2004)** found that door openings (every 40 minutes, with each door opening lasting for 14s) in refrigerator/freezer units resulted in a 10% increase in energy consumption over steady conditions. Moreover, **Gin et al. (2010)** highlighted that eight openings lasting 1 minutes, increase the energy consumption over steady state conditions of about 17% and 11% without and with PCM respectively. **Bansal (2001)** also showed that following door openings, at an ambient temperature of 25 °C, the increase of energy consumption was equal to 10.5-14% with respect to the reference case. Finally **Li et al. (2007)** assessed that the impact of air infiltration in an upright freezer during door openings at 100 seconds intervals, increases the energy consumption by 28%. Literature results are in a quite agreement to those obtained in this work. Energy consumption differences could be due to the prolonged door opening time with respect to the literature reference cases.

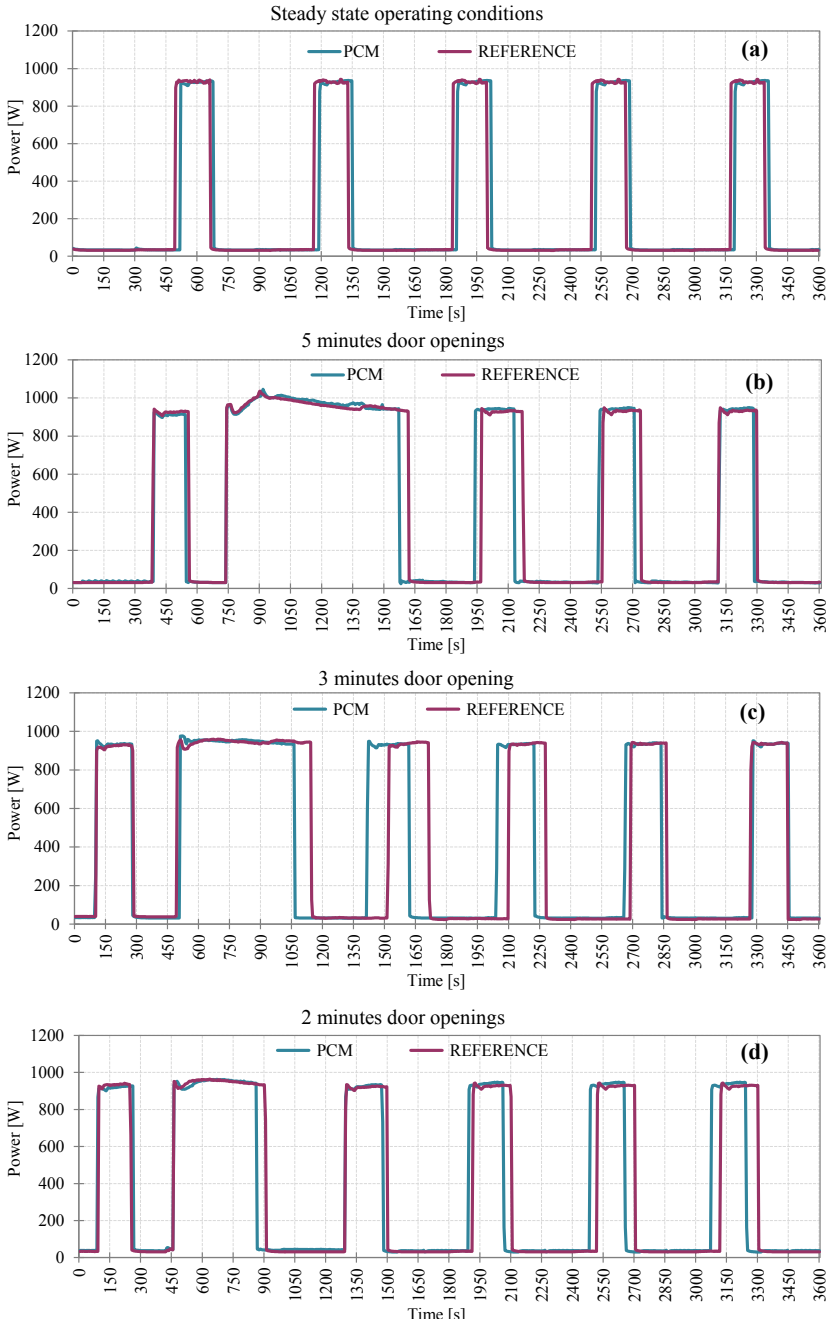

Figure 41: Electric power consumption details

4.3.2 Energy consumption

The comparison of the energy consumption (Table 11) during eight hours of steady state operating conditions, shows that there is a 1.5% difference in the energy consumption with (6808 kJ) and without PCM (6912 kJ). In accordance to **Gin et al. (2010)** the PCM addition into a refrigerated compartment has no significant effect on the energy consumption of a household refrigerator. In fact, in their study the authors found that the difference in energy consumption between the reference and PCM added system was about 1.2%. Therefore we can consider that the 1.5% difference in energy consumption with and without PCM is in accordance to **Gin et al. (2010)** and no significant.

However, as reported in Table 11, some differences in energy consumption between the reference and the novel cold room during door openings were obtained. Therefore, considering eight working hours characterized by three different door openings (5, 3 and 2 minutes) the energy consumption were 8805 [kJ] and 8504 [kJ] without and with PCM (3.4 % lower with PCM).

Table 11: Energy consumption results

REFERENCE	PCM
8 hours of steady state operating conditions	
6912 [kJ]	6808 [kJ]
8 hours of a typical working day	
8802 [kJ]	8504 [kJ]

In order to conduct a deepened study, different energy consumption scenarios have been hypothesized. Specifically the first scenario considers that during a typical working day the door was opened with different durations. Specifically once for a period of five minutes, once for a period of three minutes and five for a period of two minutes. This scenario was designed by considering door openings which normally occurs during refrigerated transport of foodstuff that have to be sold in supermarket. The second scenario considers that during the eight hours of a typical restaurant working day the door was opened six times for three minutes and twice for two minutes. Finally the third scenario considers the cold room usage in the food industry. In this case it can be assumed that door openings occurs for a longer period of time in order to charge and discharge large quantities of food stuff. Therefore this scenario considers six door openings lasting five minutes throughout the eight hours period.

In order to understand the relation between the percentages of door opening time up the operational time and the increase of energy consumption, a correlation analysis was carried out (Fig. 42). The graph perfectly shows a straight-

line relationship between the two considered variables. Therefore, increasing the percentage of door opening time up the operational time, an increase of the energy consumption is expected. Moreover by comparing the two lines it is possible to note that the energy saving absolute value remains almost constant even when the percentage value of the door opening time up the operational time increases. Specifically looking at Fig. 43 it is also worth noting that in all the considered scenarios the PCM addition to the internal compartment walls reduce the energy consumption in a range between 4.4-4.8%. However by improving the door opening time the energy saving is slightly reduced.

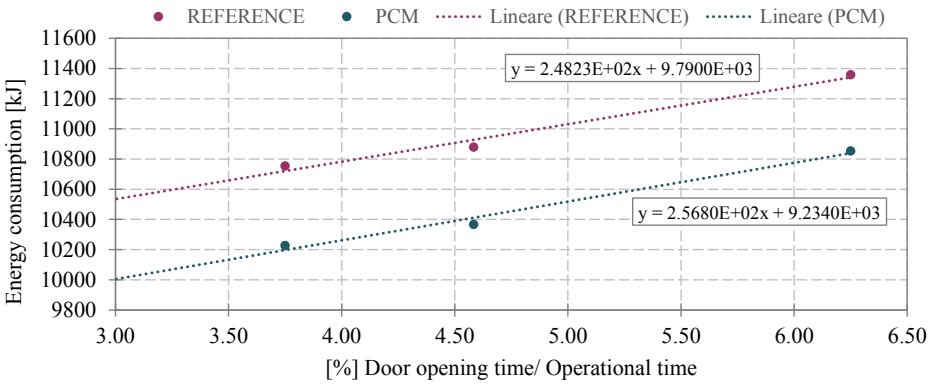

Figure 42: Linear correlation between the between the percentage of door opening time up the operational time and the increase of energy consumption

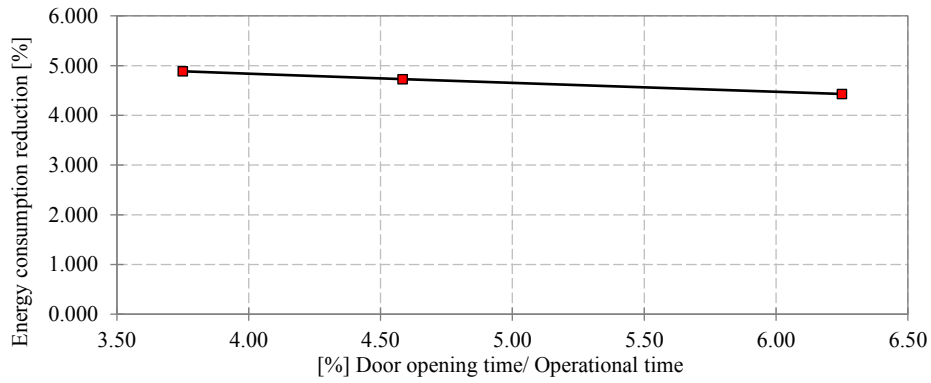

Figure 43: Linear correlation between the percentage of door opening time up the operational time and the increase of energy consumption

To the best of the authors' knowledge promising results have been obtained by integrating PCM internal compartment walls of freezer and household

refrigerators. **Gin et al. (2010)** proposed an investigation into the effectiveness of phase change materials panels inside the internal wall of a freezer in order to reduce energy consumption and temperature variation during door openings, defrost cycle and power failure event. With particular reference to door opening the authors found that the presence of PCM, resulted in a slight lower energy consumption (7% lower with PCM) with respect to reference case. Although the experimental analyses are similar, the results obtained are not comparable due to different boundary conditions and different characteristics of the refrigerated unit and the PCM packaging system. Albeit encouraging, the here presented results should be improved. The slight reduction of the energy reduction might be due to the PCM packaging system. In fact being polyethylene a highly conductive material, a reduced heat exchange between the PCM and the incoming heat load was obtained. For those reasons aluminium containers are recommended. Moreover for further reduction of energy consumption, the amount and the melting temperature of PCM should be optimized in accordance with heat gain of the cold room at environment temperature.

4.3.3 Temperature response during door openings

In this section, temperature response during the door openings was investigated. Fig. 44 plots the average air temperature inside the cold room during door openings lasting five (Fig. 44a), three (Fig. 44b) and two (Fig. 44c) minutes. In each door opening the temperature reached lower values when the PCM was applied to the internal compartment walls. As an example, the peak air temperature reached when the door was opened for five minutes (Fig. 44a) with and without PCM was equal to 15.5 °C and 17.8 °C respectively. This means that the peak air temperature in the novel cold room was reduced by 2.3 °C. Moreover, looking at Fig. 44b it is possible to note a reduction of the compartment peak air temperature of about 1.22 °C in the PCM added system with respect to the reference. Finally, data lines reported in Fig. 44c compare the compartment air temperature trend during door opening lasting two minutes. Also in this case a slight reduction of the compartment peak air temperature can be observed (13 °C without PCM, 12.3 °C with PCM). Overall the results highlight the PCM beneficial effect during door opening test. In fact, it can be assumed that the PCM absorbs the heat load introduced during its phase change from solid to liquid, keeping the compartment air temperature lower than the reference cold room.

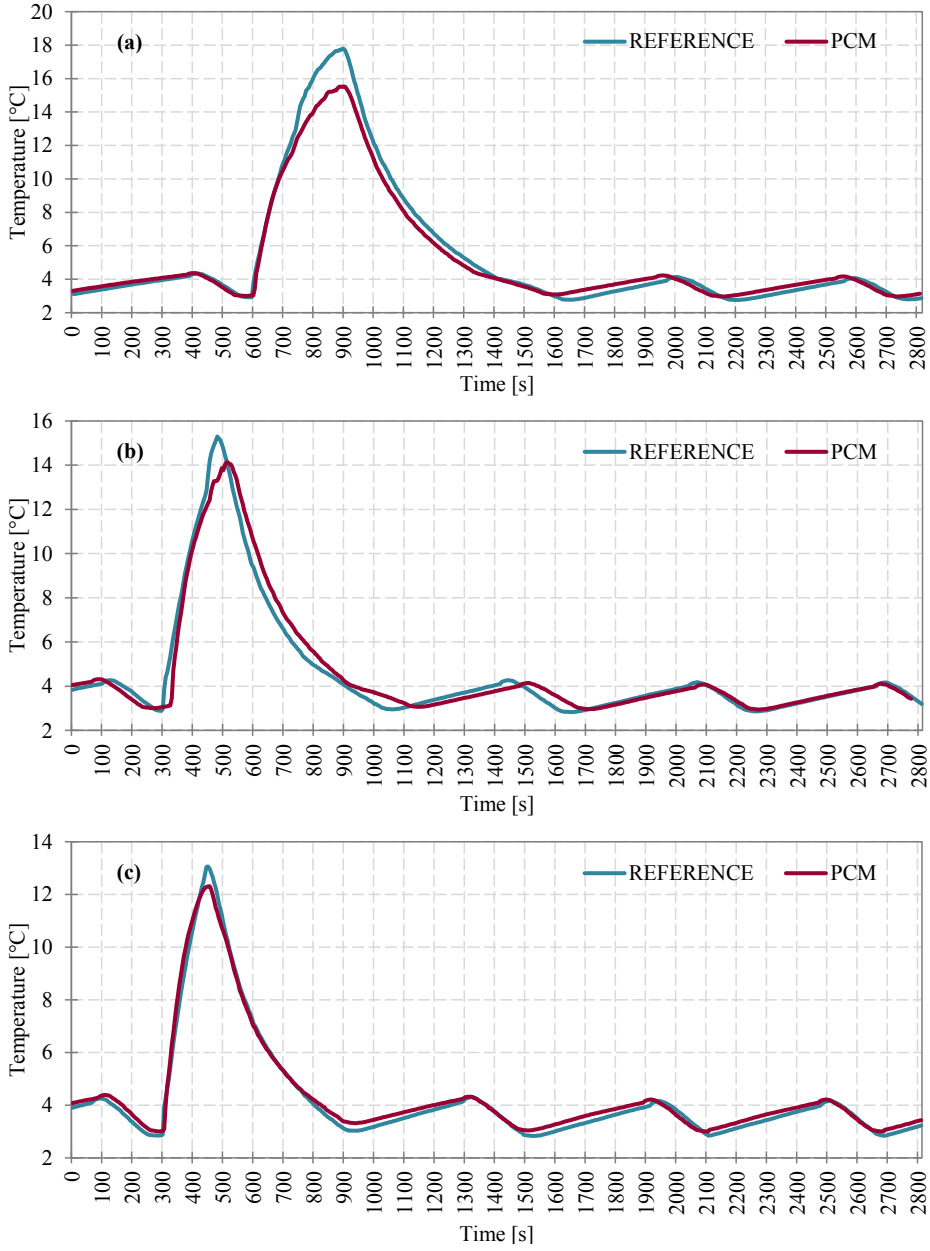

Figure 44: Compartment temperature response during five (a), three (b), and one minutes door openings

The obtained results are in a quite agreement with those obtained by **Orò et al. 2012.** The authors found that the selection of phase change material with a phase change temperature near to the storage temperature can be a valid method to reduce the compartment peak air temperature during a door openings. From Fig. 45 it is possible to appreciate that the phase change materials worked in temperature range near to its phase change temperature.

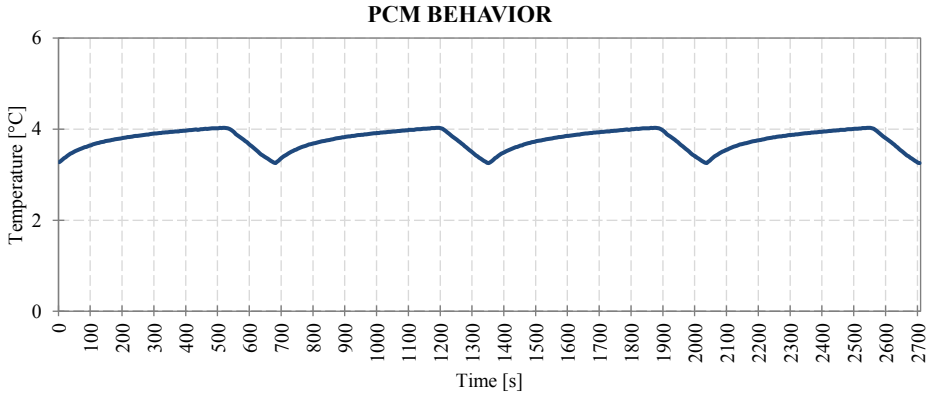

Figure 45: Phase Change Material thermal behaviour during steady state operating conditions

4.3.4 Temperature response during power loss

The cold room compartment temperature change during the event of power loss of almost 1.5 hour was also investigated. This test ("Part C") was done by shutting off the power to the cold room during normal operating conditions. Fig. 46 shows that by using PCM the cold room compartment average air temperature took 31 minutes to reach 6 °C as compared to without PCM which took only 22 minutes. Moreover it also worth noting that after 1.5 hours of electric power failure the average compartment air temperature reached the maximum value of 7.63 °C when the PCM was used. The same numerical value resulted equal to 10.21 °C in the reference case. After 1.5 hours the power to the cold room was resumed. This results shows that the PCM allowed to maintain the compartment air temperature lower for a longer period of time compared to without PCM. This result can be easily understood looking at the data lines reported in Fig. 47 which describe the compartment surface temperature with and without PCM. In fact it is evident that immediately after the power shutdown the PCM at almost 5 °C starts to melt releasing the cold energy stored during the normal operating conditions. This melting occurs at a narrow temperature range as shown by the horizontal lines at almost 5 °C. This means that the PCM acts a major source of cooling when the compressor is OFF. Moreover from the graph it is evident that the PCM did not

melt completely allowing to maintain the compartment temperature at an almost constant temperature for a longer period of time.

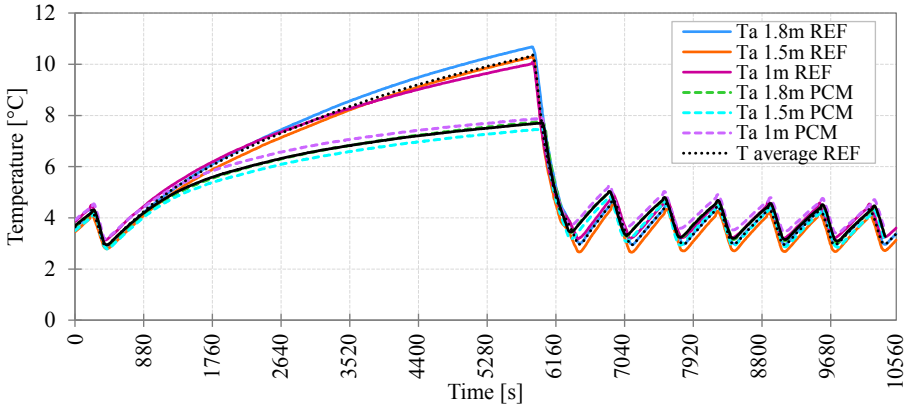

Figure 46: Compartment air temperature trend with/without PCM during power loss

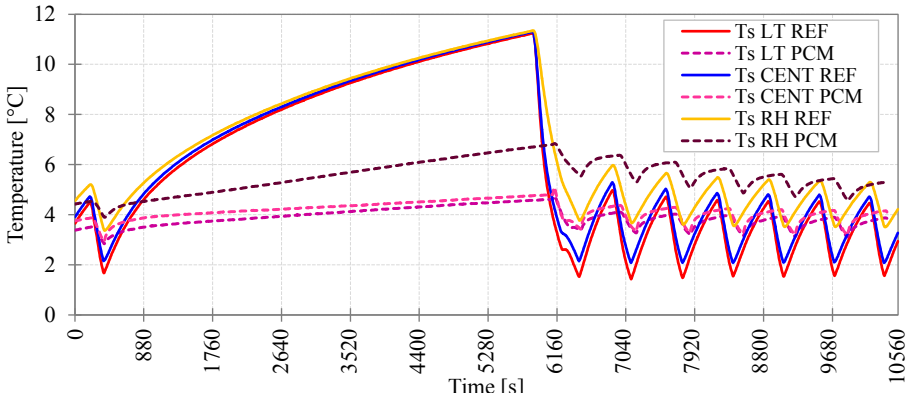

Figure 47: Compartment surface temperature trend with/without PCM during power loss

4.4 Conclusion

In this experimental study, the thermal performance of a cold room with PCM panels inside the refrigerated compartment was investigated. The experimental activity was devoted to investigate the PCM beneficial effect on limiting the peak air temperature and the rate of compartment temperature increase during door openings and power loss events respectively. Test results demonstrated that the PCM acts as cooling unit reducing the peak air temperature of almost 2.3 °C and 0.7 °C during door openings. Moreover the use of PCM reduced the rate of temperature increase during the electrical power failure event. In fact after 1.5 of absence of electrical power the compartment air temperature reached the maximum value of 7.63 °C when the PCM was used, instead of 10.21 °C when no PCM was used. Finally, regarding the energy consumption test during door opening a decrease of energy consumption of about 3.4 % in the PCM added system was reached. Moreover, the different scenarios developed, highlighted an energy saving ranging between 4.4-4.8%. For further improvement of energy saving, the amount and the melting temperature of PCM should be optimized in accordance with heat gain of the cold room at environment temperature.

Acknowledgments The author wants to thank the manufactory CN CONTINENTAL (http://www.cncontinental.it//) for the development of the phase change materials low density polyethylene panels.

References

Bansal PK. 2001. A generic approach to the determination of refrigerator energy efficiency. In: Energy efficiency in household appliances and lighting. Springer; 404–17.

Evans, J. Are doors on fridges the best environmental solution for the retail sector? Surrey, U.K. The Institute of Refrigeration, 2014.

Gin, B., Farid, M.M., Bansal P.K. 2010. Effect of door opening and defrost cycle on a freezer with phase change panels. Energ. Convers Manage. 51: 2698–2706

Li, X., Zhu, D. S., Wang, N., Zeng, X. C. Influence of door openings on temperature fluctuation and energy consumption of refrigerated display cabinet. IIR 22nd International Congress of Refrigeration, Peking, China, 21st - 26th August 2007.

Liu DY, Chang WR, Lin JY. 2004. Performance comparison with effect of door opening on variable and fixed frequency refrigerators/freezers. Appl Therm Eng. 24: 2281–92.

Orlandi, M., Visconi, F. M., Zampini, S. CFD assisted design of closed display cabinets. 2nd IIR. Paris 2013.

Oró, E., Miró, L., Farid, M.M., Cabeza, L.F. 2012. Improving thermal performance offreezers using phase change materials, Int. J. Refrig. 35: 984–991.

5. Predictive tool for optimization of energy consumption in refrigerated transport system

This chapter has been developed in collaboration with ENEA (Italian National Agency for New Technologies, Energy and Sustainable Economic Development) and published at www.enea.it (Principi et al. 2016) Report RdS-PAR2014-039.

5.1 Introduction

The reduction of energy consumption in the transport sector has become a compelling food industry concern mainly due to the increasingly energy costs and the consequent economic value behind the food chain. It is well known that refrigeration units of transport systems run on a vapor compressor system powered by electric current produced by the alternators of the carrying vehicles or by direct connection to the electric grid. Due to the external climatic conditions, door openings, the loading/unloading of cargo and fruits and vegetable respiration rate the internal temperature can be subjected to variations and consequently the compressor works at full charge when it may be not required. All of this aspects can lead to an intensively energy usage with a consequent increase of CO_2 emissions in the atmosphere (**Brito et al., 2014**). In this context, numerical tools for energy usage and global warming impact are considered an effective way for the evaluation of cold chain efficiency and sustainability (**Gwanpua et al., 2015**). By this way, the present work is aimed to give a contribution to the development of an effective methodology that allows to determines which parameters such as door opening, external temperature, products respiration rate and duration of journey have greater influence in energy consumption. Therefore the user will be able to select the most suitable PCM, in terms of phase change temperature and amount, in order to obtain a possible energy saving.

5.2 Numerical tool layout

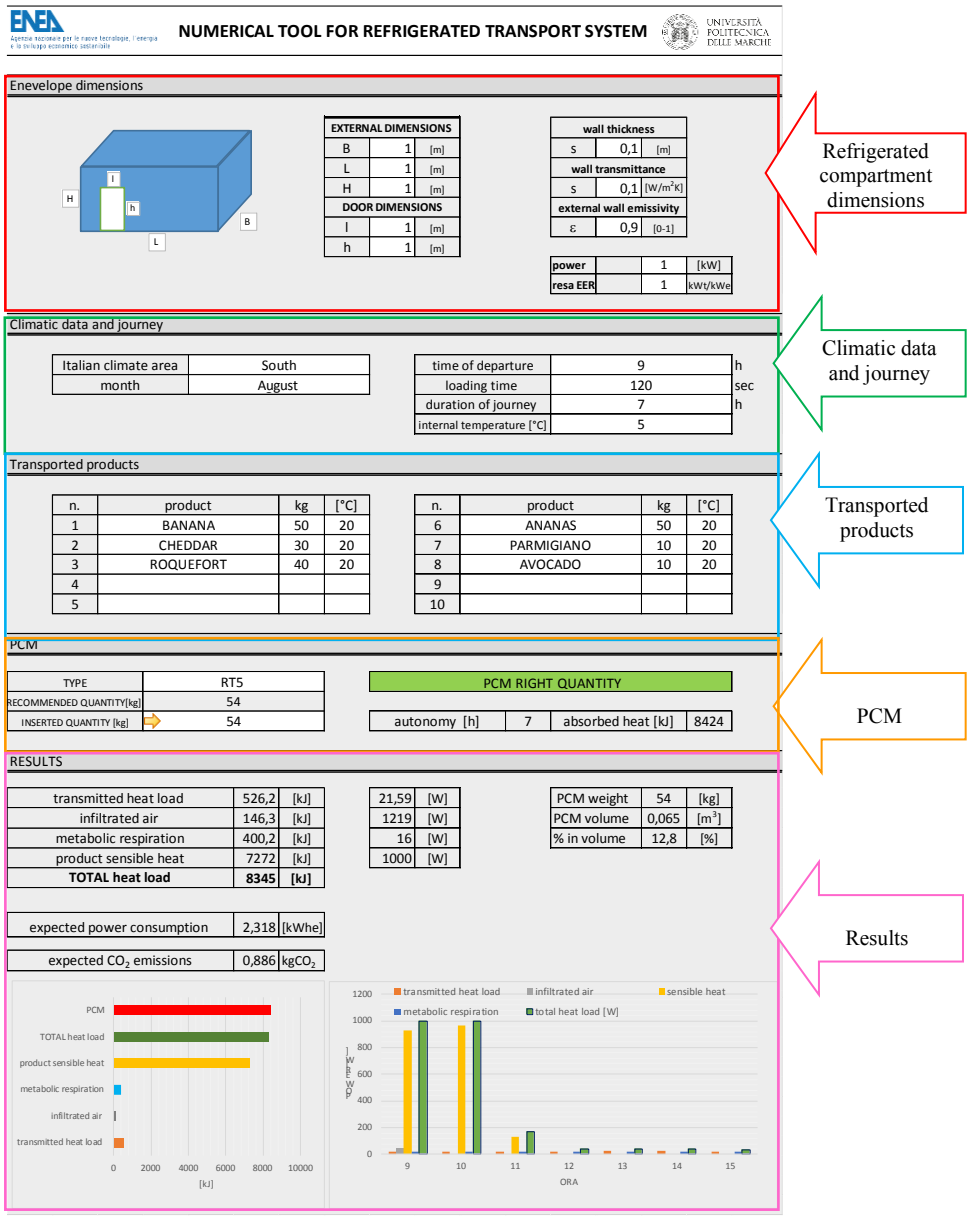

Figure 48: Numerical tool layout

5.3 Organogram

The methodology developed in this work is based on an analytical strategy aimed to determine the total heat load entering inside a refrigerated transport system through several ways. After inserting the input parameters and carefully chosen the operating temperature, it is possible to select the most suitable PCM in terms of absorbed thermal energy capacity. Moreover the numerical tool is able to verify if both the PCM phase change temperature and its amount are compatible with the operating temperature inside the refrigerated compartment. Therefore, by varying one or more data inputs it is possible to estimate the energy consumption and the expected CO_2 emissions therewith associated. This process is illustrated in more detail in Fig. 49.

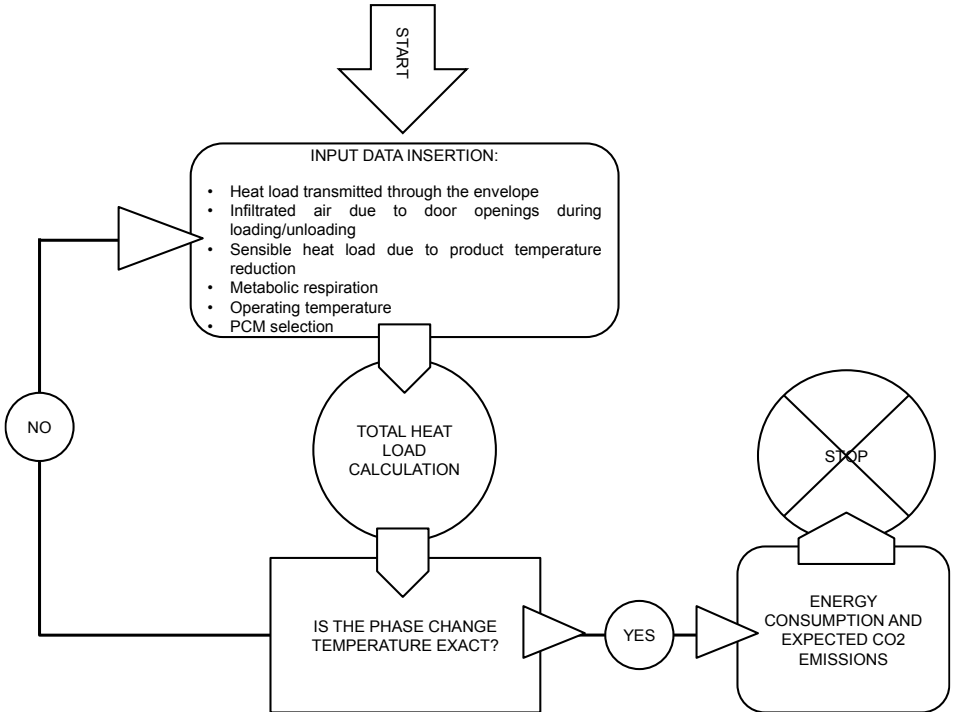

Figure 49: Numerical tool flow chart

5.4 Input data

5.4.1 Envelope dimensions and characteristics

As shown in Fig. 50, the external dimensions of the refrigerated transport system have to be inserted into the box “1”. Specifically, the parameters B, L and H represent the width, the length and the height of the compartment respectively. The door dimensions have to be insert into the box “2”. In the same way the wall thickness, the envelope thermal transmittance and the solar radiation absorption coefficient have to be insert into the box “3”.

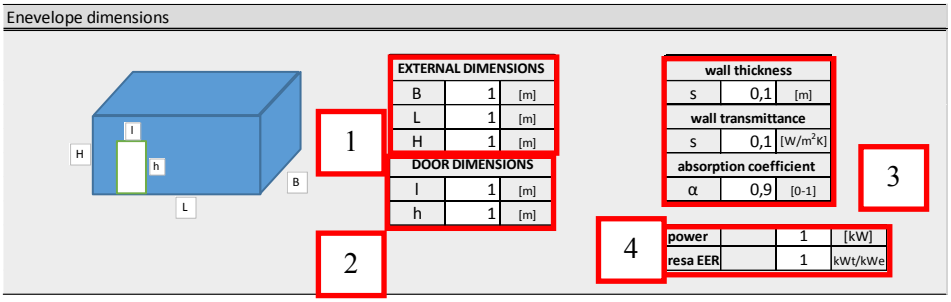

Figure 50: Calculation tool screen detail: envelope dimensions

In absence of the manufacturer technical data it is possible to use the values reported in Table 12.

Table 12: Thermal transmittance values

Thickness [cm]	Thermal transmittance U [W/m²K]
4	0.85
5	0.70
6	0.60
7	0.52
8	0.46
9	0.41
10	0.37
11	0.34
12	0.32
13	0.29
14	0.27
15	0.26
16	0.24
18	0.21
20	0.19

The letter provides a thermal transmittance value as a function of the wall made of insulating material with a thermal conductivity equal to 0.04 W/m2K (average value between polyurethane and polystyrene thermal conductivity UNI 10351).The solar radiation absorption coefficient is a dimensionless parameter ranging from 0 to 1 which represents the absorbed energy fraction respect to that absorbed by a black body. In absence of the radiation absorption coefficient it is possible to use the reported values in Table 13.

Table 13: Radiation absorption coefficient

Surface typology	Radiation absorption coefficient α
asphalt	0.93
galvanized steel	0.90
grey paint	0.75
painted aluminium	0.55
media-painting	0.50
white paint	0.29
chromed metal	0.28
polished aluminium	0.15

5.4.2 Climatic data and journey

The climatic data for the three Italian locations were derived by "**Dati climatici per la progettazione edile ed impiantistica" Appendice 1 alla "Guida al controllo energetico della progettazione" del Consiglio Nazionale delle Ricerche (Roma, 1982)**" and implemented in the numerical tool:

- Milano which represents the climatic area of the Northern part of Italy
- Roma which represents the climatic area of the Central part of Italy
- Messina which represents the climatic area of the Southern part of Italy

For each locations, data like air temperature, relative humidity and irradiation were also inserted in the numerical tool. The tabulated numerical value can be found in the attachment number one at the end of the chapter. Through the selection of the climatic area, the month (box "A", Fig. 51), the time of departure, the loading time and the duration of journey (box "B") it is possible to calculate the transmitted and infiltrated heat load. Finally into box "B" it is possible to insert the internal operating temperature which depends on transported products and refrigeration unit.

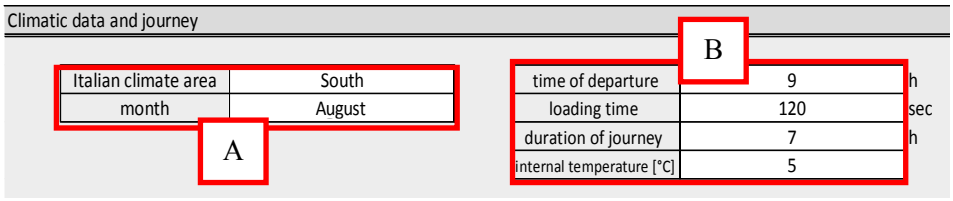

Figure 51: Calculation tool screen detail: climatic data and journey

5.4.3 Transported products

In this section (Fig. 52) it is possible to insert the transported products characteristics such as: the typology (fruits, vegetables, dairy products and met), the quantity and the initial temperature before entering in the refrigerated compartment.

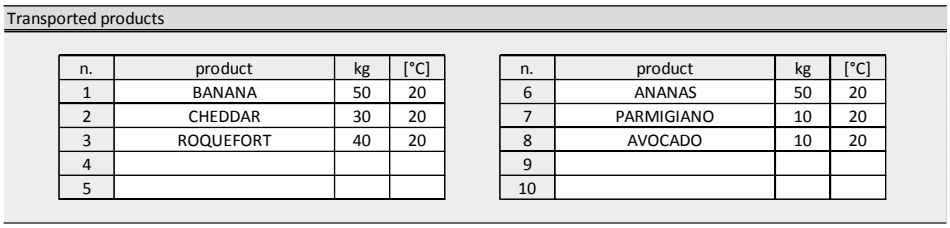

n.	product	kg	[°C]
1	BANANA	50	20
2	CHEDDAR	30	20
3	ROQUEFORT	40	20
4			
5			

n.	product	kg	[°C]
6	ANANAS	50	20
7	PARMIGIANO	10	20
8	AVOCADO	10	20
9			
10			

Figure 52: Calculation tool screen detail: transported products

By this way the numerical tool will be able to define the thermal load released by temperature reduction of products. For fruits and vegetables, it is possible to evaluate the heat emitted through the respiration activity. The tabulated product characteristics are reported in the attachment number two (**2006 ASHRAE Handbook—Refrigeration)**.

5.4.4 PCM selection

In this section it is possible to select the type and the amount of PCM to be used in the analysed application (Fig. 53). Once insert the selected PCM (**from Rubitherm and Climator**), it is possible to know the recommended quantity in order to ensure the autonomy of refrigerated compartment. Furthermore, a message will indicate if the selected PCM is suitable with the internal operating temperature (box “A”). A green and red arrow (box “B”) will indicate if the quantity is less or greater than recommended respectively.

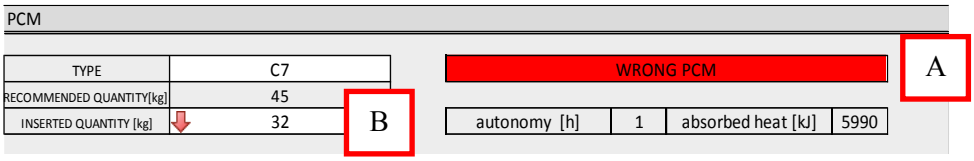

Figure 53: Calculation tool screen detail: PCM selection

5.5 Output data

5.5.1 Transmission heat load

It is well known that the heat gain through walls, floor and ceiling varies depending on the area exposed to a different temperature, the type of insulation and the temperature difference between the refrigerated space and the ambient air **(Çengel et al., 2010)**. Therefore the transmission heat load is determined as follow:

$$Q_{trasm} = \sum_{i=1}^{n} A_i \cdot U_i \cdot (T_e - T_i)$$

where A_i is the i-th element surface [m^2]; U is the i-th element overall heat transfer coefficient [W/m^2K]; T_e is the external temperature [°C] and T_i is the internal temperature [°C].

In order to take into account the combined effect of the temperature difference (between the external and the internal environment) and the solar irradiation the "Sol-air temperature" was used:

$$T_{as} = T_e + \frac{I \cdot a_s}{h_{oe}}$$

where T_e is the external temperature [°C]; I is the solar irradiation [W/m^2]; a_s is the absorption coefficient of the external surface and h_{oe} is the external adduction coefficient [W/m^2K].

In order to evaluate the overall heat transfer coefficient the following equation was used:

$$U = \frac{1}{\frac{1}{h_e} + R_t + \frac{1}{h_i}}$$

where h_i is the internal adduction coefficient and R_t is the sum of the thickness-to-thermal-conductivity ratios of the layers that make up the section under consideration.

5.5.2 Infiltration load

This type of heat load occurs when all the warm air comes into the refrigerated compartment each time the door is opened, because of the differences in air mass density. Therefore the following empirical equation was used **(Holder, 2005)**:

$$v = \frac{4.88 \cdot \sqrt{h \cdot 3.2808} \cdot \sqrt{\Delta T \cdot 1.8 + 32}}{60 \cdot 3.2808} = 0.044903 \cdot \sqrt{h} \cdot \sqrt{\Delta T \cdot 1.8 + 32}$$

where v is the average air velocity through the upper or lower half of door opening [m/s]; h is the door height and ΔT is the difference between the external and internal temperature [°C].

The volume flow rate of air ($\dot{V}_{air}$) entering inside the refrigerated space can be evaluated as follow [m^3/sec]:

$$\dot{V}_{air} = \frac{v \cdot h \cdot l}{2}$$

where l is the door weight [m]; h is the door height [m] and v is the average air velocity through the upper and lower half of door opening [m/s].

The sensible and latent infiltration loads of the cold storage room can be determined from **(Çengel et al., 2010)**:

$$Q_{sensible} = \dot{V}_{air} \cdot \rho \cdot (h_{external} - h_{internal})$$

$$Q_{latent} = \dot{V}_{air} \cdot \rho \cdot h_{fg} \cdot (X_{external} - X_{internal})$$

where V_{air} is the mass flow rate [m^3/sec]; ρ is the air density [kg/m^3]; $h_{external}$ is the enthalpy of external air [J/kg], h_{fg} is the heat of vaporization of water and $h_{internal}$ is the enthalpy of the internal air [J/kg]. Therefore, the total infiltration heat load is equal to:

$$Q_{inf} = Q_{sensibile} + Q_{latente}$$

5.5.3 Product sensible heat

In refrigeration technology lowering the temperature of all transported products implies the release of sensible heat. Therefore, the sensible heat load [kJ] can be calculated as follow (**Çengel et al., 2010**):

$$Q_{sen} = \sum_{i=1}^{n} c_{p,i} \cdot m_i \cdot \left(T_{product,i} - T_{internal}\right)$$

where $C_{p,i}$ is the i-th products sensible heat [kJ/kg*K]; m_i is the i-th products mass [kg]; $T_{products,i}$ is the i-th products temperature when insert into the refrigerated compartment [°C]; $T_{internal}$ is the internal operating temperature [°C]. The sensible heat of products is calculated considering its water content:

$$c_p = 3{,}35 \cdot a + 0{,}48$$

where C_p is the product sensible heat [kJ/kg*K] and a is the product water content [%].

5.5.4 Respiration heat load

In the refrigeration technology the respiration heat load derives from the metabolic activity of fruits and vegetables. The respiration heat load "Q_{resp}" [W] is calculated as follow **(Çengel et al., 2010)**:

$$Q_{resp} = \sum_{i=1}^{n} m_i \cdot \dot{q_{resp}}$$

where m_i is the i-th products mass [kg] and q_{resp} is the average specific heat flux released by metabolic respiration of product [W/kg].

5.5.5 Total energy consumption

According to the principle of energy conservation, the total heat to be removed is equal to the sum of all thermal loads:

$$Q = Q_{transm} + Q_{infiltr} + Q_{sens} + Q_{resp}$$

The numerical tool shows both the numerical and graphical results (Fig. 54).

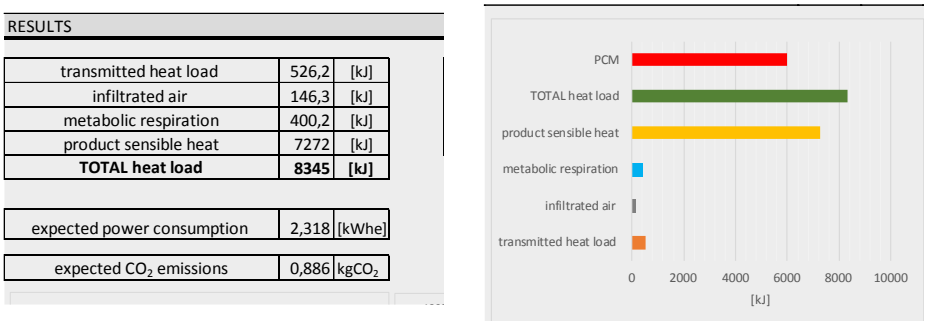

Figure 54: Calculation tool screen detail: results section

5.5.6 Carbon dioxide emission evaluation

Once evaluated the total electric power consumption it is possible to evaluate the related CO_2 emissions. In fact, by using the conversion factor of the Italian electricity mix (0,382 $kgCO_2$/kWhe- **report ISPRA 172/2012 valore 2010)** and multiplying this value with the electricity consumption it is possible to obtain the carbon dioxide value.

5.6 Conclusion

In this study a numerical tool for the optimization of energy consumption in refrigerated transport system has been developed. The proposed numerical tool showed its importance in assessing which parameters such as door opening, external temperature, products respiration rate and duration of journey have a greater influence in energy consumption and related CO_2 emission. Moreover it can be easily used by food logistic companies in order to evaluate and determine which type and amount of PCM is necessary to absorb the estimated heat load. Obviously the numerical tool should be further developed and implemented in order to combine the PCM utilization advantages together with energy and environmental aspects **(Gwanpua et al., 2015)**. Only in this way will be possible to develop efficient transport technologies providing more advanced and sustainable alternatives to the current technologies.

Attachment 1−Climatic Data

Milano: Air temperature [°C]

Hour	January	February	March	April	May	June	July	August	September	October	November	December
1	0,2	1	7,1	10,4	13,7	17,1	19,4	19,5	16,8	11,2	6,8	1,6
2	0,1	0,7	6,9	10	13,2	16,7	18,8	19,1	16,5	11	6,6	1,4
3	0	0,6	6,6	9,5	12,7	16,3	18,3	18,7	16,2	10,8	6,4	1,2
4	-0,3	0,5	6,5	9	12,3	15,9	17,8	18,4	15,9	10,7	6,1	1
5	-0,5	0,4	6,2	8,8	12,3	16	17,9	18,2	15,7	10,5	6,1	0,9
6	-0,7	0,2	6	8,7	12,5	16,5	18,2	18,2	15,5	10,4	6,1	0,8
7	-1	0,1	5,7	8,8	12,9	17,1	18,9	18,4	15,3	10,3	6,3	0,7
8	-1	0,4	6,1	9,9	14,1	18,1	20,2	19,2	16	10,7	6,4	0,9
9	-0,9	1	6,7	11,4	15,8	19,3	22	20,6	17,3	11,3	6,6	1,2
10	-0,7	1,8	7,6	13,5	18,1	20,8	24,2	22,3	19	12,2	6,9	1,6
11	-0,1	2,8	8,5	14,6	19,2	21,8	25,6	23,5	20,2	13,2	7,5	2,3
12	0,7	4,1	9,5	15,4	20,1	22,7	26,7	24,5	21,5	14,4	8,3	3,3
13	1,8	5,5	10,6	16	20,6	23,6	27,6	25,5	22,9	15,7	9,3	4,4
14	2,3	6,4	11,3	16,5	21,1	23,9	28,1	26,1	23,5	16,4	9,7	4,9
15	2,7	7,1	11,7	17	21,4	24	28,3	26,6	23,7	16,9	9,8	5,1
16	3	7,6	12	17,3	21,6	23,8	28,3	26,8	23,6	17,2	9,8	5,1
17	2,8	7	11,8	17	21,2	23,5	27,9	26,4	23	16,6	9,4	4,6
18	2,2	5,9	11,2	16,3	20,6	23,1	27,2	25,5	22	15,6	8,7	3,9
19	1,3	4,2	10,3	15,3	19,6	22,5	26,2	24,1	20,6	14	7,8	2,8
20	0,9	3,4	9,6	14,3	18,5	21,4	25	23,1	19,6	13,3	7,4	2,4
21	0,5	2,8	9	13,1	17,2	20,1	23,6	22	18,6	12,7	7,2	2,2
22	0,3	2,4	8,3	11,8	15,8	18,4	22	20,9	17,6	12,3	7,1	2,2
23	0,1	1,9	7,8	11,1	14,9	17,7	21	20,2	17,1	11,8	6,9	2
24	0,1	1,5	7,4	10,7	14,3	17,3	20,2	19,7	16,9	11,5	6,7	1,7

Relative humidity

Hour	January	February	March	April	May	June	July	August	September	October	November	December
1	92	93	93	90	82	90	76	88	96	99	93	93
2	92	93	94	91	84	91	78	89	96	99	93	94
3	91	93	94	92	85	93	80	90	96	99	93	94
4	91	93	94	93	86	94	81	91	97	99	94	95
5	92	93	94	93	87	94	82	91	97	99	94	95
6	92	92	95	93	87	92	81	91	97	99	94	95
7	93	92	95	92	87	90	79	91	97	99	94	95
8	93	91	94	88	82	86	74	87	95	98	93	95
9	93	89	92	82	74	82	66	82	91	97	92	94
10	93	88	89	74	64	76	56	74	87	95	92	94
11	91	85	85	70	60	72	51	70	82	92	89	91
12	89	80	81	66	57	68	47	66	77	88	86	86
13	85	75	75	64	56	64	45	63	72	83	82	79
14	84	72	72	62	54	62	44	60	69	80	81	77
15	83	69	69	61	52	63	43	58	67	78	80	77
16	82	67	67	61	51	64	44	56	67	76	81	78
17	84	69	68	62	53	66	45	58	70	79	82	79
18	86	74	71	66	55	67	47	63	76	85	85	83
19	89	82	76	71	60	70	51	70	84	93	89	87
20	90	85	80	75	64	74	55	74	89	95	91	89
21	92	88	84	81	69	80	59	79	92	97	92	91
22	93	90	88	87	74	87	65	83	96	98	93	92
23	94	91	91	90	78	90	69	86	97	98	93	93
24	93	92	92	91	80	91	73	88	97	99	93	93

Solar irradiation−South [W/m^2]

Hour	January	February	March	April	May	June	July	August	September	October	November	December
1	0	0	0	0	0	0	0	0	0	0	0	0
2	0	0	0	0	0	0	0	0	0	0	0	0
3	0	0	0	0	0	0	0	0	0	0	0	0
4	0	0	0	0	0	0	0	0	0	0	0	0
5	0	0	0	0	12	19	11	0	0	0	0	0
6	0	0	0	24	44	51	44	25	1	0	0	0
7	0	14	66	72	79	86	80	75	84	14	0	0
8	42	112	163	170	151	142	163	197	223	164	49	12
9	124	191	251	26	244	239	276	315	353	287	152	121
10	176	249	320	339	319	316	367	410	455	377	217	190
11	207	284	364	387	367	367	426	471	520	433	255	228
12	217	297	379	404	384	384	447	492	542	452	268	240
13	207	284	364	387	367	367	426	471	520	433	255	228
14	176	249	320	339	319	316	367	410	455	377	217	190
15	124	191	251	264	244	239	276	315	353	287	152	121
16	42	112	163	170	151	142	163	197	223	164	49	12
17	0	14	66	72	79	86	80	75	84	14	0	0
18	0	0	0	24	44	51	44	25	1	0	0	0
19	0	0	0	0	12	19	11	0	0	0	0	0
20	0	0	0	0	0	0	0	0	0	0	0	0
21	0	0	0	0	0	0	0	0	0	0	0	0
22	0	0	0	0	0	0	0	0	0	0	0	0
23	0	0	0	0	0	0	0	0	0	0	0	0
24	0	0	0	0	0	0	0	0	0	0	0	0

Solar irradiation−West [W/m^2]

Hour	January	February	March	April	May	June	July	August	September	October	November	December
1	0	0	0	0	0	0	0	0	0	0	0	0
2	0	0	0	0	0	0	0	0	0	0	0	0
3	0	0	0	0	0	0	0	0	0	0	0	0
4	0	0	0	0	0	0	0	0	0	0	0	0
5	0	0	0	0	12	19	11	0	0	0	0	0
6	0	0	0	24	44	51	44	25	1	0	0	0
7	0	8	32	59	79	86	80	62	34	8	0	0
8	15	37	65	93	112	119	114	97	70	40	15	6
9	38	63	93	123	140	147	144	129	102	69	39	29
10	56	83	115	145	162	169	166	153	127	92	58	47
11	68	96	129	159	176	183	181	168	143	107	70	59
12	72	100	134	164	181	188	186	173	148	112	74	63
13	106	156	218	268	291	306	329	314	285	210	121	103
14	126	194	282	350	380	403	447	428	395	283	150	125
15	119	206	316	400	437	467	526	500	457	312	145	110
16	54	172	305	406	453	487	551	513	446	261	64	13
17	0	26	211	348	412	451	505	438	301	28	0	0
18	0	0	0	173	293	339	356	211	0	0	0	0
19	0	0	0	0	51	115	58	0	0	0	0	0
20	0	0	0	0	0	0	0	0	0	0	0	0
21	0	0	0	0	0	0	0	0	0	0	0	0
22	0	0	0	0	0	0	0	0	0	0	0	0
23	0	0	0	0	0	0	0	0	0	0	0	0
24	0	0	0	0	0	0	0	0	0	0	0	0

Solar Irradiation−East [W/m^2]

Hour	January	February	March	April	May	June	July	August	September	October	November	December
1	0	0	0	0	0	0	0	0	0	0	0	0
2	0	0	0	0	0	0	0	0	0	0	0	0
3	0	0	0	0	0	0	0	0	0	0	0	0
4	0	0	0	0	0	0	0	0	0	0	0	0
5	0	0	0	0	51	115	58	0	0	0	0	0
6	0	0	0	173	293	339	356	211	0	0	0	0
7	0	26	211	348	412	451	505	438	301	28	0	0
8	54	172	305	406	453	487	551	513	446	261	64	13
9	119	206	316	400	437	467	526	500	457	312	145	110
10	126	194	282	350	380	403	447	428	395	283	150	125
11	106	156	218	268	291	306	329	314	285	210	121	103
12	72	100	134	164	181	188	186	173	148	112	74	63
13	68	96	129	159	176	183	181	168	143	107	70	59
14	56	83	115	145	162	169	166	153	127	92	58	47
15	38	63	93	123	140	147	144	129	102	69	39	29
16	15	37	65	93	112	119	114	97	70	40	15	6
17	0	8	32	59	79	86	80	62	34	8	0	0
18	0	0	0	24	44	51	44	25	1	0	0	0
19	0	0	0	0	12	19	11	0	0	0	0	0
20	0	0	0	0	0	0	0	0	0	0	0	0
21	0	0	0	0	0	0	0	0	0	0	0	0
22	0	0	0	0	0	0	0	0	0	0	0	0
23	0	0	0	0	0	0	0	0	0	0	0	0
24	0	0	0	0	0	0	0	0	0	0	0	0

Solar Irradiation−Horizontal [W/m^2]

Hour	January	February	March	April	May	June	July	August	September	October	November	December
1	0	0	0	0	0	0	0	0	0	0	0	0
2	0	0	0	0	0	0	0	0	0	0	0	0
3	0	0	0	0	0	0	0	0	0	0	0	0
4	0	0	0	0	0	0	0	0	0	0	0	0
5	0	0	0	0	22	41	22	0	0	0	0	0
6	0	0	1	58	127	159	141	65	1	0	0	0
7	0	14	82	180	259	297	296	211	99	14	0	0
8	28	90	189	305	387	431	448	363	246	113	29	11
9	87	167	286	415	499	548	581	498	380	220	95	67
10	135	227	362	499	586	638	685	603	485	305	151	118
11	166	265	409	553	640	695	750	669	551	359	187	151
12	176	278	425	571	659	714	772	692	574	378	199	163
13	166	265	409	553	640	695	750	669	551	359	187	151
14	135	227	362	499	586	638	685	603	485	305	151	118
15	87	167	286	415	499	548	581	498	380	220	95	67
16	28	90	189	305	387	431	448	363	246	113	29	11
17	0	14	82	180	259	297	296	211	99	14	0	0
18	0	0	1	58	127	159	141	65	1	0	0	0
19	0	0	0	0	22	41	22	0	0	0	0	0
20	0	0	0	0	0	0	0	0	0	0	0	0
21	0	0	0	0	0	0	0	0	0	0	0	0
22	0	0	0	0	0	0	0	0	0	0	0	0
23	0	0	0	0	0	0	0	0	0	0	0	0
24	0	0	0	0	0	0	0	0	0	0	0	0

Solar Irradiation−North [W/m^2]

Hour	January	February	March	April	May	June	July	August	September	October	November	December
1	0	0	0	0	0	0	0	0	0	0	0	0
2	0	0	0	0	0	0	0	0	0	0	0	0
3	0	0	0	0	0	0	0	0	0	0	0	0
4	0	0	0	0	0	0	0	0	0	0	0	0
5	0	0	0	0	30	67	33	0	0	0	0	0
6	0	0	46	0	108	138	125	53	1	0	0	0
7	0	8	59	32	104	130	112	62	34	8	0	0
8	15	37	93	65	112	119	114	97	70	40	15	6
9	38	63	123	93	140	147	144	129	102	69	39	29
10	56	83	145	115	162	169	166	153	127	92	58	47
11	68	96	159	129	176	183	181	168	143	107	70	59
12	72	100	164	134	181	188	186	173	148	112	74	63
13	68	96	159	129	176	183	181	168	143	107	70	59
14	56	83	145	115	162	19	166	153	127	92	58	47
15	38	63	123	93	140	147	144	129	102	69	39	29
16	15	37	93	65	112	119	114	97	70	40	15	6
17	0	8	59	32	104	130	112	62	34	8	0	0
18	0	0	46	0	108	138	125	53	1	0	0	0
19	0	0	0	0	30	67	33	0	0	0	0	0
20	0	0	0	0	0	0	0	0	0	0	0	0
21	0	0	0	0	0	0	0	0	0	0	0	0
22	0	0	0	0	0	0	0	0	0	0	0	0
23	0	0	0	0	0	0	0	0	0	0	0	0
24	0	0	0	0	0	0	0	0	0	0	0	0

Roma: Air temperature [°C]

Hour	January	February	March	April	May	June	July	August	September	October	November	December
1	5,6	6	8,1	10	13,4	17,5	20,3	20,8	18	13,4	10,9	7,5
2	5,4	5,7	7,8	9,6	13,1	17,1	19,7	20,3	17,6	12,8	10,6	7,4
3	5,2	5,4	7,4	9,3	12,8	16,8	19,2	19,8	17,2	12,3	10,1	7,3
4	5,1	5,2	7	9,1	12,6	16,4	18,8	19,3	16,8	11,8	9,6	7,2
5	5,1	5	6,8	9	12,9	16,8	19,1	19,2	16,5	11,5	9,4	7
6	5,3	4,9	6,6	9	13,4	17,5	19,7	19,3	16,4	11,3	9,3	6,9
7	5,5	4,9	6,6	9,2	14,3	18,6	20,6	19,6	16,3	11,1	9,3	6,6
8	5,9	5,5	7,5	10,5	15,7	19,9	22,2	21	17,8	12,2	9,9	6,8
9	6,5	6,6	9	12,6	17,7	21,4	24,1	23,2	20,1	14,1	11	7,2
10	7,2	8	11,1	15,3	20,1	23,2	26,5	26	23,2	16,6	12,5	7,8
11	8,2	9,2	12,3	16,4	21,2	24,2	27,9	27,4	24,8	18,4	13,7	8,6
12	9,6	10,5	13,4	17,2	21,8	25	28,9	28,5	26,1	20,2	15	9,6
13	11,1	11,8	14,4	17,6	22	25,5	29,7	29,2	27	21,9	16,4	10,8
14	11,6	12,3	14,7	17,7	22,1	25,6	29,9	29,4	27,3	22,4	16,8	11,2
15	11,8	12,4	14,6	17,6	21,9	25,4	29,7	29,3	27	22,2	16,8	11,3
16	11,5	12,2	14,1	17,1	21,5	24,8	29,1	28,7	26,2	21,4	16,3	11,1
17	10,8	11,5	13,4	16,4	20,8	24,2	28,4	28	25,2	20,4	15,5	10,6
18	9,6	10,4	12,3	15,4	19,8	23,6	27,4	26,9	23,8	18,8	14,3	9,8
19	8	8,9	10,9	14,2	18,6	22,7	26,2	25,6	22,1	16,9	12,7	8,7
20	7,4	8,2	10,1	13,3	17,5	21,7	25	24,6	21,1	16	12	8,3
21	7	7,6	9,6	12,5	16,3	20,5	23,7	23,5	20,2	15,3	11,6	7,9
22	6,9	7,2	9,2	11,8	15	19,1	22,2	22,5	19,6	15	11,5	7,7
23	6,6	6,9	8,8	11,1	14,2	18,3	21,4	21,7	19	14,4	11,3	7,5
24	6,3	6,5	8,5	10,6	13,7	17,9	20,7	21,2	18,5	13,7	11,1	7,3

Relative humidity

Hour	January	February	March	April	May	June	July	August	September	October	November	December
1	88	87	77	82	86	89	78	82	85	88	87	84
2	89	88	79	84	87	90	80	83	86	90	88	84
3	89	89	81	86	87	91	82	85	87	91	89	84
4	90	90	83	88	88	92	84	87	88	92	90	84
5	90	91	83	88	88	91	83	87	89	93	91	85
6	89	90	83	89	88	89	81	86	89	92	91	86
7	89	89	81	89	87	86	78	85	90	91	91	87
8	88	88	78	84	81	79	71	80	85	88	89	87
9	86	85	74	77	72	71	62	72	76	83	86	85
10	84	82	69	66	59	61	51	61	64	77	82	83
11	80	76	64	62	55	57	46	56	58	71	77	81
12	74	68	59	58	54	55	43	53	53	64	73	78
13	68	59	54	56	56	54	42	51	48	57	67	74
14	65	56	53	55	56	54	41	49	48	56	66	73
15	64	57	54	56	56	55	42	49	49	57	66	72
16	64	59	57	58	56	58	44	51	53	60	67	72
17	66	63	61	62	59	61	47	54	59	65	71	74
18	72	68	66	67	64	64	51	59	66	71	77	77
19	80	75	72	74	70	68	56	65	75	80	84	81
20	82	79	74	76	75	74	61	70	79	83	86	82
21	84	81	76	78	80	80	67	75	81	85	87	83
22	84	83	76	79	85	88	73	81	82	85	86	83
23	85	85	77	80	87	90	76	83	83	86	86	84
24	86	86	77	82	88	90	78	83	85	87	87	84

Solar Irradiation−South [W/m^2]

Hour	January	February	March	April	May	June	July	August	September	October	November	December
1	0	0	0	0	0	0	0	0	0	0	0	0
2	0	0	0	0	0	0	0	0	0	0	0	0
3	0	0	0	0	0	0	0	0	0	0	0	0
4	0	0	0	0	0	0	0	0	0	0	0	0
5	0	0	0	0	7	12	6	0	0	0	0	0
6	0	0	0	23	41	46	37	21	1	0	0	0
7	0	29	75	68	79	83	73	65	93	33	0	0
8	117	158	186	175	145	125	144	202	250	226	127	65
9	260	257	287	277	252	235	269	337	395	378	292	241
10	351	330	365	359	339	324	370	446	508	489	398	344
11	405	375	415	411	395	382	436	516	581	558	459	402
12	423	390	432	429	414	401	458	540	605	581	480	421
13	405	375	415	411	395	382	436	516	581	558	459	402
14	351	330	365	359	339	324	370	446	508	489	398	344
15	260	257	287	277	252	235	269	337	395	378	292	241
16	117	158	186	175	145	125	144	202	250	226	127	65
17	0	29	75	68	79	83	73	65	93	33	0	0
18	0	0	0	23	41	46	37	21	1	0	0	0
19	0	0	0	0	7	12	6	0	0	0	0	0
20	0	0	0	0	0	0	0	0	0	0	0	0
21	0	0	0	0	0	0	0	0	0	0	0	0
22	0	0	0	0	0	0	0	0	0	0	0	0
23	0	0	0	0	0	0	0	0	0	0	0	0
24	0	0	0	0	0	0	0	0	0	0	0	0

Solar Irradiation−West [W/m^2]

Hour	January	February	March	April	May	June	July	August	September	October	November	December
1	0	0	0	0	0	0	0	0	0	0	0	0
2	0	0	0	0	0	0	0	0	0	0	0	0
3	0	0	0	0	0	0	0	0	0	0	0	0
4	0	0	0	0	0	0	0	0	0	0	0	0
5	0	0	0	0	7	12	6	0	0	0	0	0
6	0	0	0	23	41	46	37	21	1	0	0	0
7	0	12	35	61	79	83	73	58	35	11	0	0
8	23	45	72	99	115	118	108	95	73	48	23	13
9	52	75	104	131	146	149	139	128	108	82	53	41
10	75	98	129	156	171	172	162	153	134	108	77	64
11	89	113	144	172	186	187	177	168	151	125	93	78
12	94	118	150	177	191	192	182	174	156	131	98	83
13	179	200	254	298	332	343	359	354	325	268	197	165
14	239	261	335	395	448	468	506	503	461	375	267	220
15	252	287	380	455	525	552	607	601	543	426	283	220
16	159	253	371	464	548	581	642	624	539	376	174	82
17	0	66	263	396	499	538	588	534	373	79	0	0
18	0	0	0	180	339	390	396	235	0	0	0	0
19	0	0	0	0	19	79	19	0	0	0	0	0
20	0	0	0	0	0	0	0	0	0	0	0	0
21	0	0	0	0	0	0	0	0	0	0	0	0
22	0	0	0	0	0	0	0	0	0	0	0	0
23	0	0	0	0	0	0	0	0	0	0	0	0
24	0	0	0	0	0	0	0	0	0	0	0	0

Solar Irradiation−East [W/m^2]

Hour	January	February	March	April	May	June	July	August	September	October	November	December
1	0	0	0	0	0	0	0	0	0	0	0	0
2	0	0	0	0	0	0	0	0	0	0	0	0
3	0	0	0	0	0	0	0	0	0	0	0	0
4	0	0	0	0	0	0	0	0	0	0	0	0
5	0	0	0	0	19	79	19	0	0	0	0	0
6	0	0	0	180	339	390	396	235	0	0	0	0
7	0	66	263	396	499	538	588	534	373	79	0	0
8	159	253	371	464	548	581	642	624	539	376	174	82
9	252	287	380	455	525	552	607	601	543	426	283	220
10	239	261	335	395	448	468	506	503	461	375	267	220
11	179	200	254	298	332	343	359	354	325	268	197	165
12	94	118	150	177	191	192	182	174	156	131	98	83
13	89	113	144	172	186	187	177	168	151	125	93	78
14	75	98	129	156	171	172	162	153	134	108	77	64
15	52	75	104	131	146	149	139	128	108	82	53	41
16	23	45	72	99	115	118	108	95	73	48	23	13
17	0	12	35	61	79	83	73	58	35	11	0	0
18	0	0	0	23	41	46	37	21	1	0	0	0
19	0	0	0	0	7	12	6	0	0	0	0	0
20	0	0	0	0	0	0	0	0	0	0	0	0
21	0	0	0	0	0	0	0	0	0	0	0	0
22	0	0	0	0	0	0	0	0	0	0	0	0
23	0	0	0	0	0	0	0	0	0	0	0	0
24	0	0	0	0	0	0	0	0	0	0	0	0

Solar Irradiation−Horizontal [W/m^2]

Hour	January	February	March	April	May	June	July	August	September	October	November	December
1	0	0	0	0	0	0	0	0	0	0	0	0
2	0	0	0	0	0	0	0	0	0	0	0	0
3	0	0	0	0	0	0	0	0	0	0	0	0
4	0	0	0	0	0	0	0	0	0	0	0	0
5	0	0	0	0	12	26	11	0	0	0	0	0
6	0	0	1	56	129	159	135	60	1	0	0	0
7	0	23	97	197	290	327	317	234	115	23	0	0
8	56	125	228	343	449	491	498	420	291	159	58	28
9	155	226	346	472	588	635	658	586	452	300	167	119
10	237	306	437	571	689	746	782	714	578	413	258	200
11	289	356	495	634	764	816	860	796	657	484	317	252
12	307	373	514	656	787	840	886	823	684	508	337	269
13	289	356	495	634	764	816	860	796	657	484	317	252
14	237	306	437	571	696	746	782	714	578	413	258	200
15	155	226	346	472	588	635	658	586	452	300	167	119
16	56	125	228	343	449	491	498	420	291	159	58	28
17	0	23	97	197	290	327	317	234	115	23	0	0
18	0	0	1	56	129	159	135	60	1	0	0	0
19	0	0	0	0	12	26	11	0	0	0	0	0
20	0	0	0	0	0	0	0	0	0	0	0	0
21	0	0	0	0	0	0	0	0	0	0	0	0
22	0	0	0	0	0	0	0	0	0	0	0	0
23	0	0	0	0	0	0	0	0	0	0	0	0
24	0	0	0	0	0	0	0	0	0	0	0	0

Solar Irradiation−North [W/m^2]

Hour	January	February	March	April	May	June	July	August	September	October	November	December
1	0	0	0	0	0	0	0	0	0	0	0	0
2	0	0	0	0	0	0	0	0	0	0	0	0
3	0	0	0	0	0	0	0	0	0	0	0	0
4	0	0	0	0	0	0	0	0	0	0	0	0
5	0	0	0	0	13	47	12	0	0	0	0	0
6	0	0	47	0	122	156	136	55	1	0	0	0
7	0	12	61	35	123	153	128	58	35	11	0	0
8	23	45	99	72	115	118	108	95	73	48	23	13
9	52	75	131	104	146	149	139	128	108	82	53	41
10	75	98	156	129	171	172	162	153	134	108	77	64
11	89	113	172	144	186	187	177	168	151	125	93	78
12	94	118	177	150	191	192	182	174	156	131	98	83
13	89	113	172	144	186	187	177	168	151	125	93	78
14	75	98	156	129	171	172	162	153	134	108	77	64
15	52	75	131	104	146	149	139	128	108	82	53	41
16	23	45	99	72	115	118	108	95	73	48	23	13
17	0	12	61	35	123	153	128	58	35	11	0	0
18	0	0	47	0	122	156	136	55	1	0	0	0
19	0	0	0	0	13	47	12	0	0	0	0	0
20	0	0	0	0	0	0	0	0	0	0	0	0
21	0	0	0	0	0	0	0	0	0	0	0	0
22	0	0	0	0	0	0	0	0	0	0	0	0
23	0	0	0	0	0	0	0	0	0	0	0	0
24	0	0	0	0	0	0	0	0	0	0	0	0

Messina: Air temperature [°C]

Hour	January	February	March	April	May	June	July	August	September	October	November	December
1	10	11,7	11,4	13	17	20,1	23,5	24,3	22,4	17,7	15,1	12,8
2	9,9	11,6	11,4	12,9	16,9	19,9	23,3	24,2	22,3	17,6	15	12,8
3	9,9	11,4	11,5	12,7	16,7	19,6	23,2	24	22,2	17,4	14,8	12,8
4	9,9	11,2	11,6	12,7	16,5	19,3	23,1	24	21,1	17,4	14,7	13
5	9,9	11,2	11,6	12,7	16,6	19,4	23,1	23,9	22	17,2	14,6	12,9
6	9,9	11,1	11,5	12,8	16,9	19,7	23,4	23,8	21,9	17,1	14,7	12,9
7	10	11	11,5	13	17,3	20,3	23,7	23,8	21,9	16,9	14,7	12,7
8	10,3	11,3	11,9	13,6	18	21	24,3	24,7	22,5	17,6	15,3	12,9
9	10,8	11,9	12,5	14,3	19	21,8	25,2	25,9	23,4	18,9	16,1	13,1
10	11,4	12,6	13,4	15,3	20,3	22,9	26,3	27,7	24,6	20,5	17,1	13,5
11	11,8	12,9	13,8	15,9	20,8	23,5	27	28,3	25,1	21	17,7	13,8
12	12,2	13,2	14	16,3	21,1	24,1	27,6	28,7	25,5	21,2	18,2	14,1
13	12,5	13,5	14,1	16,5	21,2	24,5	28,1	28,7	25,8	21	18,5	14,8
14	12,6	13,6	14,1	16,6	21,1	24,6	28,2	28,7	25,6	20,9	18,6	14,5
15	12,5	13,6	14,2	16,4	20,8	24,5	28	28,4	25,1	20,7	18,5	14,4
16	12,2	13,5	14,1	16,1	20,4	24,1	27,5	28	24,3	20,3	18,2	14,2
17	11,9	13,2	13,8	15,7	20	23,6	27	27,6	24	20	17,7	14
18	11,5	12,8	13,3	15,2	19,6	22,9	26,4	27	23,7	19,5	17	13,7
19	11,1	12,3	12,7	14,7	19,1	22	25,6	26,4	23,6	19	16	13,3
20	10,9	12,1	12,4	14,4	18,7	21,5	25,1	25,9	23,3	18,7	15,7	13,2
21	10,7	12	12,1	14,2	18,3	21,1	24,6	25,5	22,8	18,5	15,4	13,1
22	10,5	12	11,9	14,1	18	20,8	24,1	25,1	22,3	18,3	15,4	13,1
23	10,4	11,9	11,8	13,8	17,8	20,6	23,8	24,8	22,2	18,1	15,3	13
24	10,3	11,7	11,6	13,6	17,5	20,3	23,5	24,5	22,1	17,9	15,2	12,9

Relative Humidity

Hour	January	February	March	April	May	June	July	August	September	October	November	December
1	70	66	71	72	78	81	74	64	72	71	75	75
2	70	66	71	73	78	81	74	64	72	72	75	75
3	70	66	69	73	78	81	75	65	73	73	75	76
4	70	66	68	73	78	80	75	66	73	73	74	76
5	69	67	68	73	79	79	75	66	73	74	73	76
6	69	69	68	73	80	78	75	67	73	74	72	76
7	69	71	70	73	81	77	75	67	72	75	71	76
8	67	69	68	71	78	75	71	64	69	71	69	74
9	66	66	66	68	73	72	67	59	65	66	67	72
10	63	61	63	63	66	68	61	52	59	59	63	69
11	61	59	61	60	63	65	57	50	56	56	61	68
12	59	58	59	57	61	63	54	49	54	55	59	67
13	56	58	58	55	59	60	50	49	53	55	57	66
14	56	58	56	56	60	60	50	50	54	55	58	66
15	57	57	56	58	63	61	52	51	57	57	59	67
16	59	57	55	62	67	63	55	53	61	59	62	68
17	61	58	57	65	69	66	58	55	63	60	64	68
18	63	61	61	67	72	70	62	58	65	62	67	69
19	66	65	65	69	74	75	67	61	67	64	69	70
20	67	67	67	70	75	77	69	62	69	65	71	71
21	68	67	68	71	75	78	70	63	70	67	73	72
22	68	67	68	71	75	78	70	62	71	68	75	74
23	69	67	68	72	76	79	71	63	72	69	75	75
24	70	67	69	72	77	81	73	64	72	70	75	76

Solar Irradiation−South [W/m^2]

Hour	January	February	March	April	May	June	July	August	September	October	November	December
1	0	0	0	0	0	0	0	0	0	0	0	0
2	0	0	0	0	0	0	0	0	0	0	0	0
3	0	0	0	0	0	0	0	0	0	0	0	0
4	0	0	0	0	0	0	0	0	0	0	0	0
5	0	0	0	0	3	8	2	0	0	0	0	0
6	0	0	0	21	37	41	31	18	1	0	0	0
7	0	46	79	62	77	80	67	55	96	53	0	0
8	150	190	192	168	126	116	116	186	255	251	193	117
9	283	299	295	271	230	208	240	319	401	403	373	280
10	370	380	375	353	314	296	341	427	516	515	490	377
11	422	430	425	406	369	352	407	497	589	584	559	434
12	440	447	442	424	387	372	430	521	614	608	583	453
13	422	430	425	406	369	352	407	497	589	584	559	434
14	370	380	375	353	314	296	341	427	516	515	490	377
15	283	299	295	271	230	208	240	319	401	403	373	280
16	150	190	192	168	126	116	116	186	255	251	193	117
17	0	46	79	62	77	80	67	55	96	53	0	0
18	0	0	0	21	37	41	31	18	1	0	0	0
19	0	0	0	0	3	8	2	0	0	0	0	0
20	0	0	0	0	0	0	0	0	0	0	0	0
21	0	0	0	0	0	0	0	0	0	0	0	0
22	0	0	0	0	0	0	0	0	0	0	0	0
23	0	0	0	0	0	0	0	0	0	0	0	0
24	0	0	0	0	0	0	0	0	0	0	0	0

Solar Irradiation−West [W/m^2]

Hour	January	February	March	April	May	June	July	August	September	October	November	December
1	0	0	0	0	0	0	0	0	0	0	0	0
2	0	0	0	0	0	0	0	0	0	0	0	0
3	0	0	0	0	0	0	0	0	0	0	0	0
4	0	0	0	0	0	0	0	0	0	0	0	0
5	0	0	0	0	3	8	2	0	0	0	0	0
6	0	0	0	21	37	41	31	18	1	0	0	0
7	0	15	38	62	77	80	67	55	35	14	0	0
8	30	53	77	101	115	116	103	94	75	54	31	21
9	61	86	112	136	148	148	134	127	110	90	65	51
10	86	112	138	162	174	173	158	153	138	118	92	76
11	101	128	155	179	190	188	173	169	155	136	109	91
12	107	134	161	185	195	194	178	175	161	142	115	96
13	196	234	272	313	339	352	370	366	344	292	242	186
14	261	310	360	417	458	483	531	525	494	410	336	248
15	280	346	410	481	536	572	642	630	586	470	369	259
16	206	316	403	490	558	601	681	655	587	429	270	149
17	0	115	290	415	502	551	619	558	415	135	0	0
18	0	0	0	170	322	381	393	219	0	0	0	0
19	0	0	0	0	3	29	3	0	0	0	0	0
20	0	0	0	0	0	0	0	0	0	0	0	0
21	0	0	0	0	0	0	0	0	0	0	0	0
22	0	0	0	0	0	0	0	0	0	0	0	0
23	0	0	0	0	0	0	0	0	0	0	0	0
24	0	0	0	0	0	0	0	0	0	0	0	0

Solar Irradiation−East [W/m^2]

Hour	January	February	March	April	May	June	July	August	September	October	November	December
1	0	0	0	0	0	0	0	0	0	0	0	0
2	0	0	0	0	0	0	0	0	0	0	0	0
3	0	0	0	0	0	0	0	0	0	0	0	0
4	0	0	0	0	0	0	0	0	0	0	0	0
5	0	0	0	0	3	29	3	0	0	0	0	0
6	0	0	0	170	322	381	393	219	0	0	0	0
7	0	115	290	415	502	551	619	558	415	135	0	0
8	206	316	403	490	558	601	681	655	587	429	270	149
9	280	346	410	481	536	572	642	630	586	470	369	259
10	261	310	360	417	458	483	531	525	494	410	336	248
11	196	234	272	313	339	352	370	366	344	292	242	186
12	107	134	161	185	195	194	178	175	161	142	115	96
13	101	128	155	179	190	188	173	169	155	136	109	91
14	86	112	138	162	174	173	158	153	138	118	92	76
15	61	86	112	136	148	148	134	127	110	90	65	51
16	30	53	77	101	115	116	103	94	75	54	31	21
17	0	15	38	62	77	80	67	55	35	14	0	0
18	0	0	0	21	37	41	31	18	1	0	0	0
19	0	0	0	0	3	8	2	0	0	0	0	0
20	0	0	0	0	0	0	0	0	0	0	0	0
21	0	0	0	0	0	0	0	0	0	0	0	0
22	0	0	0	0	0	0	0	0	0	0	0	0
23	0	0	0	0	0	0	0	0	0	0	0	0
24	0	0	0	0	0	0	0	0	0	0	0	0

Solar Irradiation−Horizontal [W/m^2]

Hour	January	February	March	April	May	June	July	August	September	October	November	December
1	0	0	0	0	0	0	0	0	0	0	0	0
2	0	0	0	0	0	0	0	0	0	0	0	0
3	0	0	0	0	0	0	0	0	0	0	0	0
4	0	0	0	0	0	0	0	0	0	0	0	0
5	0	0	0	0	5	14	4	0	0	0	0	0
6	0	0	1	51	115	144	120	52	1	0	0	0
7	0	33	108	203	286	324	318	238	126	33	0	0
8	79	159	252	363	456	502	517	440	321	190	91	50
9	189	279	382	504	604	657	693	619	498	348	229	157
10	277	374	483	613	719	778	829	759	636	472	341	245
11	334	433	546	681	792	854	915	847	724	551	413	302
12	353	454	568	705	817	880	944	878	754	578	437	322
13	334	433	546	681	792	854	915	847	724	551	413	302
14	277	374	483	613	719	778	829	759	636	472	341	245
15	189	279	382	504	604	657	693	619	498	348	229	157
16	79	159	252	363	456	502	517	440	321	190	91	50
17	0	33	108	203	286	144	318	238	126	33	0	0
18	0	0	1	51	115	144	120	52	1	0	0	0
19	0	0	0	0	5	14	4	0	0	0	0	0
20	0	0	0	0	0	0	0	0	0	0	0	0
21	0	0	0	0	0	0	0	0	0	0	0	0
22	0	0	0	0	0	0	0	0	0	0	0	0
23	0	0	0	0	0	0	0	0	0	0	0	0
24	0	0	0	0	0	0	0	0	0	0	0	0

Solar Irradiation−North [W/m^2]

Hour	January	February	March	April	May	June	July	August	September	October	November	December
1	0	0	0	0	0	0	0	0	0	0	0	0
2	0	0	0	0	0	0	0	0	0	0	0	0
3	0	0	0	0	0	0	0	0	0	0	0	0
4	0	0	0	0	0	0	0	0	0	0	0	0
5	0	0	0	0	3	19	3	0	0	0	0	0
6	0	0	45	0	119	156	136	51	1	0	0	0
7	0	15	62	38	133	166	142	59	35	14	0	0
8	30	53	101	77	115	132	103	94	75	54	31	21
9	61	86	136	112	148	148	134	127	110	90	65	51
10	86	112	162	138	174	173	158	153	138	118	92	76
11	101	128	179	155	190	188	173	169	155	136	109	91
12	107	134	185	161	195	194	178	175	161	142	115	96
13	101	128	179	155	190	188	173	169	155	136	109	91
14	86	112	162	138	174	173	158	153	138	118	92	76
15	61	86	136	112	148	148	134	127	110	90	65	51
16	30	53	101	77	115	132	103	94	75	54	31	21
17	0	15	62	38	133	166	142	59	35	14	0	0
18	0	0	45	0	119	156	136	51	1	0	0	0
19	0	0	0	0	3	19	3	0	0	0	0	0
20	0	0	0	0	0	0	0	0	0	0	0	0
21	0	0	0	0	0	0	0	0	0	0	0	0
22	0	0	0	0	0	0	0	0	0	0	0	0
23	0	0	0	0	0	0	0	0	0	0	0	0
24	0	0	0	0	0	0	0	0	0	0	0	0

Attachment 2−Thermal properties of food

VEGETABLES	WATER CONTENT [%]	HEAT OF RESPIRATION (mW/kg)				
		0 °C	5 °C	10 °C	15 °C	20 °C
Artichokes	84,94	100,4	136,3	153,85	226,55	366,2
Asparagus	92,4	159,3	283,25	611,05	721,85	1146,7
Beans	90,27	60,1	82,45	167,3	333,15	462,65
Beet	87,58	18,65	27,65	37,6	59,45	
Broccoli	90,69	59	288		761,6	917,55
Brussels Sprouts	86	58,45	119,75	218,95	299,5	415,5
Cabbage	92,15	19	31,5	44,85	69,1	113,95
Carrots	87,79	45,6	58,2	93,1	117,4	209
Cauliflowers	91,91	52,9	60,6	100,4	136,8	238,1
Celery	94,64	21,3	32,5	54,5	110,6	191,6
Beet	90,55	18,65	27,65	37,6	59,45	
Crop	75,96	126,1	230,4	332,2	483	855
Cucumbers	96,01			76,5	84,5	117
Garlic	58,58	20,5	22,5	27,8	56,75	41,4
Radish	78,66	16,75	23,5	70,8	89,5	143
Lettuce	95,89	31	39,3	64,5	106,7	168,8
Mushrooms	91,81	106,25	210,5			860,45
Green peppers	89,58			42,7	67,9	130
Onion	89,68	8,7	10,2	21,3	33	50
Parsley	87,71	117,25	223,5	437	544	668,5
Peas	78,86	126,5	194,5		565	900
Potatoes	78,96		34,9	51,5	66	93
Rhubarbs	93,61	31,5	42,5		112,5	143
Spinach	91,58	48,5	136,3	328,3	530,5	682,3
Tomatoes	93				60,6	102,8

FRUITS	WATER CONTENT [%]	HEAT OF RESPIRATION (mW/kg)				
		0 °C	5 °C	10 °C	15 °C	20 °C
Apples	83,93	20,4	35,9	50,2	106,2	166,8
Apricots	86,35	16,5	22,5	44	82	121,1
Avocado	74,27				324,3	623,55
Banana	74,26				94,5	121,1
Blueberries	84,61	18,9	31,5		142	206,35
Blackberries	85,64	56,5	109,9	218	319,5	484,5
Melon	89,78		27	46,1	106,5	161,8
Cherries	86,13	28	38		114,5	131,5
Figs	79,11		31	66	166	224,5
Grapes	90,89	8,2	16	22,8	47	97
Lemon	87,4				47	67,4
Lime	88,26			13	26	37,5
Mango	81,71				133,4	335,5
Peaches	86,28	11,2	19,4	46,6	101,8	181,9
Olive	79,99				89,5	129,75
Orange	82,3	9,2	18,9	36,4	62,1	89,2
Pear	83,81	15	21,5	39	111	146,5
Persimmons	64,4		17,5		37	65
Pineapple	86,5			16,5	38,3	71,8
Plums	85,2	7	18,5	29,5	35	65
Raspberries	86,57	63	102,5	123	271,5	173,35
Strawberries	91,57	44	73	213	241	442

MEET	WATER CONTENT [%]
BEEF	65,15
PIG	44,45
SAUSAGE	48,32
CHICKEN	65,99
DUCK	48,5
TURKEY	70,4
LAMB	74,11

FISH	WATER CONTENT [%]
COD	81,22
HERRING	59,7
MACKEREL	63,55
PERCH	78,7
YELLOW COD	78,18
SALMON	76,35
TUNA	68,09
WHITING	80,27
CLAMS	81,82
LOBSTER	76,76
OYSTER	85,16
SCALLOPS	78,57
SHRIMP	75,86

DAIRY	WATER CONTENT [%]
BUTTER	17,94
MOZZARELLA	54,14
PARMIGIANO	29,16
EMMENTALER	37,21
ROQUEFORT	39,38
CHEDDAR	36,75

References

ASHRAE Handbook—Refrigeration (SI) Thermal properties of food, 2006. Thermal properties of food. Section 9.

Brito, P., Lopes, P., Reis, P., Alves, O., 2014. Simulation and optimization of energy consumption in cold storage chambers from the horticultural industry. Int. J. Energy Environ. Eng. 5, 88.

Çengel, Y.A., Ghajar, A. 2010. Heat and mass transfer: Fondamental & Applications - McGraw-Hill Editor, 4 edition Chapter17 - Refrigeration and freezing of foods.

Climator Sweden AB. www.climator.com

Consiglio Nazionale delle Ricerche, CNR, Dati climatici per la Progettazione edile ed impiantistica, Pubblicazione Piano Finalizzato Energia, Roma, 1982.

Gwanpua, S.G., Verboven, P., Leducq, D., Brown, T., Verlinden, B.E., Bekele, E., Aregawi, W., Evans, J., Foster, A., Duret, S., Hoang, H.M., Van der Sluis, S., Wissink, E., Hendriksen, L.J.A.M., Taoukis, P., Gogou, E., Stahl, V., El Jabri, M., Le Page, J.F., Claussen, I., Indergård, E., Nicolai, B.M., Alvarez, G., Geeraerd, A.H., 2015. The FRISBEE tool, a software for optimising the trade-off between food quality, energy use, and global warming impact of cold chains. J. Food Eng.148, 2–12.

Holder, R.D. 2005. Heat load in Refrigeration Systems.

ISPRA – "Fattori di emissione di CO2 nel settore elettrico e analisi della decomposizione delle emissioni" – Rapporto 172 / 2012 - ISBN: 978-88-448-0580-7.

Rubiterm Technologies GmbH. www.rubitherm.de

UNI 10351- Materiali da costruzione. Conduttività termica e permeabilità al vapore.

Conclusion

Conclusion and recommendations for future research directions

Nowadays, refrigeration plays an essential role within food industry, since preserving the quality of foodstuff and satisfying an increasingly wide range of consumer's needs. On the other hand, refrigeration sector is responsible for ozone depletion and global warming because of the leakage of refrigerants used (20%) and the energy consumption of refrigerating equipment (80%) respectively. In Italy, the Ministry of Economic Development within the "Electrical System Research" has funded a number of research activities, between ENEA (National Agency for New Technologies, Energy and Sustainable Economic Development) and several Italian universities, aimed at reducing the national electricity consumption. In this context, present research focuses on technologies for the reduction of energy consumption over refrigerated cold storage and transportation systems. It is well known that the maintenance of a proper temperature along the entire cold chain, determines a high-energy consumption and related greenhouse gasses (GHGs) emissions into the atmosphere. Therefore, small improvements in energy performance of refrigerated storage and transport systems can lead to interesting reduction in overall energy impact on an already high-tech sector.

The aim of this dissertation was to assess the effectiveness of PCMs application in a commercial cold room in terms of energy saving amount and the consequent CO2-equivalent emissions reduction. Therefore, considering the main heat loads affecting a refrigerated compartment, the application of PCM on three different thermal energy storage systems have been assessed. The first analysis was focused on the reduction of cooling energy required to break down the heat load deriving from the external environment (e.g. heat conducted through the insulated envelope). In this context, a PCM layer was added to the external side of a refrigerated container envelope. Afterwards, an experimental campaign was aimed at the reduction of cooling energy required to run a low efficiency-refrigerating unit and to contrast the incoming heat load, occurring during a power outage event. By this way, an air heat exchanger containing PCM was positioned near the evaporator of a cold room. Finally, the third analysis was devoted at reducing the heat load infiltration, occurring during refrigerated compartment door opening events. In this regard, the application of PCM on the internal compartment walls would be an ultimate step for significant energy saving on refrigeration technologies. Results underline that the improvement of the envelope thermal inertia, by adding PCM layer, leads to a consistent reduction (between 5.55% and 8.57%) and phase displacement (between 4.30h-3.30h) of the daily heat load. Thanks to higher thermal inertia, the heat load stored during the day reaches the internal refrigerated environment during the night, characterized by high

refrigeration system performance and reduced energy costs. In fact, the refrigeration unit operates with high efficiency due to a reduced temperature gradient between the external and the internal environment therefore requiring lower energy amount. Results obtained by the positioning of a PCM air heat exchanger near the evaporator highlighted a lowered number of compressor ON-OFF cycles (6 cycles instead of 13 cycles) and in an increased of their length. By this way, the refrigerating unit energy efficiency was improved and the electric power consumption reduced as well (about 16%). Furthermore, the present technology has been proved a valid method for reducing both the compartment air (of about 3.06 °C) and stored product temperature (of about 1.4 °C) during a power outage event. Finally, the PCM panels addition to the internal compartment walls, leads to a reduction of both peak air temperature (of almost 2.3 °C and 0.7 °C) and energy consumption (3.4%) during door openings. Moreover, the different operational scenarios considered, highlighted an energy saving ranging between 4.4-4.8%.

Summing up a comprehensive study on PCM application in a cold room was carried out during the three research years. Experimental and numerical campaigns provided encouraging results. However, the highest energy consumption reduction can be only reached carefully calibrating planning settings in function of the operational conditions on which PCMs are employed. In each investigation, has been possible to appreciate the importance of selecting a PCM with a proper phase change temperature. This means that the selection of a PCM with a too high or too low melting temperature with respect to the operating condition, can limit the PCM functioning. This was true for first two PCM applications investigated. As an example, regarding the PCM addition to the external surfaces of a refrigerated container, although the numerical analysis identified the RT35HC as optimal, the external climatic conditions, which characterized the summer season, determined a partial PCM melting. Therefore, along with the heat flux peak reduction, a consistent decrease of the total amount of heat per unit area was not obtained. Moreover, concerning the application of a PCM air heat exchanger near the evaporator of a cold room, the selection of a PCM characterized by a melting temperature closer to the evaporator outgoing air temperature, could determine a further improvement of the refrigerating unit energy efficiency. Another aspect to be considered is the PCM packaging system and its construction material. The first consideration was well-thought-out during the experimentation regarding the PCM application to the external side of a refrigerated container envelope. However, two main drawbacks such as PCM losses (during its melting phase) and PCM partially discharge process were found. Specifically the latter occurred because of a thin air layer, between the PCM and the polyurethane foam, which behaving as a thermal resistance not allowed the PCM to discharge the stored energy, determining non satisfactory achievements in

terms of energy saving. Therefore, in order to avoid the previously described drawbacks it is advisable to insert the PCM layer during the polyurethane foaming. On the other hand, another aspect to carefully consider regards the selection of PCM packaging system material. This aspect was pointed out following the weak results obtained by placing the PCM to the internal compartment walls of a cold room. In fact, by using aluminum containers, the heat exchange between the PCM and the warm air entering during door opening could be improved. By this way, a higher reduction of both internal compartment peak air temperature and energy consumption could be achieved. One of the last point to consider carefully focuses to the PCM thickness, which should be sized based on the thermal load. In fact the selection of a too high thickness does not allow the PCM to fully participate to the phase change process. On the other hand too low thickness does not allow the PCM to store all the thermal energy. This aspect should be better reviewed in the experimentation, which considered the PCM application to the internal walls of a refrigerated compartment. In this case, the PCM thickness should be reduced allowing the PCM to store the entire incoming heat load due to the door openings. Anyway, the selected PCM thickness resulted able to meet the entire thermal load determining by 1,5h of power failure event. Therefore, a careful sizing in accordance with heat gain of the cold room at environmental temperature is recommended.

Given the above, it is concluded that an industrial manufacturing will further increase the feature performances, reducing some of previously describe technology limitations due to handmade-construction. Finally, it is also worth noting that the presented technologies can be easily applicable to the other compartment involved in refrigerated transport and storage systems and have not to be considered alternatives to each other. In fact, assuming a possible research development it would be interesting the study of a refrigerated compartment (travelling by rail, ship or road) fully integrated of all described technologies. By this way will be desirable the development of energetically “independent” refrigerated compartments whose are able to meet the required cooling energy in different environmental conditions. On the other hand, in case of cold rooms operating in the food industry, hotels and restaurants the PCM application inside the refrigerated compartment results more useful than the thermal shield. A possible research development would be focused on comprehension of PCM beneficial effect in lowering product temperature abuse due to power failure and door opening events. Finally, all the physical properties of the entire refrigerated system would be implemented on a numerical model allowing a sharper identification of the most suitable features in function of the particular operational condition.

Acknowledgments

My deep gratitude goes first to Professor Paolo Principi, who expertly guided me throughout the doctoral research activity. My appreciation also extends to PhD Roberto Fioretti with whom I shared three long years and the "paper publication anxiety". To the technical team of Department of Industrial Engineering and Mathematical Sciences, thank you – especially to Ing. Giuliano Giuliani for always helping me. I would also like to thank the external rapporteurs Professor Marco Perino from Politecnico di Torino and Professor Mohamed Safi from Ecole Nationale d'Ingénieurs de Tunis for having expertly revised the present research work.